AD-A276 060

Technical Report EL-93-25
December 1993

US Army Corps of Engineers
Waterways Experiment Station

2

Microwave Dielectric Behavior of Soils

Report 3
Measurements and Modeling

by John O. Curtis
Environmental Laboratory

DTIC
ELECTE
FEB 23 1994
S B D

Approved For Public Release; Distribution Is Unlimited

94-05751

DTIC QUALITY INSPECTED 1

94 2 22 128

Prepared for Headquarters, U.S. Army Corps of Engineers

The contents of this report are not to be used for advertising, publication, or promotional purposes. Citation of trade names does not constitute an official endorsement or approval of the use of such commercial products.

PRINTED ON RECYCLED PAPER

Technical Report EL-93-25
December 1993

Microwave Dielectric Behavior of Soils

Report 3
Measurements and Modeling

by John O. Curtis
Environmental Laboratory

U.S. Army Corps of Engineers
Waterways Experiment Station
3909 Halls Ferry Road
Vicksburg, MS 39180-6199

Report 3 of a series

Approved for public release; distribution is unlimited

Prepared for U.S. Army Corps of Engineers
Washington, DC 20314-1000

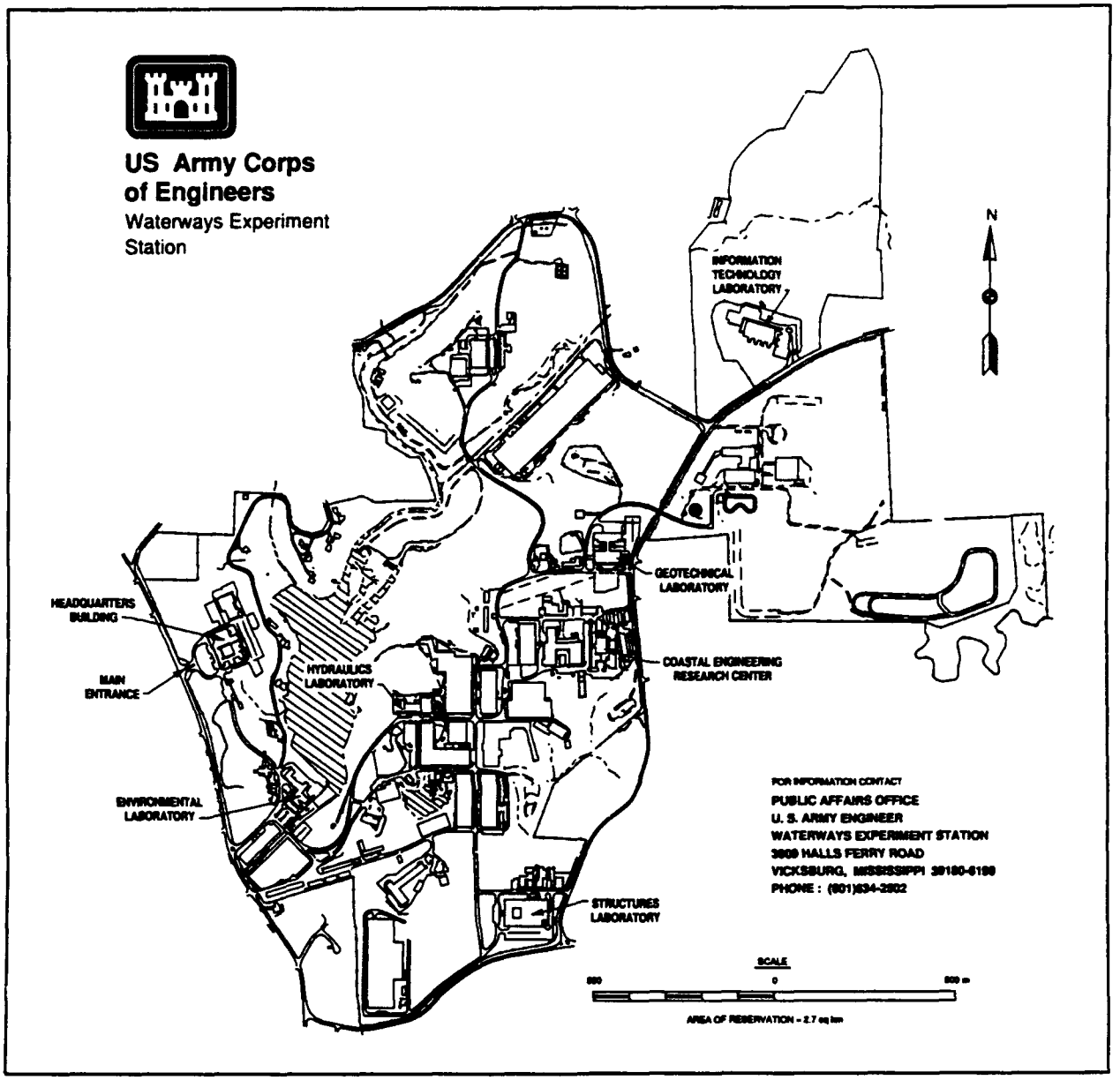

Waterways Experiment Station Cataloging-in-Publication Data

Curtis, John O.

Microwave dielectric behavior of soils / by John O. Curtis ; prepared for U.S. Army Corps of Engineers.

3 v. : ill. ; 28 cm. — (Technical report ; EL-93-25)

Contents: Report 1, Summary of related research and applications — Report 2, A unique coaxial measurement apparatus — Report 3, Measurements and modeling.

Includes bibliographical references.

1. Soils — Electric properties. 2. Dielectric measurements. 3. Microwave measurements. 4. Remote sensing. I. United States. Army. Corps of Engineers. II. U.S. Army Engineer Waterways Experiment Station. III. Title. IV. Series: Technical report (U.S. Army Engineer Waterways Experiment Station) ; EL-93-25.

TA7 W34 no.EL-93-25

Contents

List of Figures

Accession For
NTIS GRA&I ☑
DTIC TAB ☐
Unannounced ☐
Justification
By
Distribution/
Availability Codes
Dist | Avail and/or Special
A-1

Preface

The study reported herein was conducted within the facilities of the Environmental Laboratory (EL) of the U.S. Army Engineer Waterways Experiment Station (WES) during the period of May 1991 to June 1992 for Headquarters, U.S. Army Corps of Engineers.

General supervision was provided by Drs. Daniel Cress and Victor Barber, Acting Chiefs, Environmental Systems Division (ESD), EL, Dr. Raymond L. Montgomery, Chief, Environmental Engineering Division, EL, and Dr. John Harrison, Acting Director, EL.

Dr. John O. Curtis collected the data and developed the models reported herein. Dr. Curtis prepared the report under the direct supervision of Messrs. Malcolm Keown and Kenneth Hall, Chiefs, Environmental Constraints Group, ESD.

At the time of publication of this report, Director of WES was Dr. Robert W. Whalin. Commander was COL Bruce K. Howard, EN.

This report should be cited as follows:

> Curtis, J. O. (1993). "Microwave dielectric behavior of soils; Report 3, Measurements and Modeling," Technical Report EL-93-25, U.S. Army Engineer Waterways Experiment Station, Vicksburg, MS.

1 Introduction

New and improved methods of remote sensing have increased the understanding of Earth's origins, its resources, and those processes that contribute to its dynamic (on a large time scale) nature. Scientists and engineers from many disciplines are constantly exploring new ways to quantify the Earth's properties for their particular applications. Among these methods are measurements of electromagnetic energy in many different wavelength regimes, both passive and active. The development of small powerful sources and ultrasensitive receivers along with improved data processing capabilities has fostered renewed interest in measurements of the Earth within the microwave region of the spectrum where wavelengths in air range from a few millimeters to several meters.

Natural terrain surfaces consist of bare soils, rocks, vegetation, and water. This study was initiated with the hope of making a meaningful contribution to the understanding of microwave interactions with natural terrain. The first report in this series attempts to summarize what is currently known about the measurement and modeling of the electrical properties of well-characterized soils (Curtis, "Microwave Dielectric Behavior of Soils; Report 1, Summary of Related Research and Applications," In Preparation), while the second report contains a description of a new dielectric property measurement capability recently developed at the U.S. Army Engineer Waterways Experiment Station (WES) in Vicksburg, MS (Curtis, "Microwave Dielectric Behavior of Soils; Report 2, A Unique Coaxial Measurement Apparatus," In Preparation). It is hoped that this new measurement apparatus will be used in the future to establish a comprehensive database of soil properties covering a broad spectrum of soil types, measurement frequencies, sample moisture contents, and sample temperatures. This final report presents some initial measurement results and discusses two modeling approaches to interpreting those data. Most of the information contained in this series of reports is drawn from a doctoral research program recently completed by the author (Curtis 1992).

In an effort to make each report of this series as self-contained as possible, the rationale for pursuing this research program as well as some supporting information in appendices is included within each report. Hopefully, this will be useful for the individual who might read only one of the reports.

Reasons for Studying Electrical Properties of Soils

Soil moisture measurements

The dominant factor that controls the electrical behavior of soils is the presence of water (Topp, Davis, and Annan 1980). Obviously, one would hope to take advantage of this experimental fact to develop a means of accurately and quickly measuring the moisture in soils without having to collect numerous samples in the field, weigh them, dry them for extended periods of time, and weigh them again to obtain either a gravimetric (weight of water/weight of dry soil) moisture content or a more useful volumetric (volume of water/volume of soil sample) moisture content.

Numerous attempts have been made to develop a useful method for measuring soil moisture content. All have met with varying degrees of success, and none has proven accurate under all conditions. For example, a technique that essentially amounts to burying radar transmit and receive antennas in the soil and relating the measurements of attenuated received signals to moisture content (Birchak et al. 1974) is destructive to the soil fabric (the way in which soil particles are arranged), is very much controlled by the fabric and the size distribution of particles, and precludes the use of the same instrument in multiple locations (nature is not homogeneous), as well as the ability to easily repair defective equipment.

Another approach taken by some researchers for making field measurements of soil moisture (that also has numerous application in the biomedical field) is that of measuring the change in fringe capacitance of an open-ended coaxial probe (Thomas 1966; Brunfeldt 1987; Gabriel, Grant, and Young 1986). When pressed against a soil whose properties are unknown, the resulting change in capacitance produced by the impedance mismatch is related to electrical properties through calibration relationships. Problems arising from these measurements include the need to have proper contact between the probe tip and the soil surface, the fact that the volume of material associated with the fringe capacitance is quite small (1 cm^3 or less), and that calibration conditions simply cannot account for all of the dielectric loss mechanisms that exist in natural soils. The losses in moist soils can be highly frequency dependent over a range of several frequency decades on the electromagnetic spectrum. A recent variation on the open-ended probe measurement scheme involves the use of a waveguide section instead of a coaxial device (Parchomchuk, Wallender, and King 1990).

The concern over small sample volumes can be overcome with a redesign of the open-ended coaxial probe that replaces the solid outer conductor with several pointed tines (Campbell 1988) which allows for the probe to be pushed into the surface of soft soils. The volume of soil enclosed by such probes can easily be tens of cubic centimeters. The tined coaxial probes that have been built to date operate in a frequency range that is very much subject to the material-dependent loss mechanisms alluded to above. Research

continues that is directed to better understanding these various mechanisms and to fabricate a probe that operates in a frequency range that is not subject to such material-dependent anomalies.

Subterranean investigations

There are many types of electrical measurements in soils (and rocks) that are used to understand what lies beneath the Earth's surface (Telford et al. 1984). Among these are various schemes for measuring soil resistivity as well as the attenuation of propagating electromagnetic waves.

Resistivity measurements. Resistivity data in soils are collected by injecting known currents (usually of a frequency less than 60 Hz; alternating current required to minimize effects of charge buildup on the probe) into the ground and measuring potential differences across pairs of nearby electrodes. Assuming homogeneous media and uniform resistivity, it is possible to calculate from the potential differences an apparent resistivity of the earth material. These measurements will be affected by the presence of water in the soil or rock, by the presence of mineral compounds that could go into ionic solution with available water, and by the physical structure of the subsurface terrain itself. This being the case, resistivity measurements are useful as a measure of subsurface water volume, the locations of mineral deposits, and subsurface structure.

Electromagnetic wave propagation. Another method of making electrical subsurface measurements involves the transmission of electromagnetic waves into the soil and detection of energy that results from waves reflected from subsurface anomalies. Having the ability to track wave propagation in time, either by pulsing the source or sweeping over a known frequency band in some controlled manner, means that electromagnetic wave propagation methods of subterranean investigations are particularly useful for locating the depth of electrical anomalies such as the water table in sandy soil (Olhoeft 1983; Stewart 1982; Wright, Olhoeft, and Watts 1984), buried pipes or wires, or cavities such as tunnels or caves (Ballard 1983). Other applications include the delineation of stratified media (Lundien 1972) and determination of the thickness of ice and frost layers (Jakkula, Ylinen, and Tiuri 1980; O'Neill and Arcone 1991).

There are some practical bounds on the utility of radio frequency systems to conduct subterranean investigations because of the phenomenon of "skin depth," a measure of the attenuation of the electromagnetic energy as it travels through the medium. For relatively low-frequency sources (approximately 200 MHz), it can be shown that low-loss soils such as dry sands can possess a skin depth of 10 to 15 m, while high-loss soils such as wet silts and clays may have skin depths of only a few centimeters. Modern radio frequency receivers are extremely sensitive devices, often having a dynamic range of 50 to 100 db. The signal at skin depth represents about an 8.7-db loss in power or a two-way loss at the receiver for reflected signals of

about 17.4 db. It is certainly not inconceivable that radio frequency receivers should be capable of successfully detecting reflected signals from subterranean anomalies at depths of two to three skin depths or more.

Remote sensing of environment

Virtually all remote sensing of our environment from airborne or spaceborne platforms involves the measurement of electromagnetic radiation from the Earth's surface and/or atmosphere. Passive surveillance involves measurements of emitted radiation and that reflected from natural sources such as the sun, the atmosphere, and surrounding terrain. Active remote sensing measurement systems include a source for illuminating the target of interest. Whether passive or active, visual, thermal infrared, microwave, or millimeter wave sensors are utilized, remote sensing is the collection and interpretation of electromagnetic radiation and, as such, demands an understanding of the dielectric properties of those materials being observed.

Environmental remote sensing applications form a list that grows yearly as electronic components are improved and data collection and processing hardware and software become faster, more reliable, and less costly. For example, satellites can provide worldwide surveys of land-use patterns to monitor the threat of urbanization, waste disposal, and erosion of the land (Colwell 1983). Similar systems (including those mounted in aircraft) can monitor the health of vegetation to keep abreast of such things as loss of forest and the potential for food shortages. Sea traffic in the far northern and southern shipping lanes can be made safer through the use of airborne and spaceborne sensors to detect ice hazards.

One of the more obvious applications for microwave remote sensing devices is that of conducting surface moisture surveys to help predict groundwater availability and the potential for flooding. Attempts have been made to relate soil moisture to both laboratory reflectance data (Lundien 1966) and to airborne sensor backscatter measurements (Ulaby, Cihlar, and Moore 1974; John 1992). Careful airborne sensor measurements might provide a first approximation to the complex dielectric constant of the soil near the surface.

Because of the difference in dielectric behavior of liquid water and various forms of ice, it may be possible to use airborne sensors to detect freezing and thawing (Wegmuller 1990) in remote locations that could be used to predict spring runoff conditions and all that that encompasses for agricultural applications, the effects on the fishing industry, and the anticipation of flooding in built-up areas. Military analysts are concerned about soil moisture conditions because of its impact on trafficability, the ability of vehicles to move effectively over natural terrain.

Another remote sensing application is the mapping of exposed soils and rocks in remote areas of the world from high-flying aircraft or satellites,

which might prove useful for geomorphological studies (Swanson et al. 1988) or even mineral exploration. A less obvious, but recent, application of microwave remote sensing in soils dealt with archeological surveys in desert areas (Berlin et al. 1986; McCauley et al. 1986)

Others

While the above paragraphs emphasize some of the most obvious and useful applications of a better understanding of soil electrical properties, others have been noted in the literature. For example, some researchers have attempted to relate electrical property measurements to the physical properties of soils (Campbell and Ulrichs 1969; Hayre 1970; Arulanandan and Smith 1973; Madden 1974). Of course, nothing has been said about the military's need to better understand the microwave response of soils that form the backgrounds to military targets; i.e., when and why does clutter become a source of target-like signatures? Outside of the topic of soils, studies of the microwave response of foodstuffs has direct application to quality control concerns in the food industry (Nelson 1973, 1983).

Another new application of this technology that is closely related to the discussion on soil moisture is that of detecting liquid ground contaminants, either near the surface or at arbitrary depths using a specially fabricated probe. If, as will be argued later, polarizable liquids can be characterized by a unique frequency of peak losses because of the dielectric relaxation phenomenon, then a probe could be designed to measure losses over a frequency span that is broad enough to detect a peak loss frequency and, coupled with the results of a thorough experimental program, to identify the particular contaminant.

Problem Statement

The overall objective of this research is to measure and model the dielectric response of moist soils in ways that will test the current understanding of loss mechanisms over a broad range of moisture levels, frequencies, and material temperatures and perhaps suggest new ways of thinking about losses as a function of these variables.

The first step in achieving this objective has already been accomplished through the development of an apparatus that allows for the measurement of attenuation in moist soils over a broad spectrum of frequencies at controlled temperatures and calculable moisture contents (Curtis, "Microwave Dielectric Behavior of Soils; Report 2, A Unique Coaxial Measurement Apparatus," In Preparation). The remainder of this report describes measurements made on a number of different soils and two approaches to modeling the measured response.

2 Experimental Results

Sample Preparation and Measurements

Soil samples were prepared from one of four distinctly different soils. These consisted of a poorly graded sand, a well-graded sand, a poorly graded clean silt, and almost pure kaolinite, a nonswelling clay mineral. The soils and their associated properties were obtained from the Geotechnical Laboratory at the WES. Each soil type batch was made as homogeneous as possible by drying, pulverizing, and mixing thoroughly. Samples were then taken to determine the usual engineering properties of grain size distribution and plasticity indices. The results of those measurements are contained in Appendix A, along with the results of specific surface measurements on each sample that were conducted by a commercial laboratory.

The normal measurement procedure, as previously described in Report 2 of this series, was the following:

a. The dry, empty sample holder was carefully weighed.

b. A nearly saturated sample of soil was prepared using distilled, deionized water (a reasonable amount of time was allowed for the silt and clay to reach some sort of equilibrium) and was placed in the sample holder. The holder was tapped against a flat, hard surface to uniformly settle the sample.

c. The sample and holder were carefully weighed, then sealed and connected to the measurement system.

d. The temperature of the bath was set at -10 °C. For each new temperature setting, the sample was given 10 min to reach equilibrium once the bath had reached the desired setting. The 10-min wait was found experimentally to be more than adequate for sample equilibrium to be achieved.

e. The frequency range for the dual directional coupler being used was stepped through, and calculations of ε' and ε'' were made.

f. The temperature of the sample was changed and measurements repeated in the following sequence: -10, -5, -2, 0, 2, 5, 10, 20, 30, and 40 °C.

g. The holder was unsealed and its cover loosened. The sample and holder were periodically weighed to determine approximate values of moisture content. When the sample was thought to be at about the desired volumetric moisture content, the holder was resealed and reconnected; the sample temperature was taken back to -10 °C, and the whole measurement sequence repeated.

h. After all measurements were conducted, the sample was carefully removed, dried, and weighed to determine its original dry density and to facilitate calculations of volumetric moisture.

As explained in Report 2, measurements had to be conducted over two different frequency ranges because of the unavailability of a single dual directional coupler that could cover the entire range desired.

Summary of Data Collected

Figure 1 serves as an indication of both data quantity and quality. On this figure are symbols that represent data collected for the four primary soil materials at one temperature, 20 °C. For most of these data points, data were collected at nine other sample temperatures. Although they are not shown on this figure, data were also collected for the empty holder and for water, alcohols, and a swelling clay mineral called hectorite. Results for hectorite are not reported because physical property information is not currently available for that material. The total number of data sweeps (a sweep of frequencies) collected during these experiments easily exceeds five hundred.

The reference above to data quality is in terms of the repeatability of sample dry density as a result of the crude sample preparation technique described above. The strong clustering of the data points for each material type indicates how closely sample dry density matched for all samples. Only one string of data is significantly shifted from the others, and that is the data for kaolinite. The four data points that lie to the right of the others represent a sample with a dry density approximately 20 percent greater than the other clay mineral samples. The starting point for this sample was a batch of kaolinite that had been allowed to dry somewhat before the sample was inserted into the sample holder.

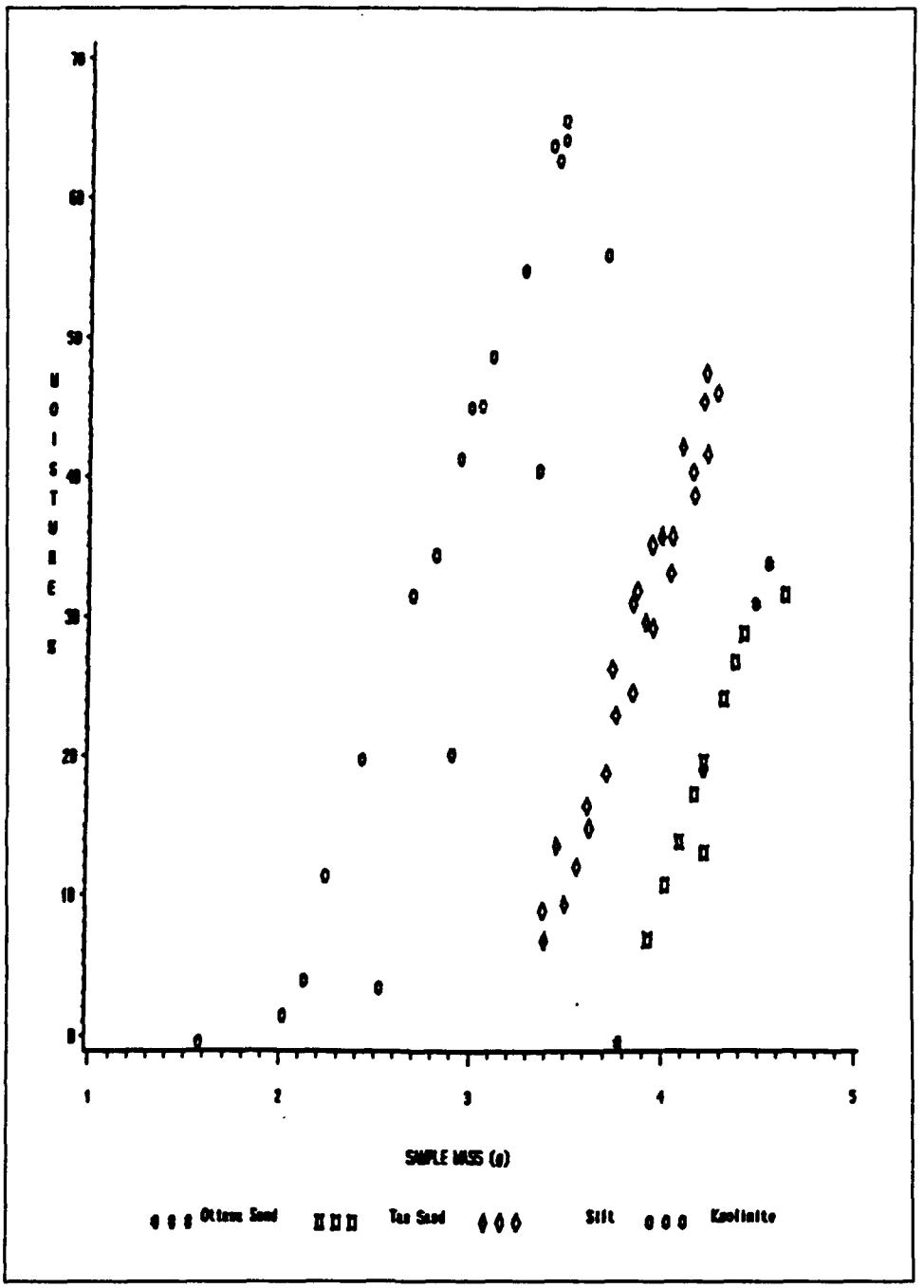

Figure 1. Data collected at 20 °C

Dispersion in Soils as a Function of Moisture Content

If the electrical behavior of moist soils is controlled by the amount and purity of water and how it fills the interstices, then one should be able to

observe high-frequency dielectric relaxation and low-frequency losses because of conductivity or Maxwell-Wagner effects or bound water (Curtis, "Microwave Dielectric Behavior of Soils; Report 1, Summary of Related Research and Applications," In Preparation), and these phenomena should be more pronounced as moisture content increases. One should also observe different responses in different soils at the same moisture content because of such factors as specific surface and the ways in which water molecules are attracted to the solid surfaces.

Figures 2-6 summarize dispersion measurements for the four soil types. Each figure contains data for sample temperatures of either -10 °C or +20 °C. These two temperatures were chosen simply to compare soils with frozen water and soils with liquid water. The vertical dashed line at 2 GHz represents the break point between measurements made with the low-frequency apparatus configuration and those made with the high-frequency setup. Three figures contain silt data, the third one representing results for a slightly different experimental procedure. In the latter case, both frequency range sweeps were conducted before the sample was incrementally dried. It is very satisfying that the results for the two setups overlap almost exactly.

Conclusions that may be drawn from these data include the following:

a. Frozen soils do not exhibit high-frequency dielectric relaxation, but do reveal some low-frequency losses.

b. Nonfrozen soils do demonstrate high-frequency relaxation, which does increase with increasing moisture content. These results are quite consistent with those published by Hallikainen et al. (1985).

c. Low-frequency losses in nonfrozen soils are also proportional to moisture content. Values are consistent with those of Campbell (1988). Minimum losses in nonfrozen soils occur in the 1- to 2-GHz range, which agrees with the observations of Hallikainen et al. (1985).

d. Comparison of sand, silt, and clay high-frequency losses at comparable moisture contents provides no indication of differences in free water content in spite of the great variation in specific surfaces.

e. If the relative magnitudes and frequency ranges of different loss mechanisms published by Hasted (1973) are correct, then bound water relaxation is a good candidate for some of the low-frequency losses seen in these data. One cannot, however, discount ionic conductivity or Maxwell-Wagner losses, or both, as contributing loss mechanisms.

f. The electrical response of frozen soils appears to be relatively insensitive to moisture content within the frequency range measured in this report, but does show some dependence on soil type at low frequencies.

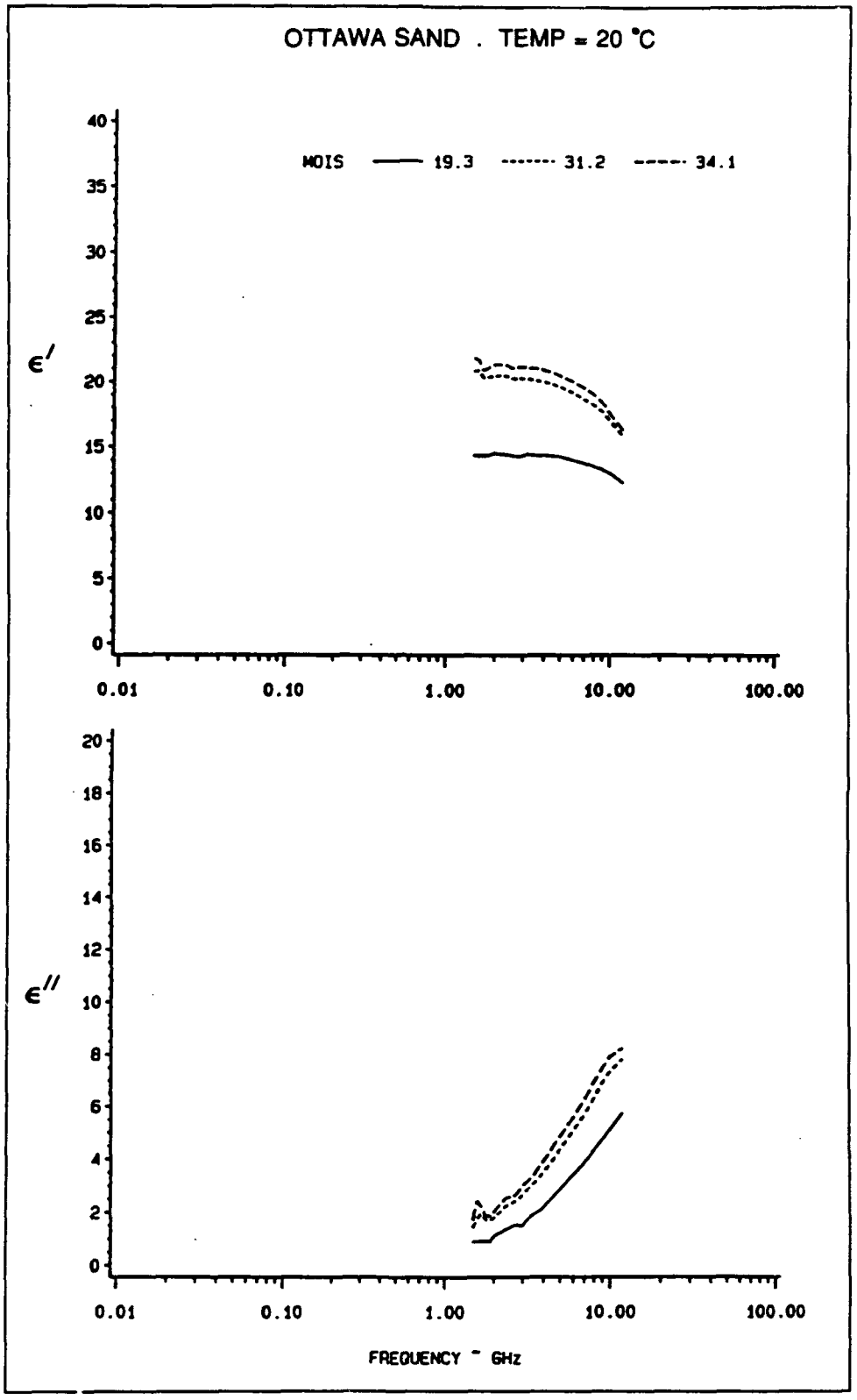

Figure 2. Dispersion in a poorly graded sand

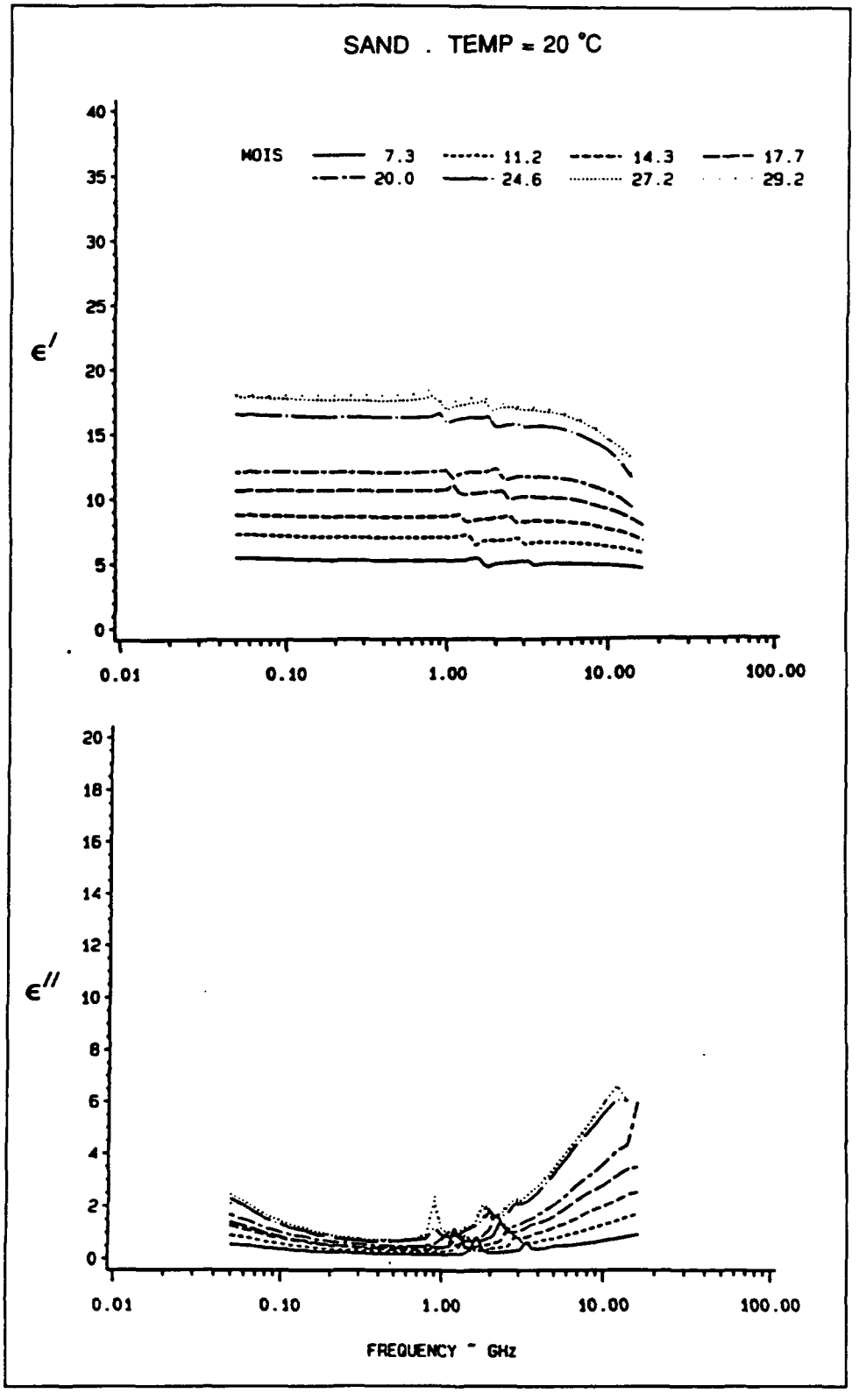

Figure 3. Dispersion in a well-graded sand

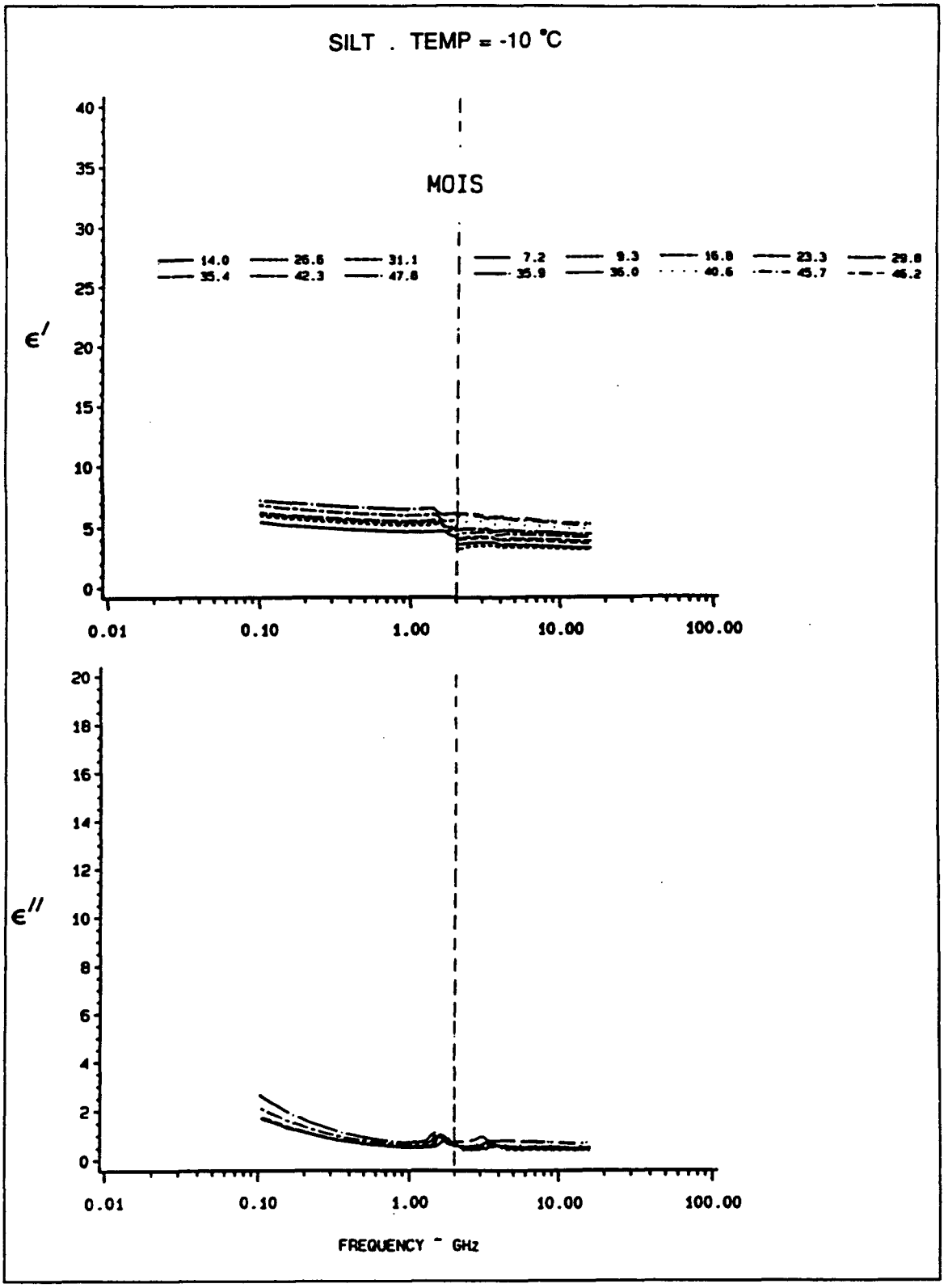

Figure 4. Dispersion in silt (first set) (Continued)

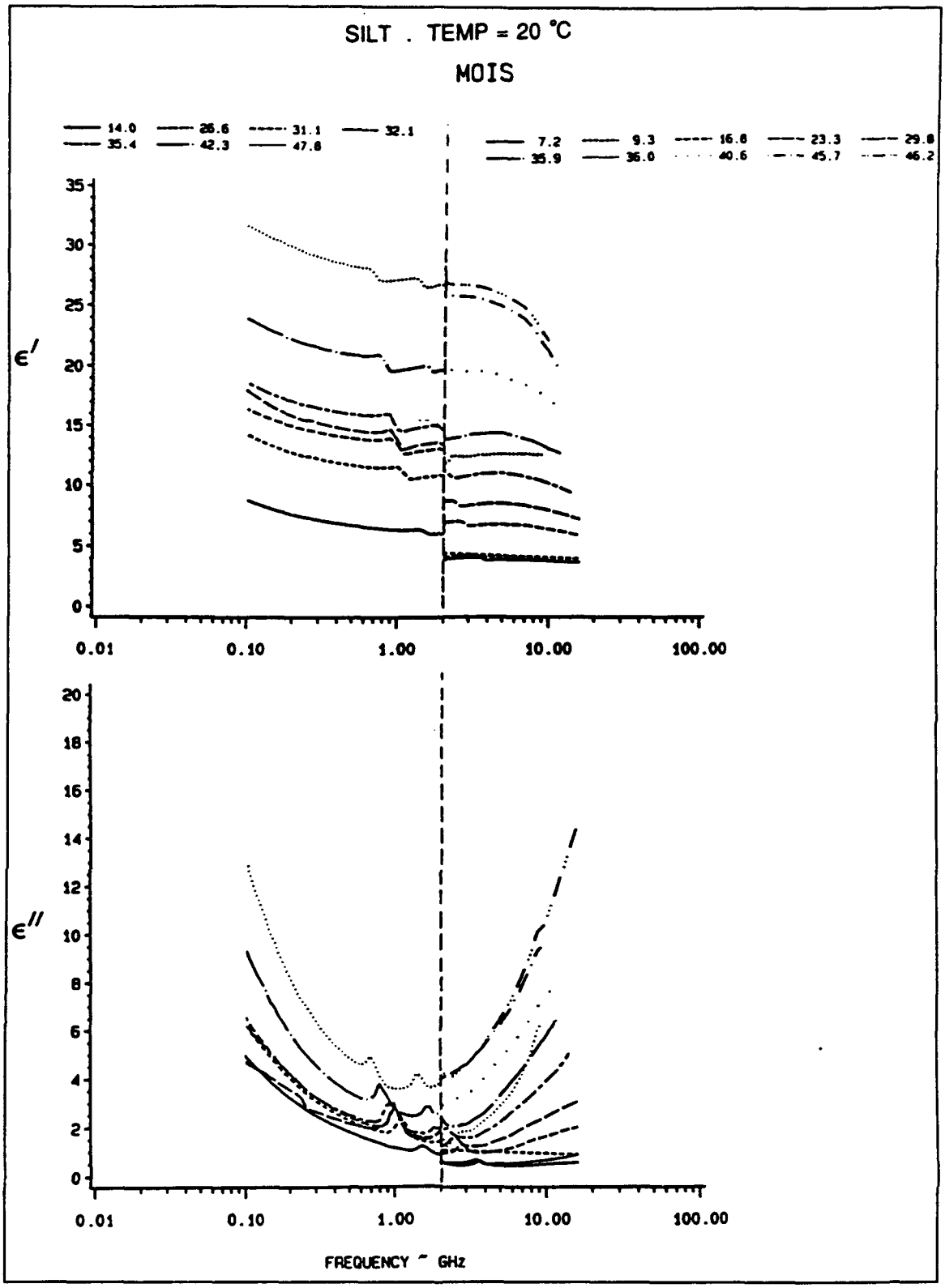

Figure 4. (Concluded)

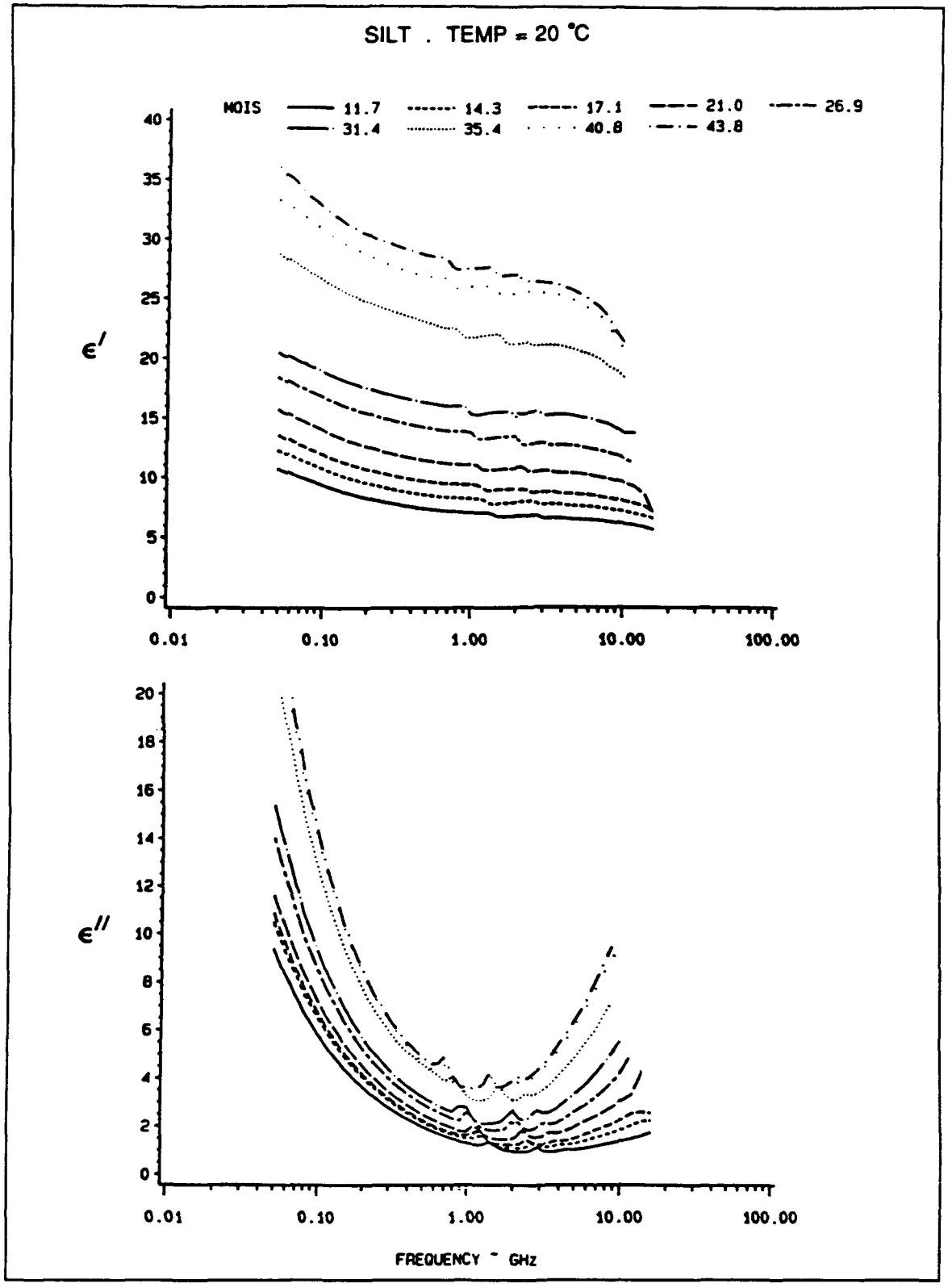

Figure 5. Dispersion in silt (second set)

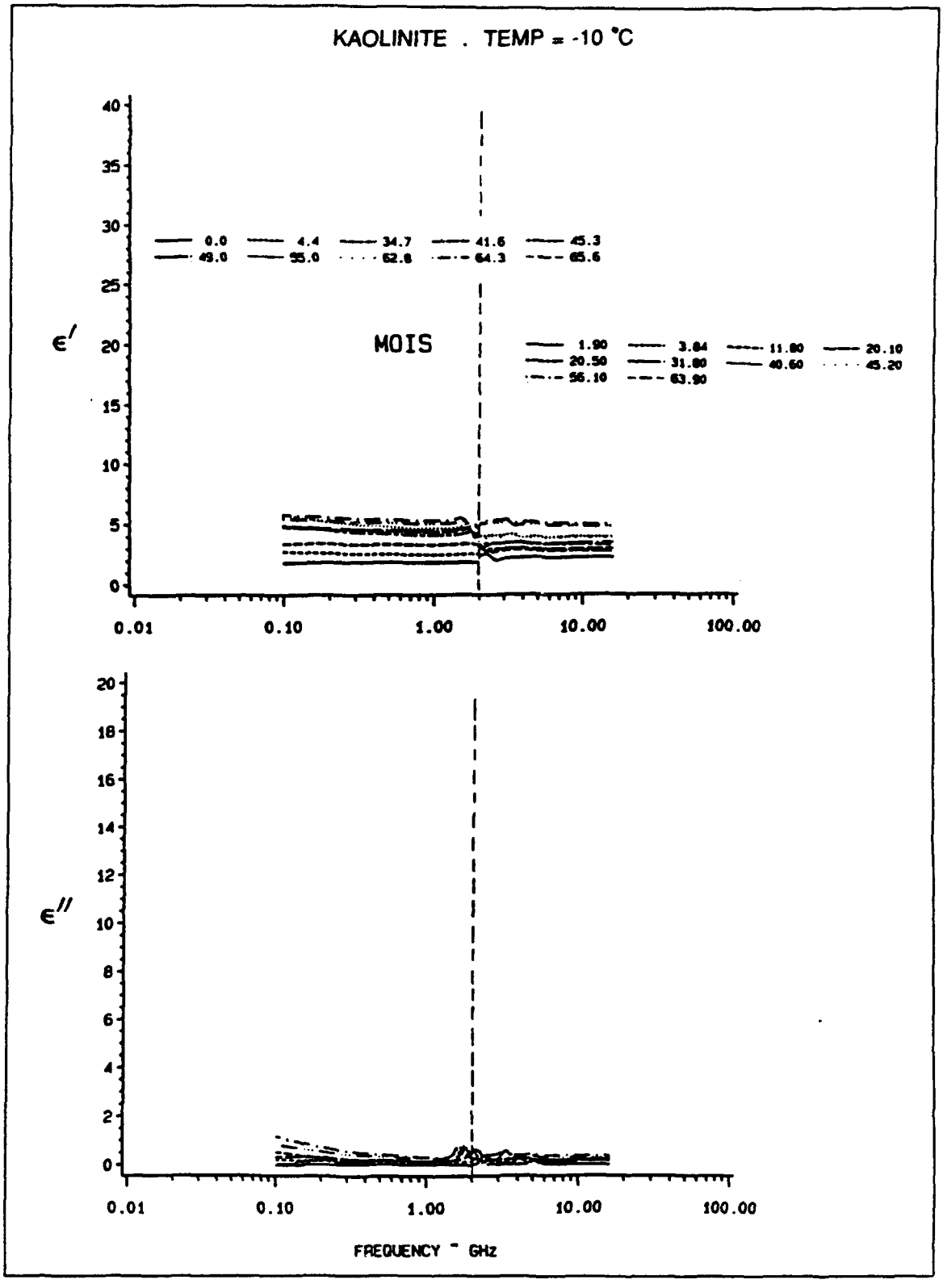

Figure 6. Dispersion in kaolinite (Continued)

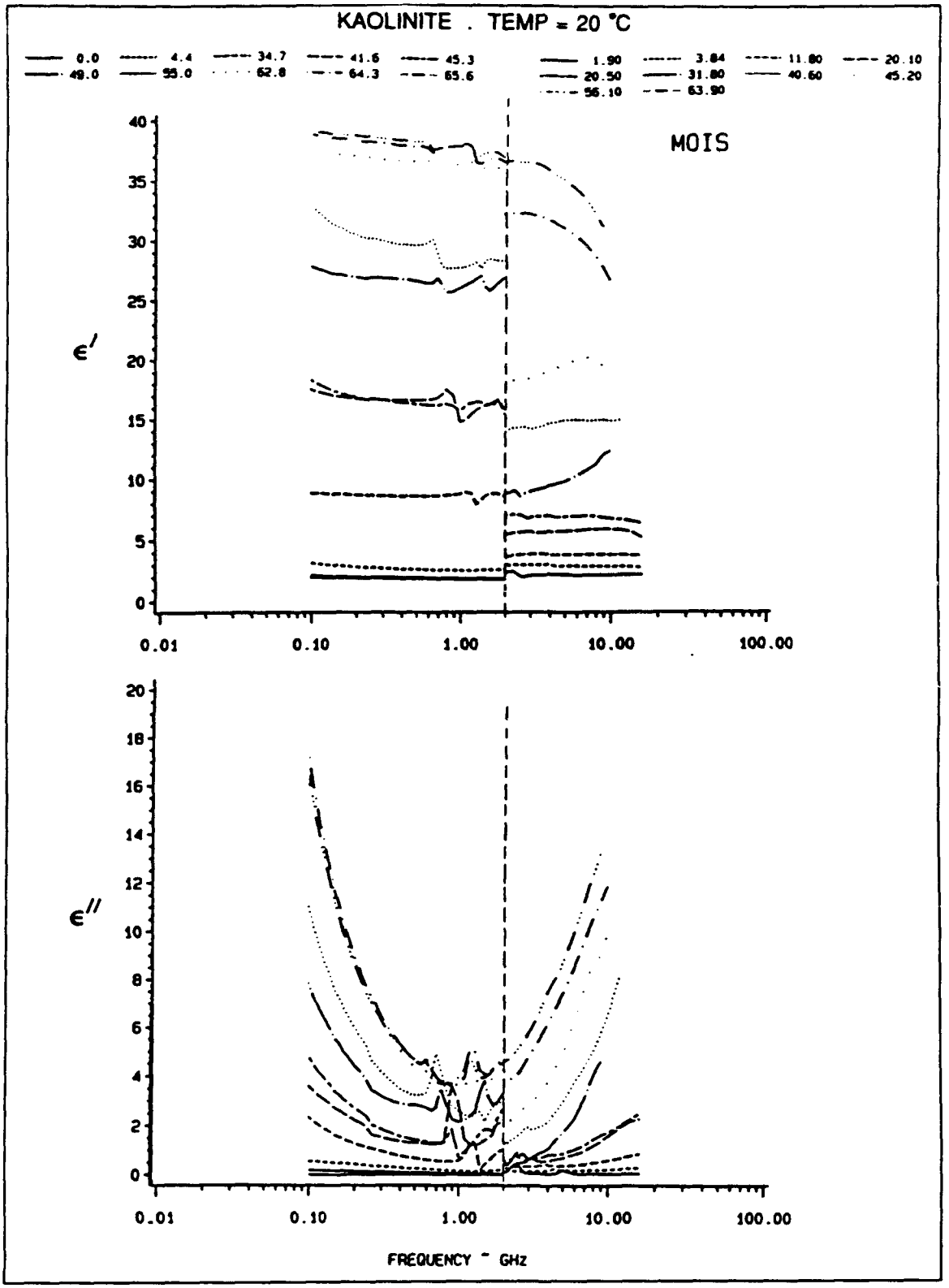

Figure 6. (Concluded)

From the results of their excellent measurements on real soils ranging from sandy loams to heavy clays, Topp, Davis, and Annan (1980) reported that, in the frequency range of 20 MHz to 1 GHz, the apparent permittivity "was strongly dependent on (moisture content) and only weakly on soil type, density, temperature, and frequency." While the measurements reported in this study have not dealt with density effects, and they do support the contention that temperature effects are minimal for unfrozen soils, they clearly demonstrate that soil type and frequency are important variables.

Single Frequency Observations

Temperature effects

Data collected at -10, -5, -2, 0, 2, 5, 10, 20, 30, and 40 °C are quite adequate for visualizing the temperature-dependent behavior of the complex dielectric constant at selected frequencies. These results are shown on Figures 7-10 and lend themselves to several observations:

a. Liquid water appears at temperatures less than 0 °C, probably somewhere between -2 and -5 °C. This is consistent with results reported by Delaney and Arcone (1982).

b. The real part of the dielectric constant for nonfrozen soils is approximately independent of temperature for all soil types.

c. The imaginary part of the dielectric constant for nonfrozen soils is not independent of temperature, showing a rise with temperature at low frequencies and a drop with temperature at high frequencies.

Because the low-frequency data show a rise in the loss term with increasing temperature, an estimate of the activation energy involved in the loss mechanism can be made following the method of Hoekstra and Doyle (1971) and Campbell (1988), which was discussed earlier in Report 1. Using their formula

$$\ln(\varepsilon'') = -\frac{A}{R}\left[\frac{1}{T_{Kelvin}}\right] \tag{1}$$

where

ε'' = imaginary part of the complex relative dielectric constant

A = activation energy, or the energy needed to overcome some equilibrium state

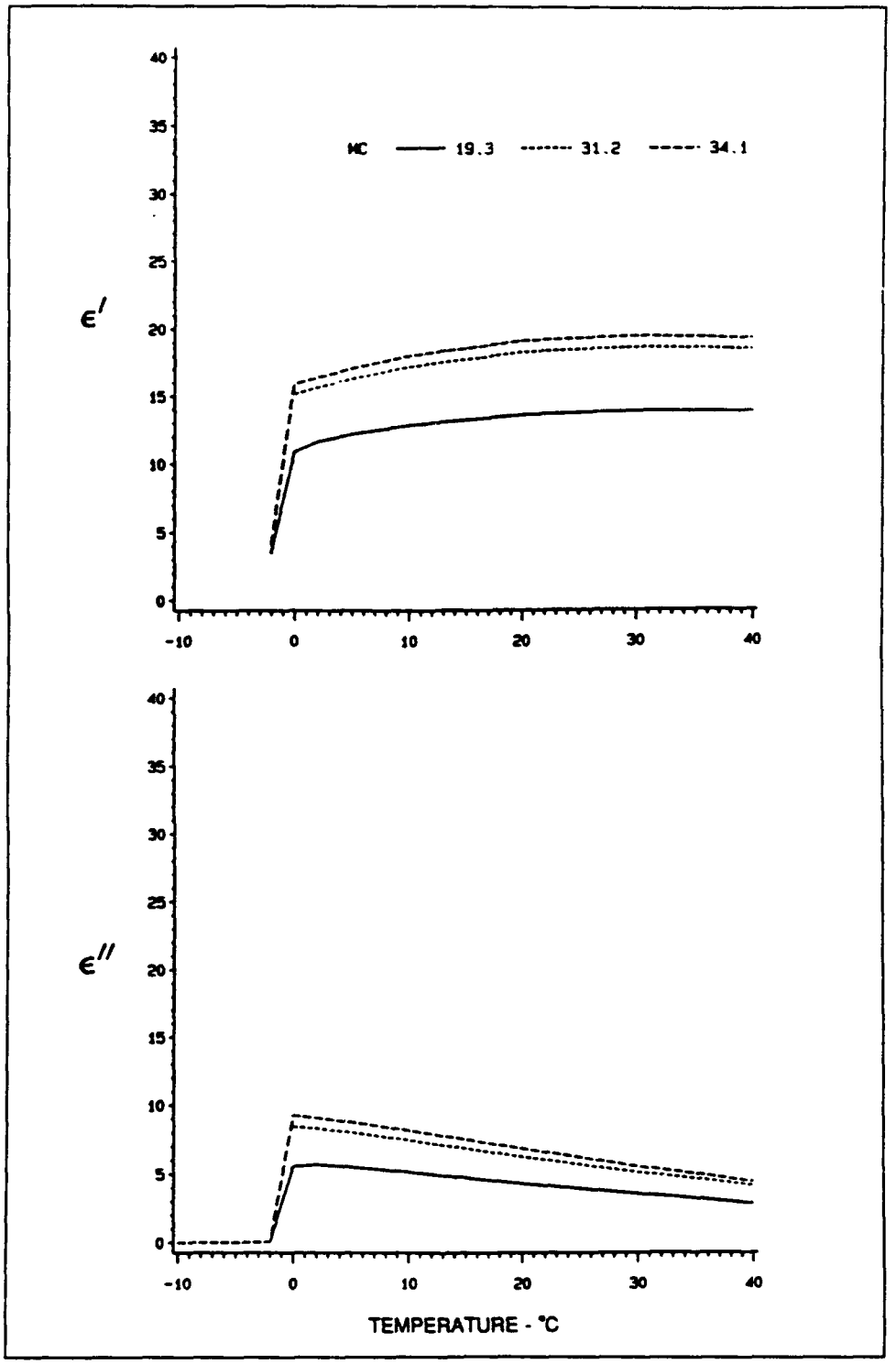

Figure 7. Temperature effects for poorly graded sand (8 GHz)

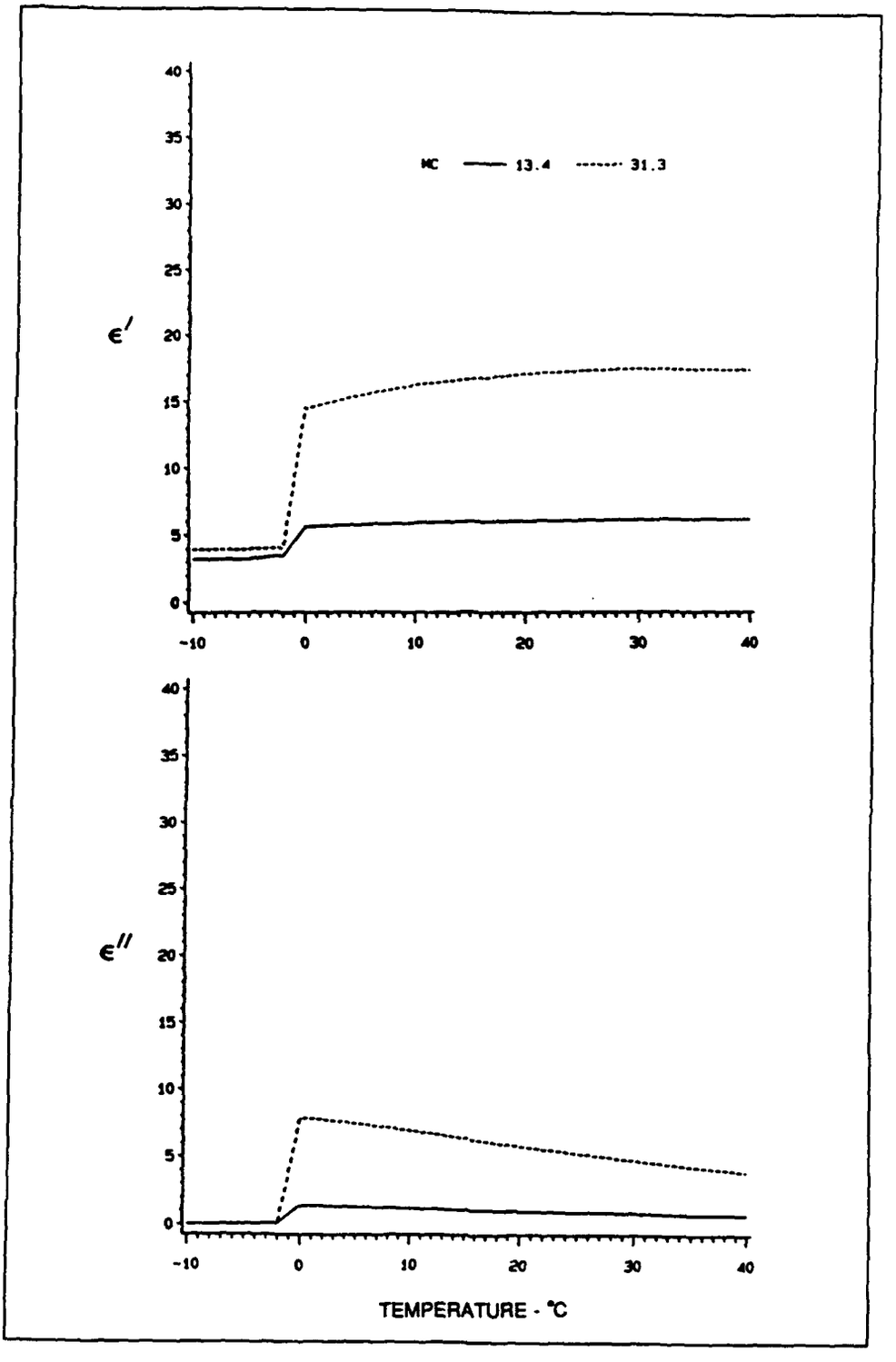

Figure 8. Temperature effects for well-graded sand (8 GHz)

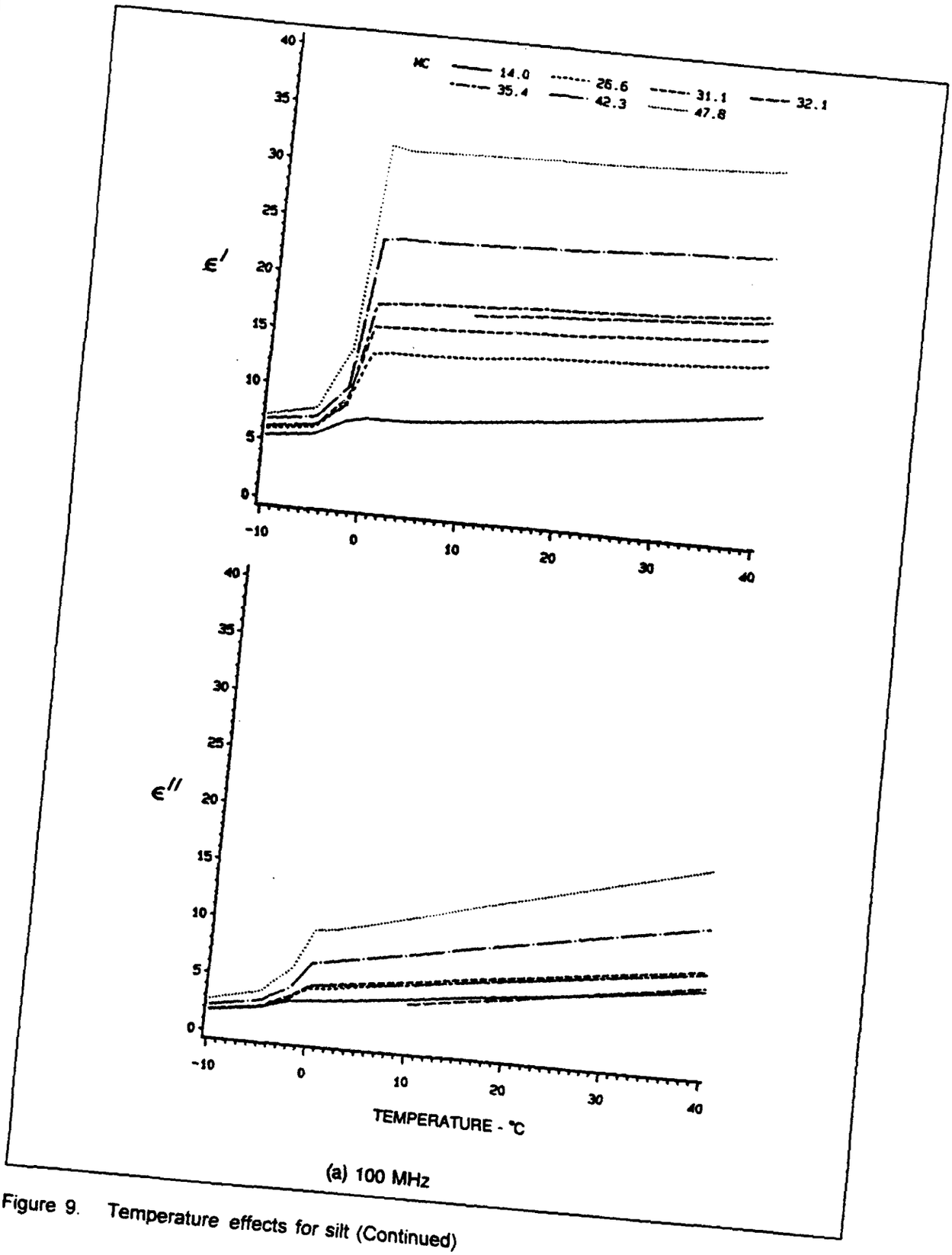

(a) 100 MHz

Figure 9. Temperature effects for silt (Continued)

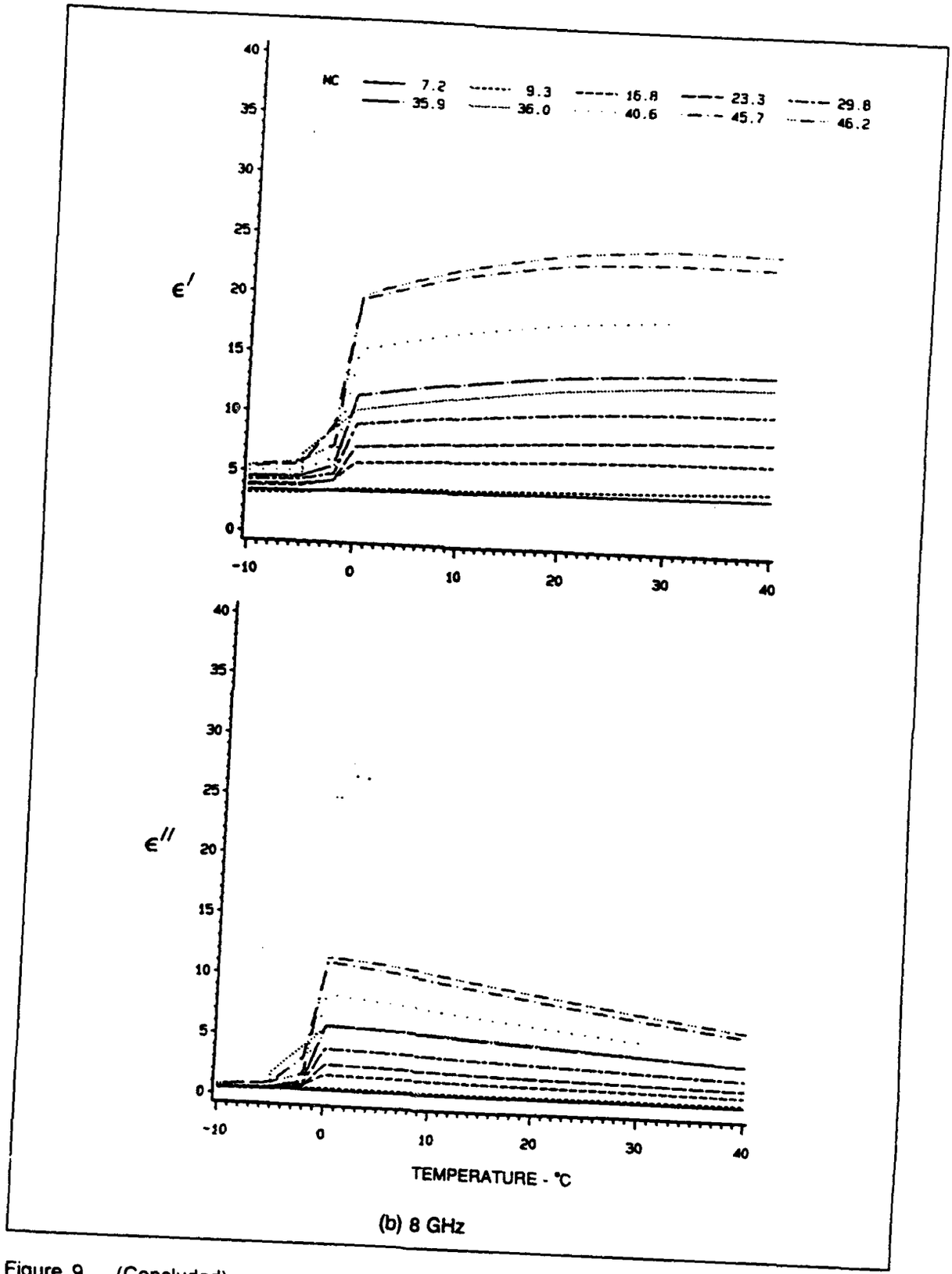

(b) 8 GHz

Figure 9. (Concluded)

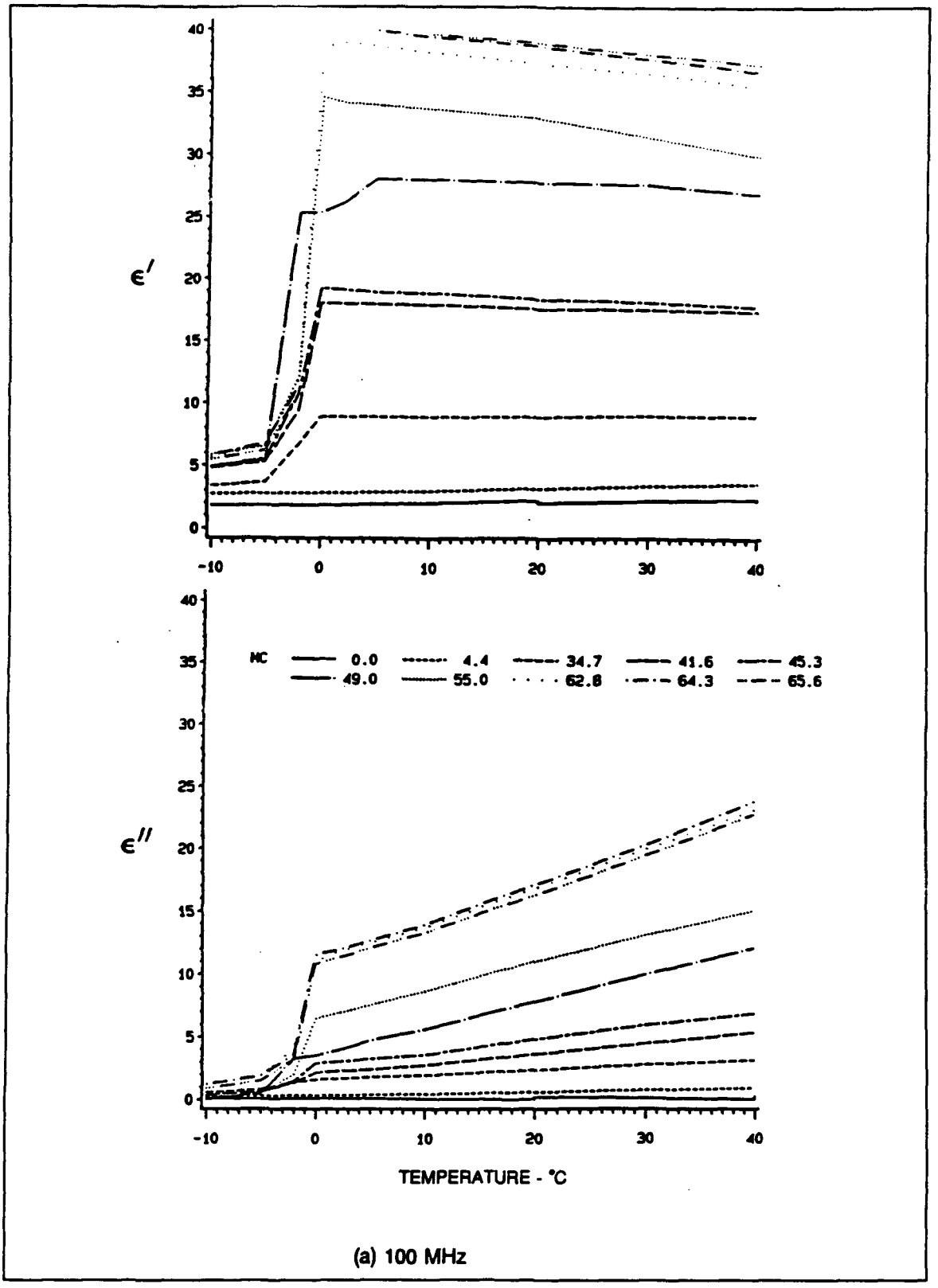

(a) 100 MHz

Figure 10. Temperature effects for kaolinite (Continued)

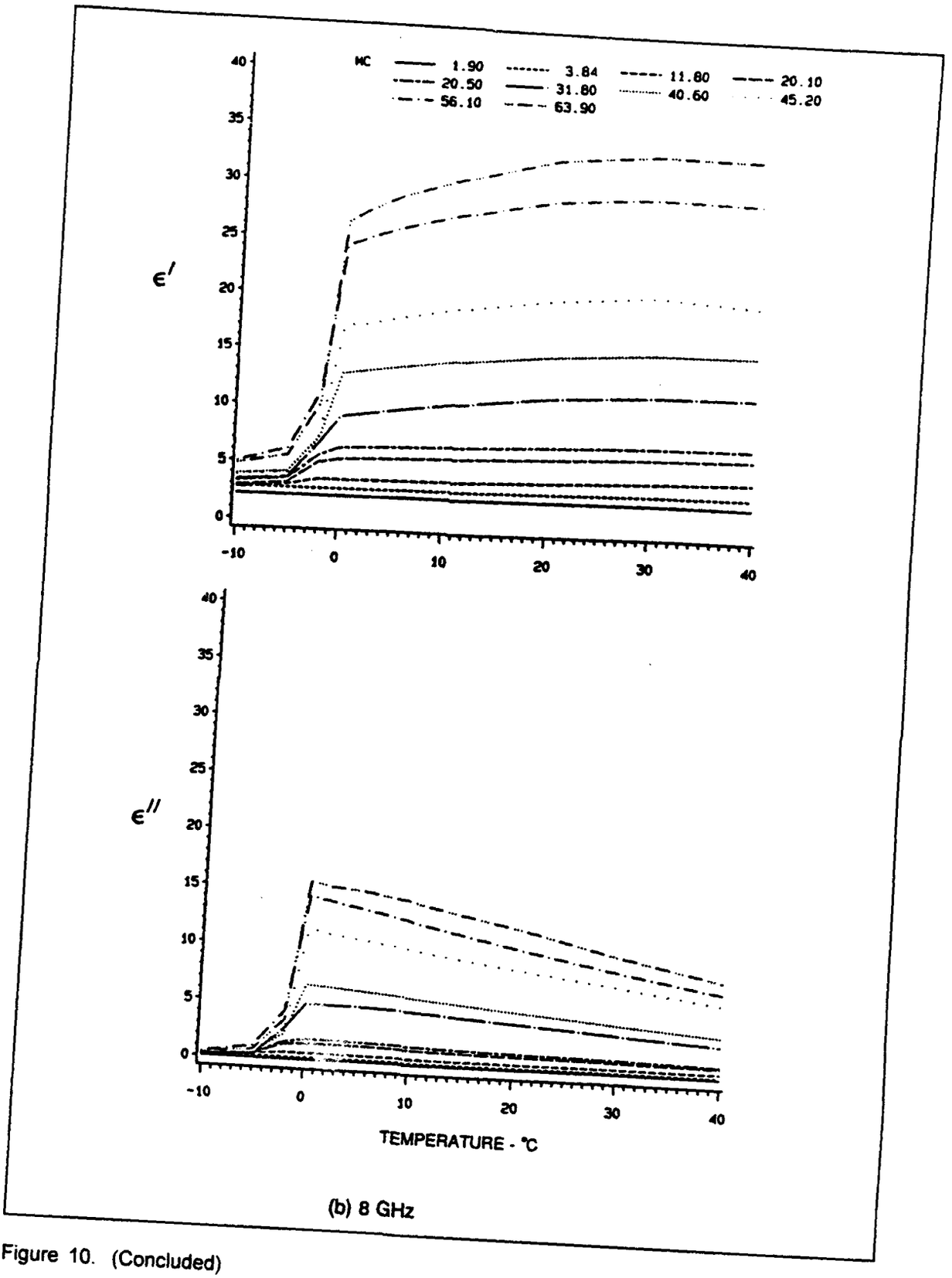

(b) 8 GHz

Figure 10. (Concluded)

R = universal gas constant

T_{Kelvin} = absolute temperature

and the temperature effects data at 100 MHz yields an average (over moisture contents) activation energy of 3.1 Kcal/mole for silt and 3.3 Kcal/mole for kaolinite. These numbers are within the range of values attributed to hydrogen bond breakage.

Moisture effects

Figures 11-14 summarize data at selected frequencies and at +20 °C as a function of volumetric moisture content for each of the materials tested. What can be said immediately from an examination of the data on moist soils presented in this format is the following:

a. The real part of the dielectric constant for all nonfrozen soils is best described by some nonlinear relationship with volumetric moisture. Bilinear fits such as those sketched in on each figure would break at critical values of moisture content in the range of 30 to 35 percent for the silt and clay minerals and in the 10- to 15-percent range for the sands. Wang and Schmugge (1980) reported critical moisture contents in the 20- to 30-percent range for the real soils that they studied.

b. The capacitive nature of nonfrozen soils as reflected in the real part of the dielectric constant varies with soil type.

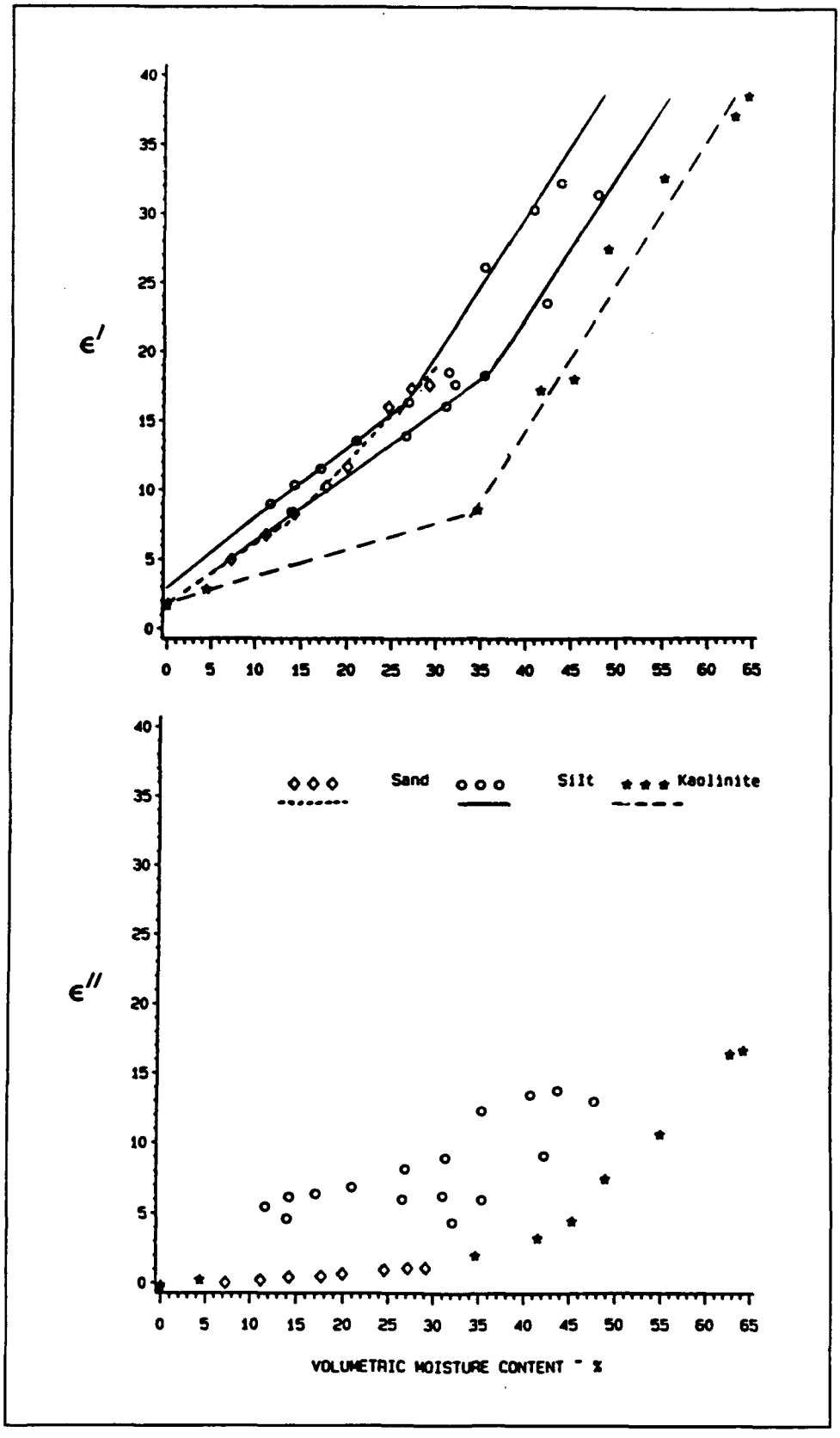

Figure 11. Moisture effects for nonfrozen soils at 100 MHz, 20 °C

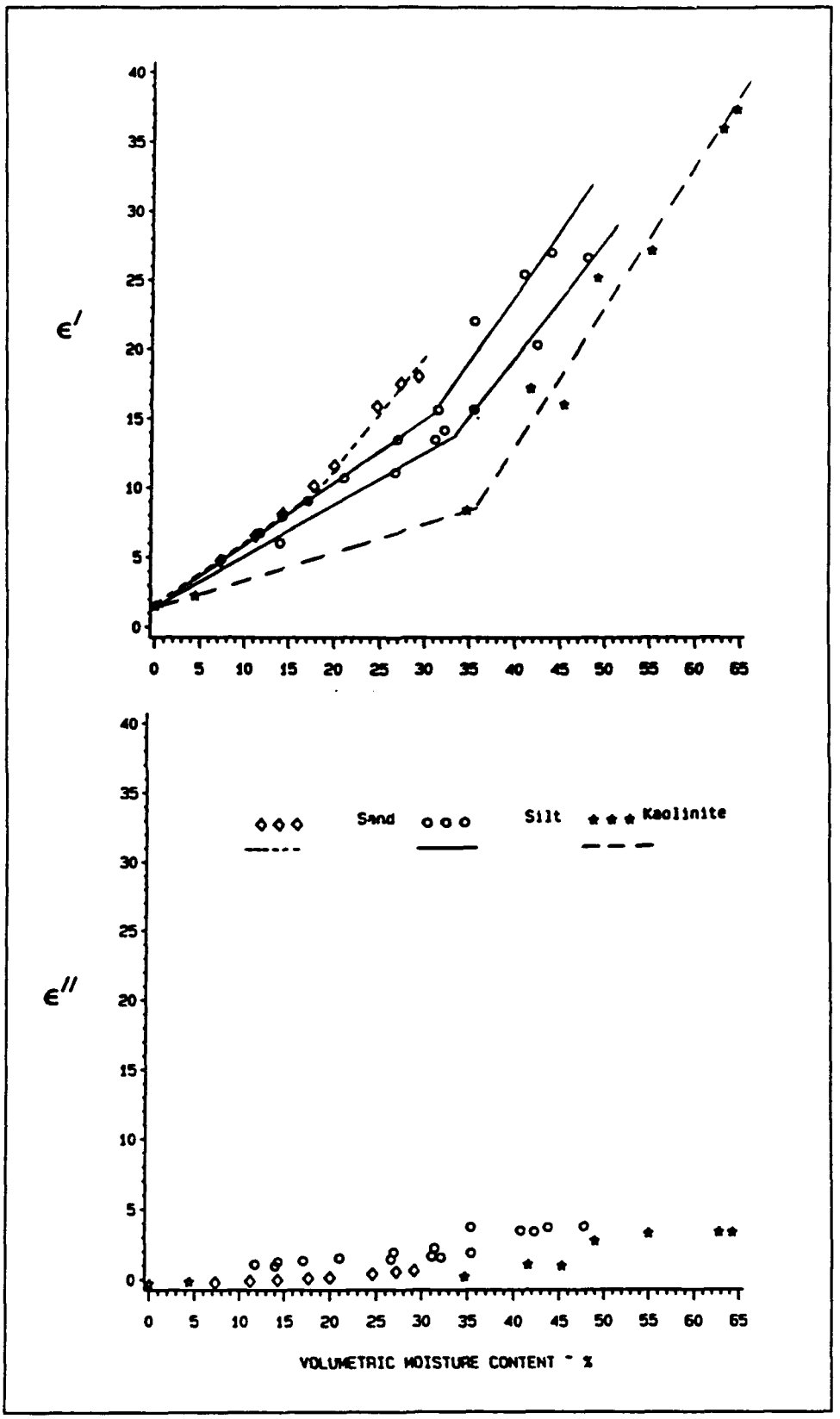

Figure 12. Moisture effects for nonfrozen soils at 800 MHz, 20 °C

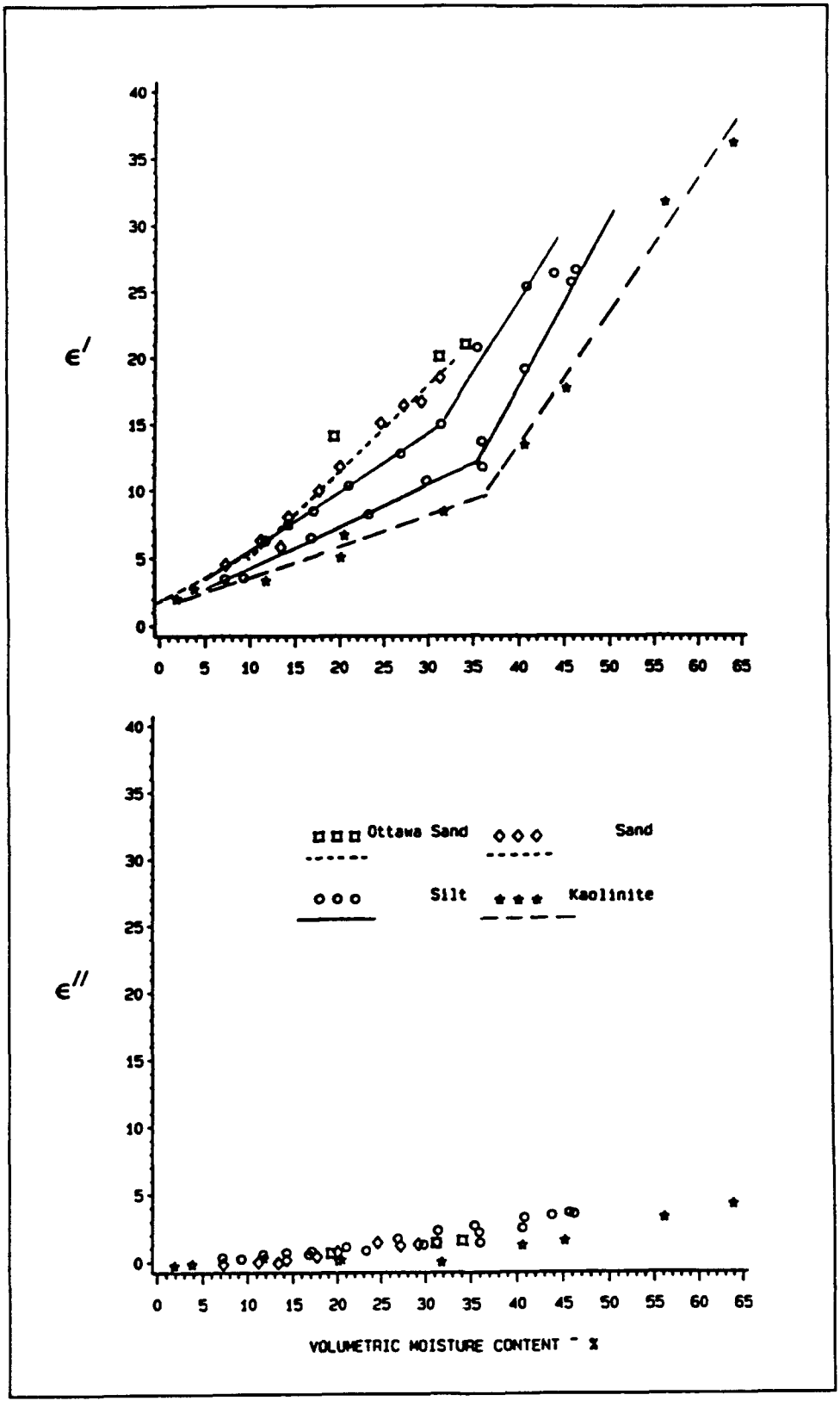

Figure 13. Moisture effects for nonfrozen soils at 2 GHz, 20 °C

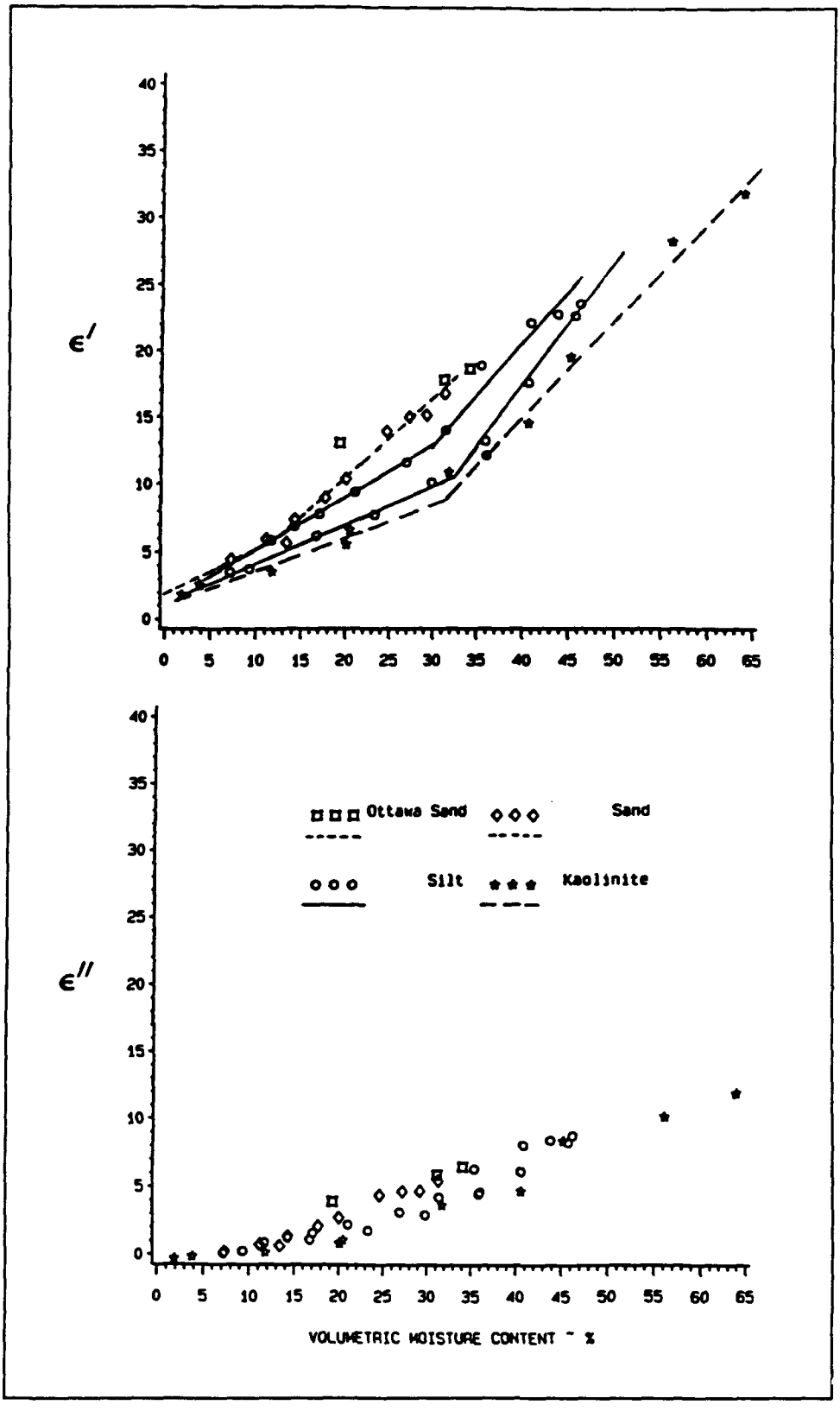

Figure 14. Moisture effects for nonfrozen soils at 8 GHz, 20 °C

3 Equivalent Circuit Modeling

The following paragraphs describe an effort to analytically model the measured soil response through an adaptation of the classical technique of representing the electrical response of an heterogeneous mixture by an equivalent circuit. The models developed here incorporate the concept of series and parallel behavior discussed in Report 1 of this series, as well as a model for water behavior that accounts for dielectric relaxation. The new features of this model are the broad frequency band of simulations through a modification of the equivalent circuit for water and the attempt to fix the values of as many circuit elements as possible while giving physical interpretations to the remaining parameters.

Equivalent Circuit Representation

If one accepts that the electrical response of soil-water mixtures is bounded on the lower end of moisture contents by a "series-like" behavior and on the upper end of moisture contents by a "parallel-like" behavior (Campbell 1988), then the most sensible simulation should include both elements. With the requirement for both series and parallel response, one sound approach to modeling the response of moist soil by the method of equivalent circuits is the three-path model first suggested by Sachs and Spiegler (1964) and adapted by Smith (1971). However, the specific representation used by Smith (see Figure 36 in Report 1) is not adequate to simulate both low-frequency loss mechanisms and losses at higher frequencies due to dielectric relaxation. A variation of the three-path model was adopted for this study using the following reasoning.

Data from the last chapter and from other sources show clearly that the response of moist soils is controlled by the presence of water in the samples. Most of the data show a high-frequency anomalous loss highly correlated with moisture content and a conductivity-like low-frequency loss mechanism. In fact, the data do not say whether the low-frequency losses are due to a conductivity effect in free water or a Maxwell-Wagner mechanism caused by the presence of the soil particles as suggested by many. Lower frequency measurements coupled with a much more thorough understanding or control of the soil chemistry would help answer this last concern. Nevertheless, the best equivalent circuit for the liquid paths has to be one that includes a

high-frequency permittivity, a direct current conductivity, and relaxation losses in the 10- to 20-GHz range of frequency (see Figure 34, Report 1).

As for the contribution by the soil, a good representation for its electrical response is felt to be one that accounts for a constant wave speed at all frequencies while including a low-frequency loss term. Therefore, a parallel circuit (see Figure 30 (b), Report 1) was chosen as the most appropriate representation for the soil component of the mixture. One implication of this selection is that one cannot model anomalous losses within the soil that result from the interaction of the soil and water particles. However, in the range of frequencies covered by these experiments, it is probably not possible to detect the difference in losses because of one mechanism or the other.

Combining these two sets of elements, the final three-path equivalent circuit used to simulate the response of the soils tested in this study is that shown in Figure 15, where the parameters "a," "b," "c," and "d" are weighting constants whose physical significance will be discussed later. A thought process for electing the model parameters is discussed later, and the results of a number of simulations will be shown; but first, a brief presentation of the governing equation for this circuit is given.

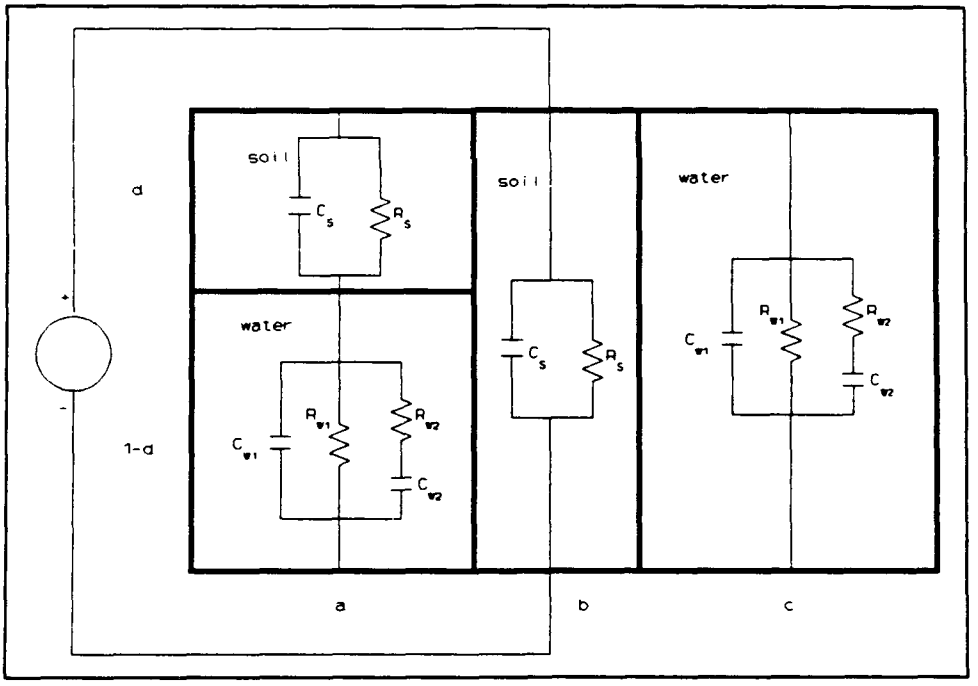

Figure 15. Three-path equivalent circuit used for this study

The macroscopic complex dielectric constant of the moist soil material is modeled as the equivalent capacitance of the circuit shown in Figure 15. Using the *w* subscript for water and the *s* subscript for soil, the macroscopic dielectric properties can be written

$$\varepsilon = \varepsilon' + i\varepsilon'' = a\varepsilon_{s+w} + b\varepsilon_s + c\varepsilon_w \tag{2}$$

where

$$\frac{1}{\varepsilon_{s+w}} = \frac{d}{\varepsilon_s} + \frac{(1-d)}{\varepsilon_w} \tag{3}$$

In terms of the simple circuit capacitances and resistances,

$$\varepsilon_s = \varepsilon'_s + i\varepsilon''_s = C_s + i\frac{1}{\omega R_s} \tag{4}$$

and

$$\varepsilon_w = \varepsilon'_w + i\varepsilon''_w \tag{5}$$

$$= C_{w1} + \frac{C_{w2}}{1 + (\omega R_{w2} C_{w2})^2} + i\left[\frac{1}{\omega R_{w1}} + \frac{\omega R_{w2} C_{w2}^2}{1 + (\omega R_{w2} C_{w2})^2}\right]$$

Parameter Selection and Model Execution

A reasonable set of circuit parameters begins with the same values chosen for water that are shown on Figure 34 of Report 1.

$C_{w1} = 4$

$C_{w2} = 76$

$R_{w1} = 5.888 \times 10^{-8}$ sec/cm

$R_{w2} = 1.25 \times 10^{-13}$ sec/cm

They allow for a dielectric relaxation peak at about 16.75 GHz and for finite values of conductivity losses at frequencies less than 1 MHz. Although the data measured in this study did not go as low as 1 MHz, it was discovered by trial and error that the low-frequency conductivity term helped improve the model's fit to data through its interaction with the soil element response.

As for the soil parameters, a static permittivity C_s was taken to be about 2. That only leaves the soil resistivity R_s to be considered. It so happens that this model allows soil resistivity to be a variable; however, it is rather easy to estimate its range in the following way. The model has associated the low- frequency losses with the soil element. They, in turn, are $1/(\omega R^s)$. A typical value of the loss term is 10 at 2 GHz for wet silt. This leads to an estimate of the resistivity as about 8×10^{-12} sec/cm.

To obtain values of the weighting parameters, "a," "b," "c," and "d," as well as the value of R_s, a simple iterative code was developed that minimized the difference between circuit predictions and real data. Smith (1971) used a similar approach to calculate the parameters associated with his three-path model and hinted that it was a rather sophisticated calculation process. In truth, it is not necessary to do anything more complicated than to increment each parameter of the equivalent circuit (element values and weighting parameters) and to calculate the difference between all data points and predicted values for each parameter change taken one at a time. That parameter increment that caused the greatest reduction in difference was applied at each step. Parameter values were both increased and decreased for each iteration, and the magnitude of these changes were decreased as the model simulation converged.

Smith (1971) also chose to allow all of the parameters in his three-path model to vary except for the permittivity of water. In this model, most of the electrical parameters were fixed because they have physical meaning. The permittivities selected for both the water element and the soil element reflect observed values that are associated with wave velocity in each media. The value of resistivity in the water element that results in the high frequency anomalous behavior was selected to properly locate the peak losses due to dielectric relaxation. In the absence of data at higher frequencies, the frequency of peak loss was taken to be constant for all moisture contents. The soil resistivity was allowed to be variable to help optimize the fits to low-frequency loss data.

Simulation Results

Figures 16-18 contain a comparison of model fits to real data for tan sand, silt, and kaolinite samples at three different volumetric moisture conditions. Besides demonstrating the ability to simulate the real response of the soil samples quite well, it is gratifying to note sensible trends in the weighting parameters. Obviously, as moisture levels rise, the contribution to sample response from the parallel (or long-range connectivity) water element should increase as reflected in an increase in the parameter "c." Because water dominates the electrical response, the soil-related parameter "b" should drop as moisture increases. Similarly, if the series elements can account for Maxwell-Wagner like behavior in the soil-water-air mixture, then it is also sensible for the losses contributed by the soil particles in the presence of an

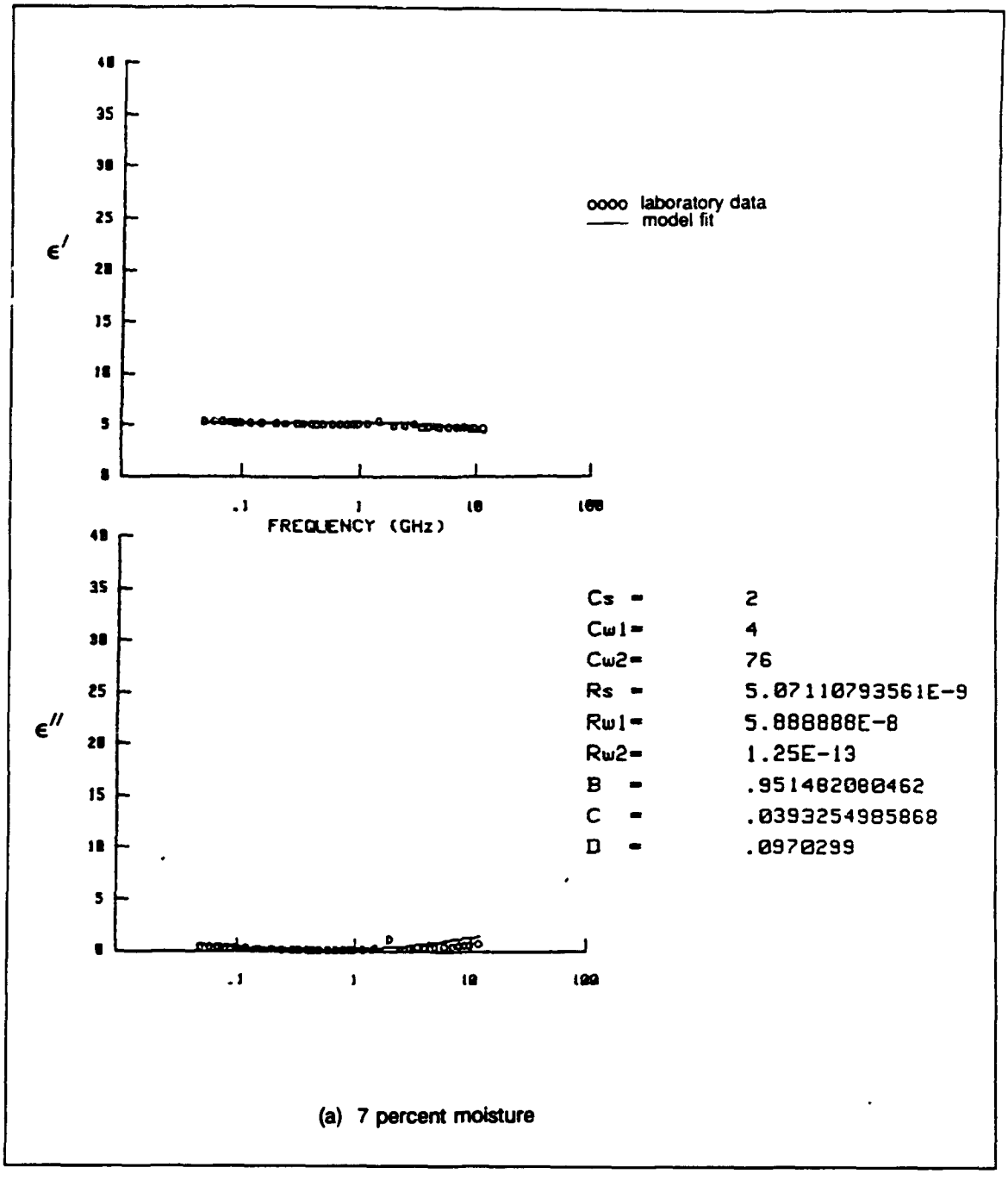

(a) 7 percent moisture

Figure 16. Equivalent circuit model-data comparisons for tan sand (Sheet 1 of 3)

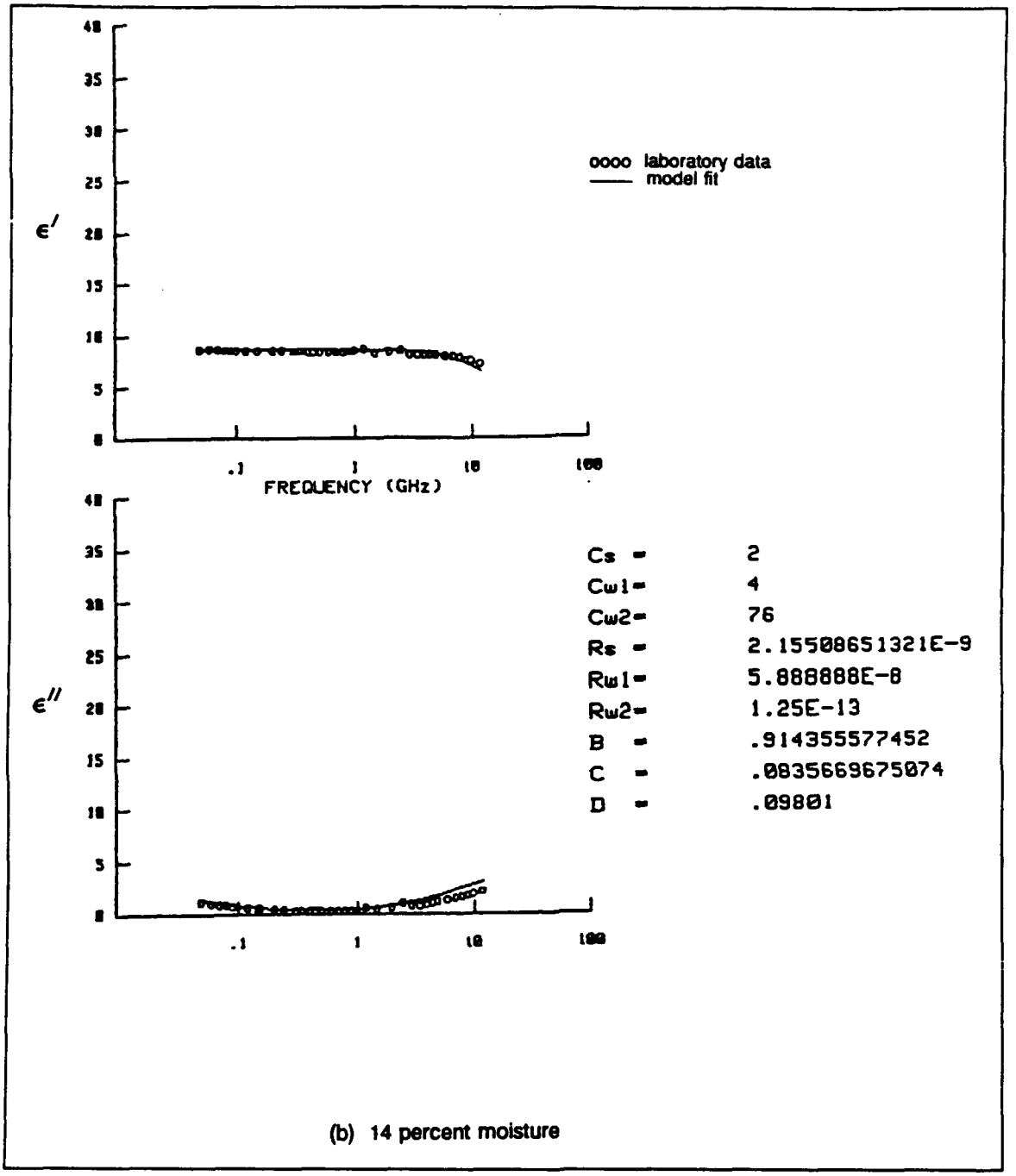

(b) 14 percent moisture

Figure 16. (Sheet 2 of 3)

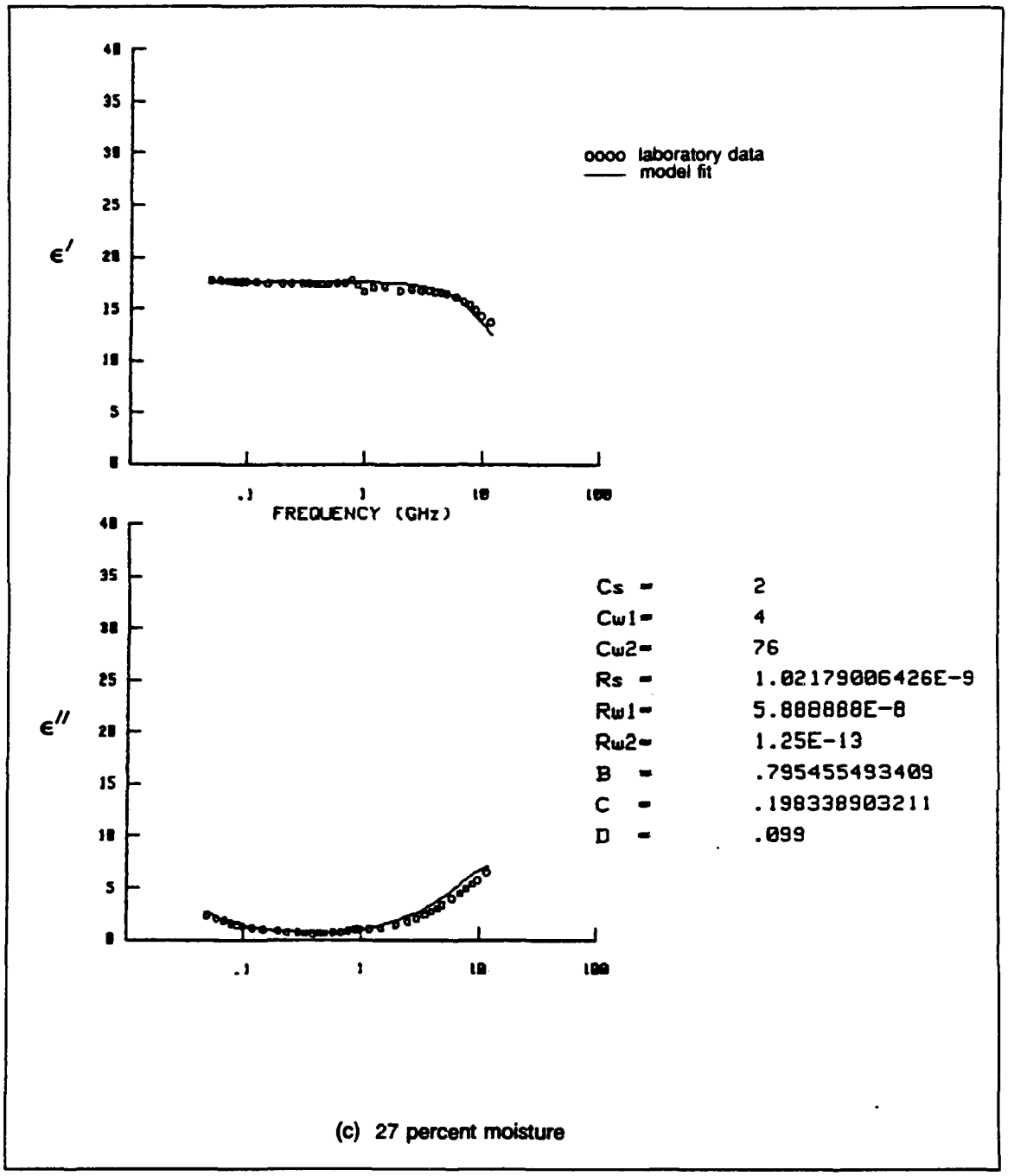

(c) 27 percent moisture

Figure 16. (Sheet 3 of 3)

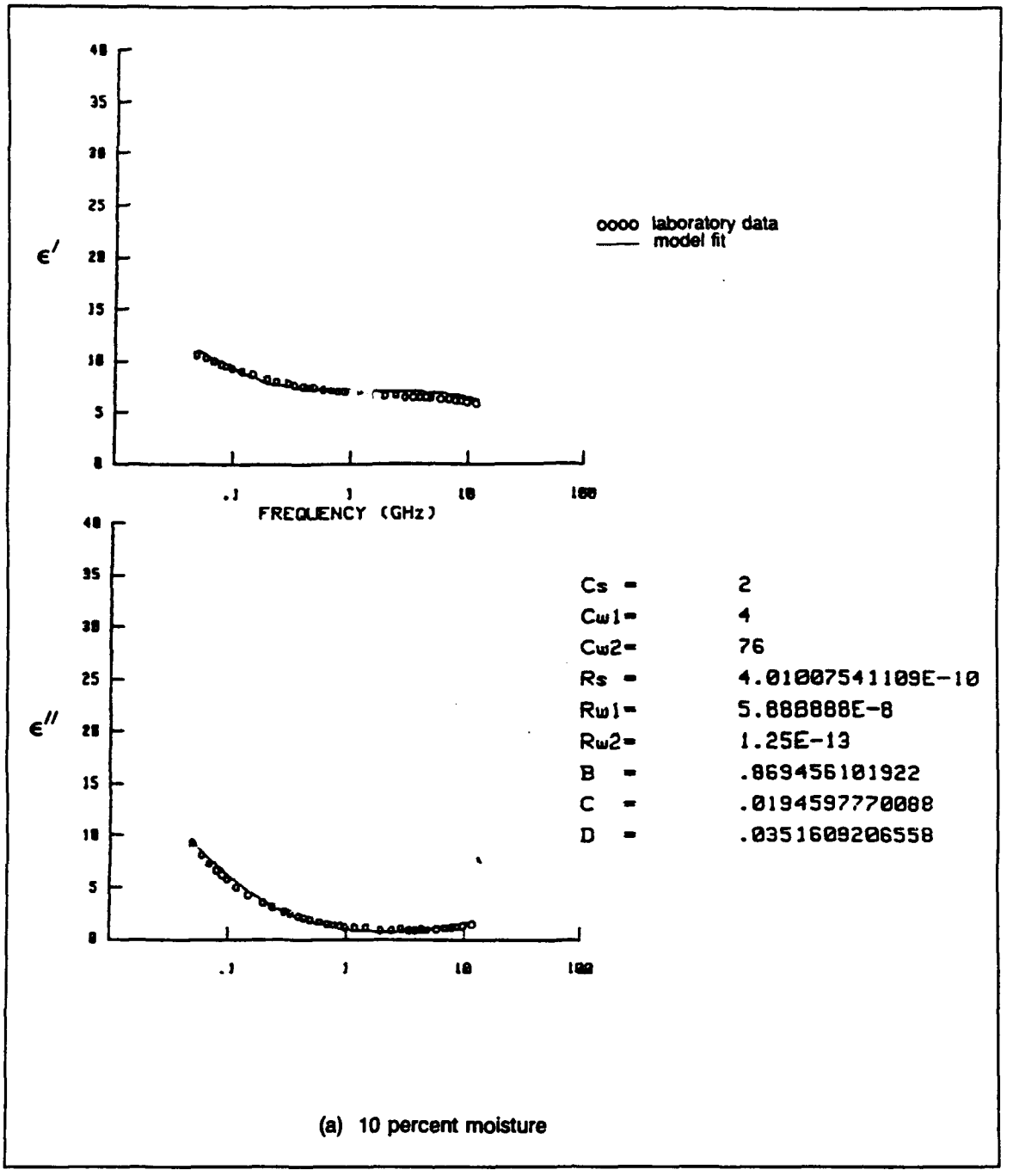

(a) 10 percent moisture

Figure 17. Equivalent circuit model-data comparisons for silt (Sheet 1 of 3)

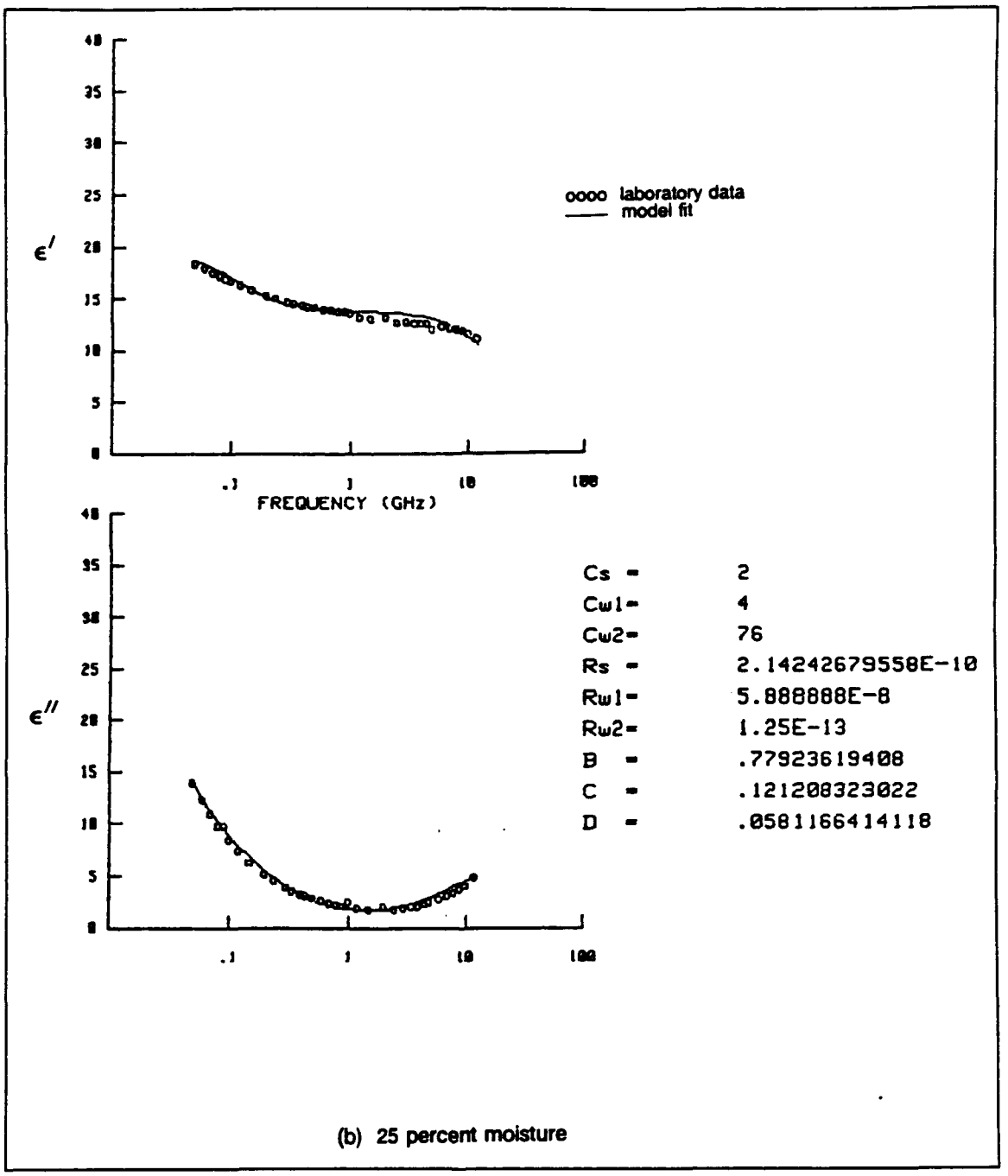

(b) 25 percent moisture

Figure 17. (Sheet 2 of 3)

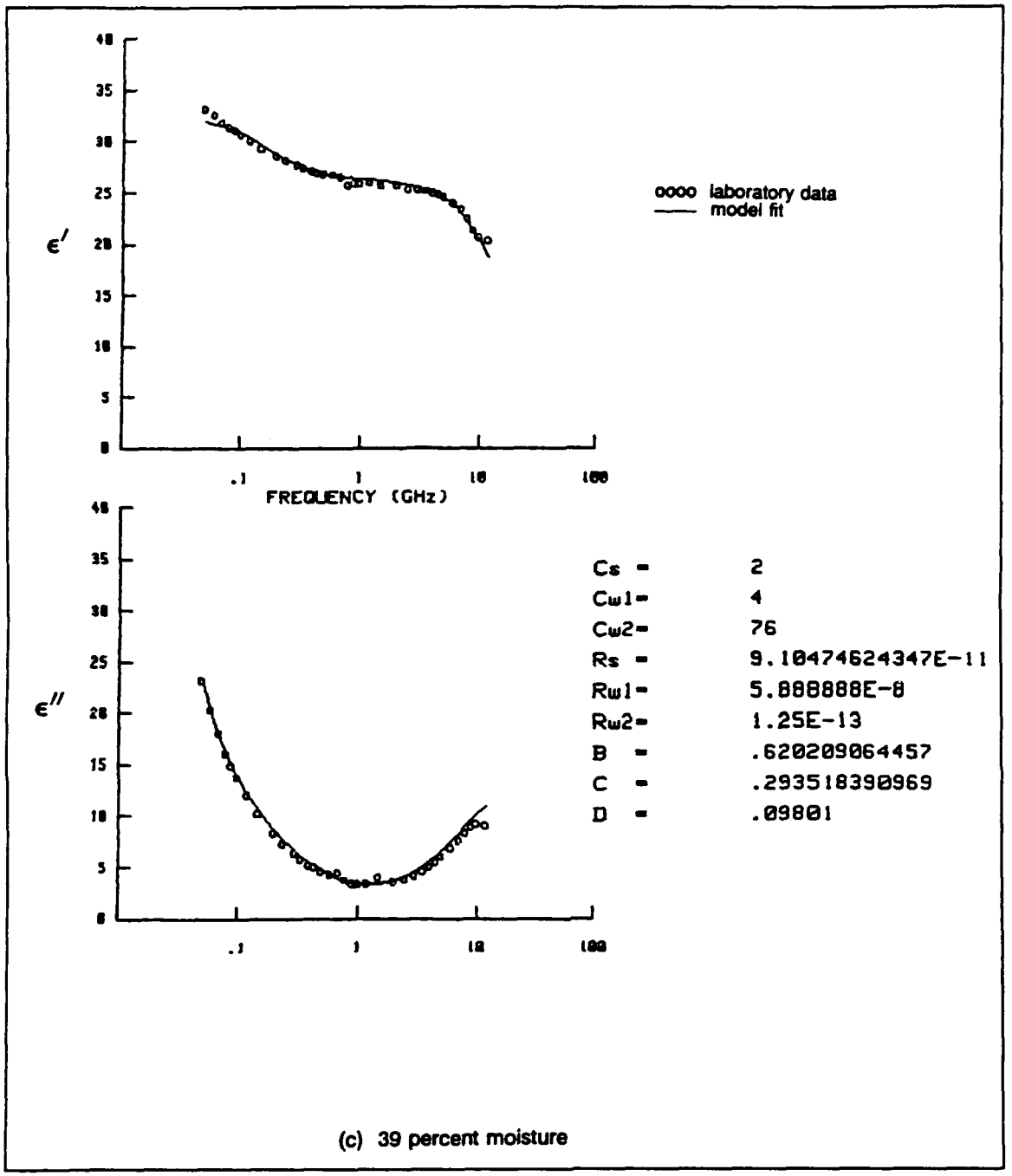

(c) 39 percent moisture

Figure 17. (Sheet 3 of 3)

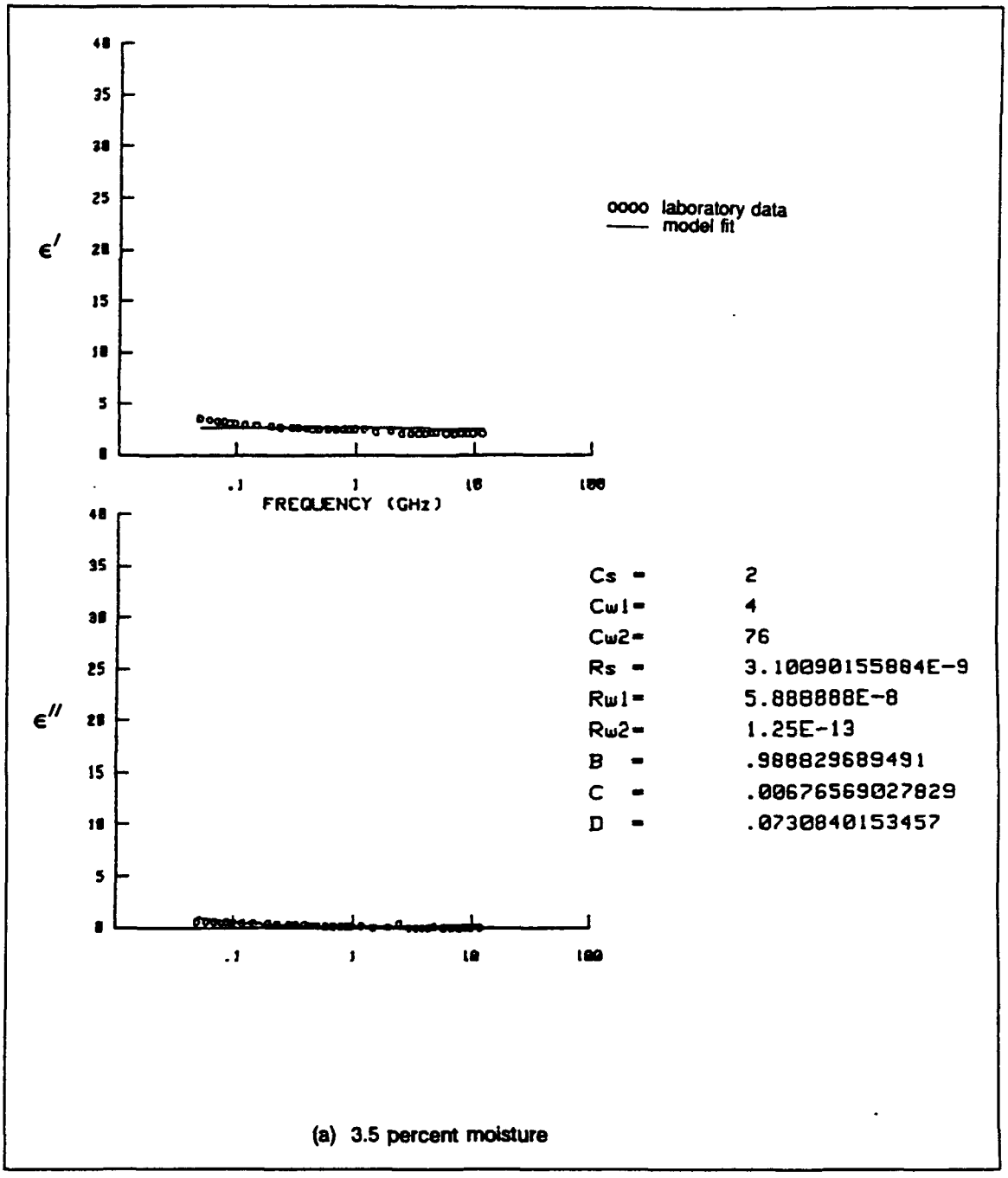

(a) 3.5 percent moisture

Figure 18. Equivalent circuit model-data comparisons for clay (Sheet 1 of 3)

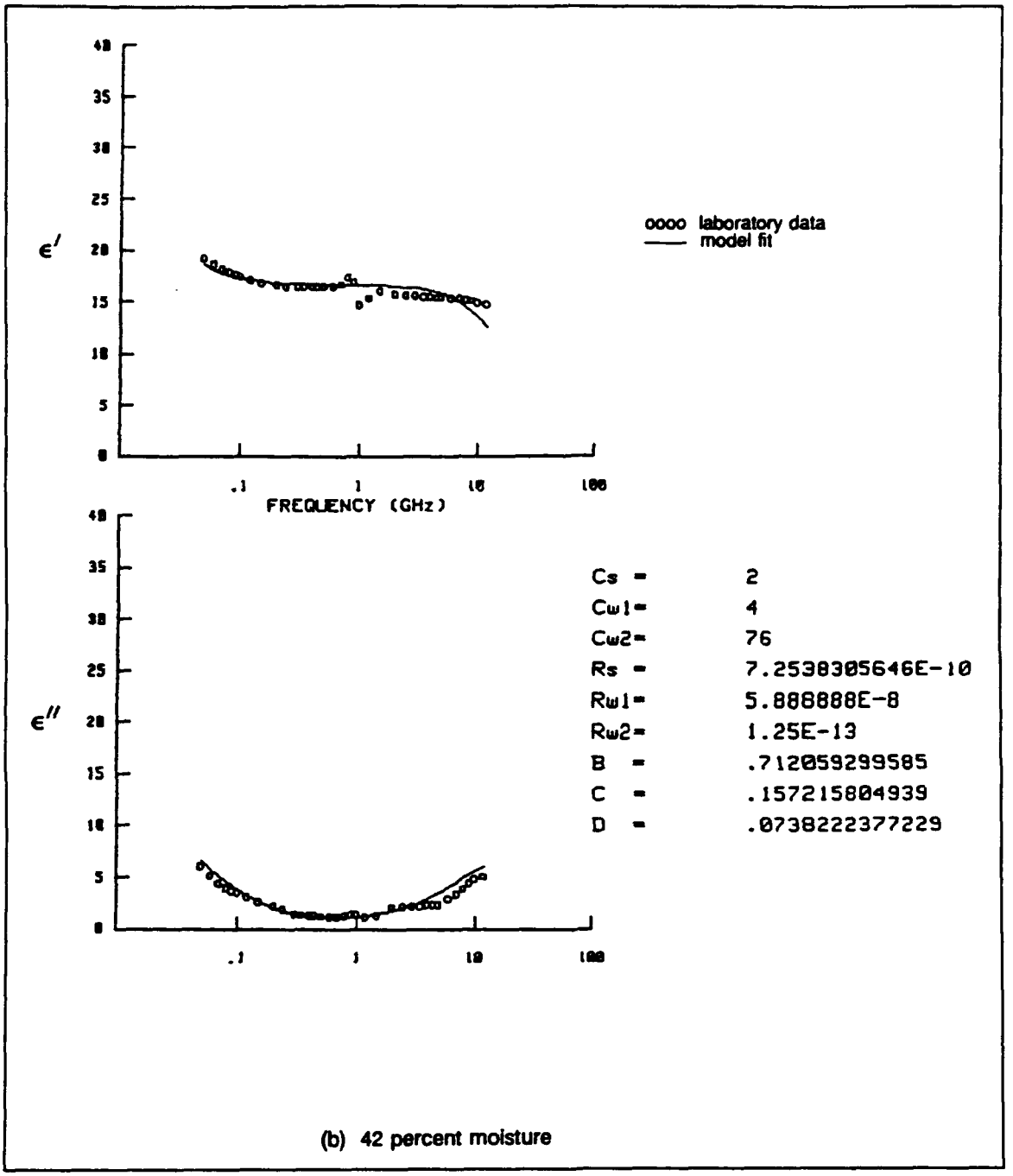

(b) 42 percent moisture

Figure 18. (Sheet 2 of 3)

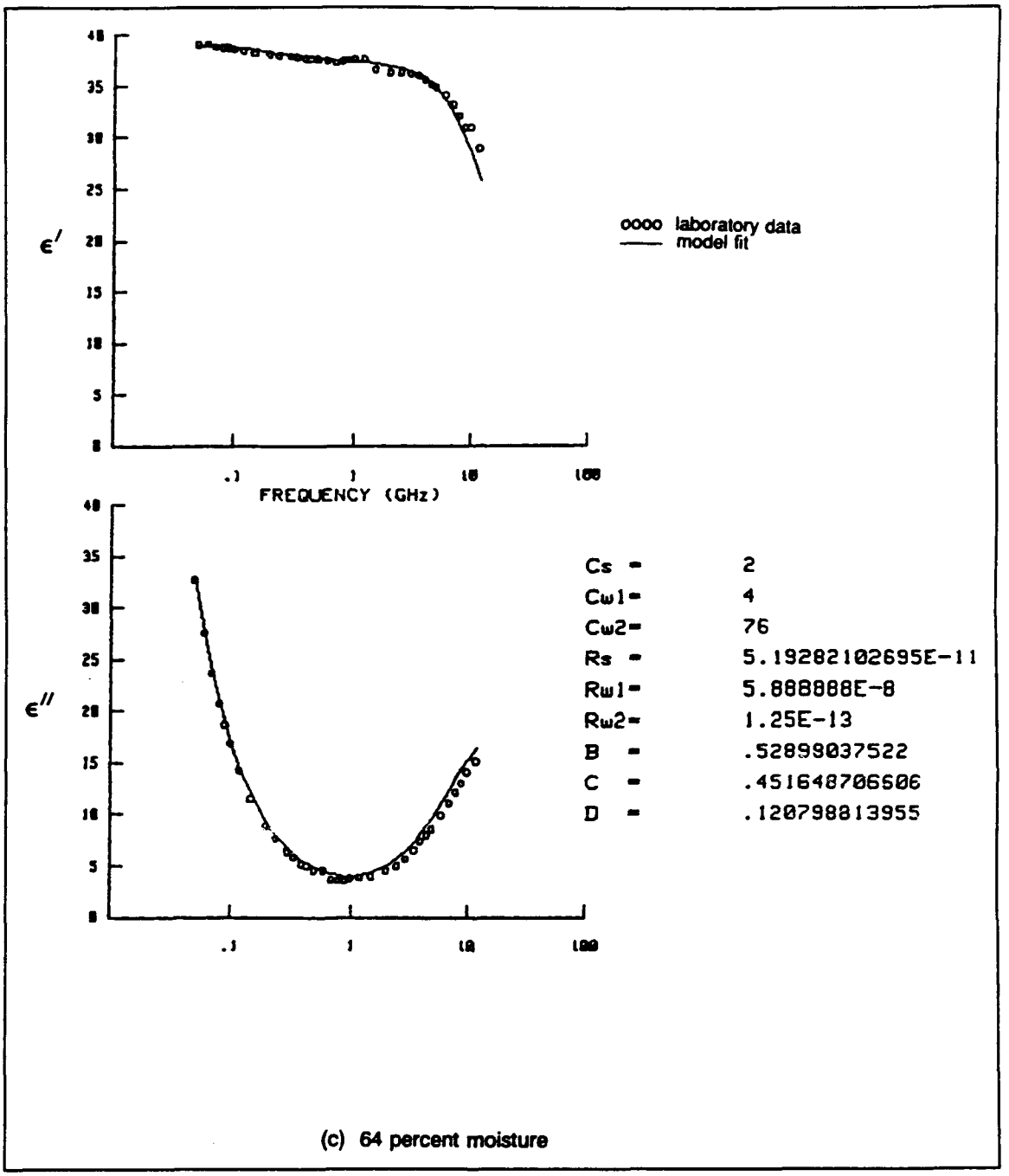

(c) 64 percent moisture

Figure 18. (Sheet 3 of 3)

increasing amount of water to increase as well. This would be reflected in an increase in the parameter "d" that, in general, is observed.

While the arrangement of elements in the three-path model is physically reasonable and the simulations are very accurate, a number of questions concerning its application remain unanswered. For example, when does one hold circuit element parameter values constant, and, if not, how should those parameters be allowed to vary? It might seem preferable, at first thought, to hold all circuit element values fixed and allow only the weighting constants to vary. In fact, this approach was tried, but with only limited success. If only the weighting coefficients could vary, then they would have to account for all of the dramatic changes that take place chemically within the mixture, and they do not appear to be able to do so. In other words, by allowing only weighting coefficients to change implies that the properties of the basic constituents do not change as the mixture changes. Even if the selected parameters for dry soil particles and unbound liquid water are quite accurate, weighting parameters, by themselves, cannot be expected to account for the loss mechanisms because of bound water or because of Maxwell-Wagner type effects, or enhanced conductivity because of salts going into solution, or enhanced capacitive response set up by the parallel plate-like structure of the clay particles being filled by water in the interlayer spaces or simply between particles in nonswelling clays.

If, then, some of the circuit parameters are allowed to vary, which ones should? Why let the resistivity of the soil element vary and not the water? A number of simulations were tried with R_s fixed and R_{wf} free. These results were unsatisfactory for the mixtures that showed increasing ε' values with decreasing frequency, with the simulation values of ε' becoming constant with decreasing frequency.

In summary, the three-path equivalent circuit is a promising tool for exploring the complex dielectric behavior of heterogeneous mixtures. Simulations done in this study very accurately reproduce measured responses. The model accounts for both series and parallel electrical responses and possesses some parameters that can be fixed to values measured in other experiments. There are still, however, unresolved issues such as what physical or chemical properties can be associated with the parameters that do vary. These issues should provide a rich opportunity for further research.

4 Fractal Geometry Model and Critical Water Content

Another analysis technique used in this study involves the application of fractal geometry (Appendix B) to model the structure of the porous media and to associate a change in the fractal dimension with the onset of long-range connectivity. While this model has been used in basic research on the properties of coal, this is its first application to soils. The proposed hypothesis is that the soil moisture content, or cumulative pore volume, at the limit of fractal behavior is equivalent to the critical moisture that defines a transition from series to parallel electrical response. This hypothesis was tested and yielded fractal dimensions for the soils tested within this study that are supported by other references.

Campbell (1988) suggested that water may fill the pore spaces of a soil sample in a fractal manner. Pursuit of this concept, particularly as it relates to the distribution of pore sizes in a soil sample, has led to the discovery of related research in pore-size distributions (Sridharan, Altschaeffl, and Diamond 1971; Arya and Paris 1981) and in the modeling of porous media as fractal geometries (Friesen and Mikula 1987) that lends itself to a relatively simple fractal interpretation of pore-size distribution data. The difference between the following study and Campbell's model is that rather than assuming pore-filling water clusters have a fractal geometry, this new approach models the soil structure, itself, using fractal concepts and makes certain assumptions to relate volumetric soil moisture content to the fractal model behavior.

Fractal Model of Pore-Size Distribution

The porous soil-water-air structure can be described as a sponge-like structure similar to that shown in Figure B3. Much of what follows has been adopted from Friesen and Mikula (1987), where additional references are given to some earlier work. Their application was toward a better way of quantifying the porous structure of coal.

Consider, first, a unit solid cube of soil minerals. Divide the cube equally into subcubes of size d = 1/m. Next, remove the subcubes necessary to give the basic structure generator shape. (In the case of the Menger sponge shown in Figure B3, m = 3, and the number of subcubes removed is 7.) That leaves a number of remaining cubes = N_c. But by the definition of fractals given in Equation B2,

$$N_c = (d)^{-D} \tag{6}$$

where D is the fractal "dimension" of the porous media. Now repeat the entire process on each subcube. After this second step, the new subcubes have a dimension of d^2 and the number of remaining subcubes is N_c^2. Continuing to the *kth* subdivision, there is a particle size of d^k and the number of remaining subcubes is N_c^k. In other words, the volume of remaining solid material at step k is

$$V_k = (N_c)^k (d)^{3k} = (d)^{-Dk}(d)^{3k} = (d)^{k(3-D)} \tag{7}$$

Noting that at each step, the particle size is identical to the smallest pore size, and renaming the particle size $(d)^k$ as l_k,

$$V_k = (l_k)^{3-D} \tag{8}$$

and the pore volume is just

$$V_{pore} = 1 - (l_k)^{3-D} \tag{9}$$

What one now has is a fractal model for a porous medium that relates pore volume (which has to be related to moisture content) and pore size. The fractal dimension of the porous media can be calculated by plotting the slope of the distribution versus pore size on a log-log plot:

$$\log\left[\frac{dV_{pore}}{dl}\right] = constant - (2-D)\log(l) \tag{10}$$

Fractal Model and Pressure Plate Data

Unfortunately, simple pore-size distribution data do not exist. What is available is a limited amount of porosimetry and/or pressure plate data that can be interpreted as pore distribution data through the capillary relationship (Bear and Verruijt 1987)

$$p = -\frac{4\delta}{D}\cos(\theta) \tag{11}$$

where

p = equilibrium pressure

δ = surface tension of nonwetting fluid

θ = contact angle between fluid meniscus and pore surface

D = capillary diameter

Substituting the capillary relationship into the fractal model for pore distribution,

$$V_{pore} = 1 - \left[-\frac{K}{p}\right]^{3-D} = 1 - K' p^{D-3} \tag{12}$$

where K and K' represent a lumping of constants. Then

$$\frac{dV_{pore}}{dp} = -K'(D-3)p^{D-4} \tag{13}$$

from which

$$\log\left[\frac{dV_{pore}}{dp}\right] = constant - (D-4)\log(p) \tag{14}$$

Therefore, the slope of a log-log plot of the derivative of a porosimetry or pressure plate curve is proportional to $D - 4$.

As a test of this relationship, real pressure plate data from Arya and Paris (1981) for five different soil samples were digitized, their slopes estimated

by difference methods, and the results plotted on Figure 19. In general, these curves reveal a bilinear response with the break point occurring at approximately the field capacity of 0.333 bars. The field capacity is associated with the amount of water that would drain from a soil sample due to gravitational forces only. At pressures higher than field capacity but less than 15 bars, which soil scientists refer to as the wilting point (Wang and Schmugge 1980), a straight line fit to the data on Figure 19 would result in a fractal dimension for the soil structure of approximately 2.67. The break in the slope of these data roughly corresponds to volumetric moisture contents of 25 to 40 percent.

An interesting question is whether or not one might be able to predict these observed moisture contents from ancillary data. For example, if the fractal behavior of the soil is, in fact, associated with water being held by capillary forces, then the field capacity can be identified with a certain pore diameter through the capillary equation. Taking conditions for pure water and clean glass (contact angle equal zero degrees and surface tension equal to 72 dynes/cm at 25 °C) as an approximation for the elements in moist soil, one can calculate from the capillary equation that the range of pressures from infinity to field capacity cover a range of pore diameters up to about 8 μm. Furthermore, if one assumes, as did Campbell (1988), that the smallest pores in soil fill first with water, then one could always estimate the moisture content below which the soil structure can be modeled as fractal in the following way. First of all, by definition

$$M_v = \frac{V_w}{V_t} = \left(\frac{V_v}{V_t}\right)\left(\frac{V_w}{V_v}\right) = n \cdot S \qquad (15)$$

where

M_v = volumetric moisture content

V_w = volume of water in a sample

V_t = total volume of the sample

V_v = volume of voids in a sample

n = sample porosity

S = degree of saturation of sample

But the sample porosity can be rewritten in terms of sample dry density ρ_d and particle density ρ_p, and the degree of saturation is (under the pore-filling assumptions) just the integral of the pore distribution curve from zero volume to the cumulative volume associated with the particular pore diameter.

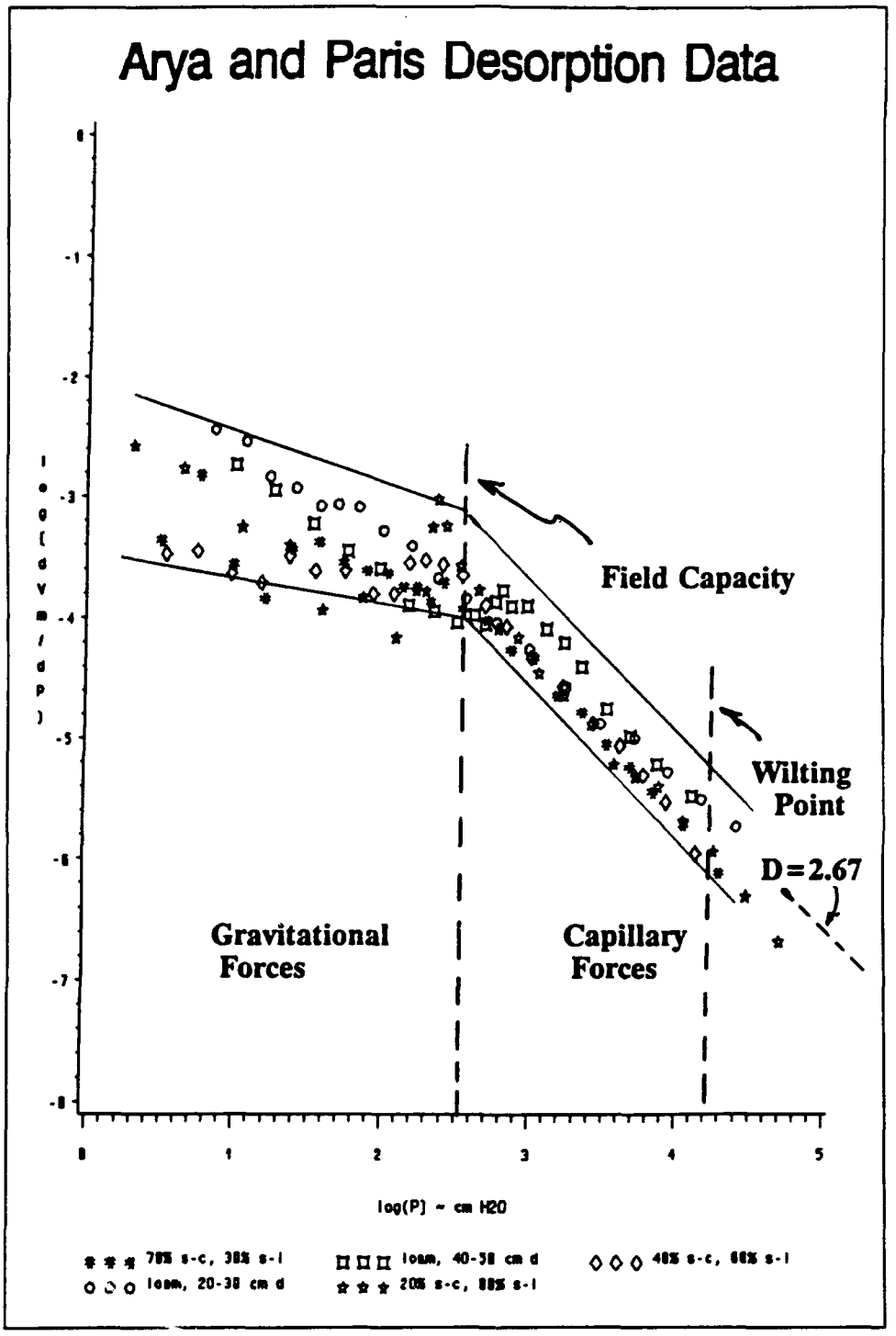

Figure 19. Fractal model applied to real soil desorption data (after Arya and Paris (1981))

The cutoff value of volumetric moisture content for fractal soil structure response can then be written simply as

$$\left(M_v\right)_{fractal} = \left(1 - \frac{\rho_d}{\rho_p}\right) S_8 \tag{16}$$

where S_8 refers to the degree of saturation (or the decimal value of cumulative pore volume) at the 8-μm mark on a pore-size distribution curve.

In summary, then, if one assumes that soil fills with water beginning with the smallest pores, and if one accepts the small-pore fractal model, then the moisture content below which the soil possesses a fractal structure can be estimated from the sample dry density and cumulative pore volume given by the 8-μm pore diameter mark on the pore-size distribution curve.

Fractal Model Related to Particle-Size Distribution Data

In the absence of porosimetry and pressure plate data (which is the case for this research), it would be advantageous to estimate pore volume distributions from other measurements that are more readily available.

At least one simple model for pore distributions does exist; namely, the physicoemperical model offered by Arya and Paris (1981). Their research centered on the need for a model to predict soil moisture characteristics from simple data like particle-size distributions and bulk (dry) density, and their key assumptions were as follows:

a. The particle-size distribution curve can be broken into segments covering a small range of diameters, and the solid fraction within each segment, or particle-size range, has a bulk density equal to that of the natural-structure sample.

b. Each solid fraction consists of uniform-size spheres having the mean radius of the fraction.

c. The pores in each segment are uniform-size cylindrical capillary tubes whose radii are related to the mean particle radius for that segment.

If there are n_i spherical particles of size R_i in the ith particle-size segment of the distribution curve (the following relationships assume that one has a unit mass of solid material; i.e., $\Sigma W_i = 1.0$), then

$$V_{p_i} = n_i \frac{4\pi R_i^3}{3} = \frac{W_i}{\rho_p} \tag{17}$$

where

V_{pi} = solid volume of the ith fraction per unit sample mass

W_i = solid mass/unit sample mass in the ith fraction, which comes from the particle-size distribution curve

ρ_p = particle density

Arya and Paris then let the total pore volume for the ith fraction be represented by a single pore of radius r_i and length h_i that threads the volume occupied by the particle-size fraction. Thus

$$V_{v_i} = \pi r_i^2 h_i = \left[\frac{W_i}{\rho_p}\right] e = n_i \frac{4\pi R_i^3}{3} e \tag{18}$$

where

V_{vi} = void volume of the ith particle-size fraction per unit sample mass

e = void ratio
= volume voids/volume solids

Not knowing exactly how this single pore threads the mass of spherical particles, Arya and Paris assumed that the total pore length would be something greater than $n_i 2R_i$ and introduced an empirical factor α defined by

$$h_i = n_i^{\alpha} 2R_i \tag{19}$$

Combining Equations 18 and 19, one arrives at their final relationship between pore radius and particle radius in the ith particle-size fraction

$$r_i = R_i \left[\frac{2e n_i^{(1-\alpha)}}{3}\right]^{1/2} \tag{20}$$

where n_i comes from Equation 17 and the manner in which the particle-size distribution curve gets subdivided.

One now has a model for deriving pore-size distributions from particle-size distributions, densities, and an emperical parameter associated with soil texture. But how can one relate this new information to soil moisture contents? The answer lies in assuming that the smallest pores first fill with water followed by larger and larger voids. Hence, a volumetric water content can be calculated by summing the void volume fractions identified above:

$$\theta_{v_i} = \sum_{j=1}^{i} V_{v_j} \rho_b \tag{21}$$

where

ρ_b = the sample bulk density

At the ith particle-size fraction, the capillary suction comes from Equation 11. Thus one has a model for soil tension versus volumetric water content. Arya and Paris exercised this model for several soils and adjusted the empirical parameter α for each to give the best fit to the experimental data. For five different soils, the best fit values of α ranged from 1.35 to 1.39.

In summary, given some knowledge of the α parameter that first appears in Equation 19, a model exists for converting a particle-size distribution curve into a pore-size distribution curve and an opportunity is presented to apply the fractal geometry model and compute a critical volumetric moisture content, below which the soil structure can be taken as a fractal geometry.

As a test of this model, consider its reapplication to the data that Arya and Paris provided in their report. Figures 20 to 24 contain a reproduction of their particle-size distribution curves for five of the soils and soil mixtures that they studied along with a pore-size distribution deduced from their soil tension data using the standard capillary relationship. The contact angle was taken to be zero degrees, and the surface tension for pure water against clean glass at 25 °C was used to convert pressure data to pore diameters. Maximum volumetric moisture (100 percent saturation) was taken to be defined by the dry density of the sample as before. The solid line on each figure is the particle-size distribution curve, and the dashed line is the pressure-plate derived pore-size distribution. The open circles on the curves represent the results of calculating a pore-size distribution curve using the model above.

Other than the large pore-size discrepancy for the sample shown in Figure 24, the two techniques for calculating pore-size distributions (one from

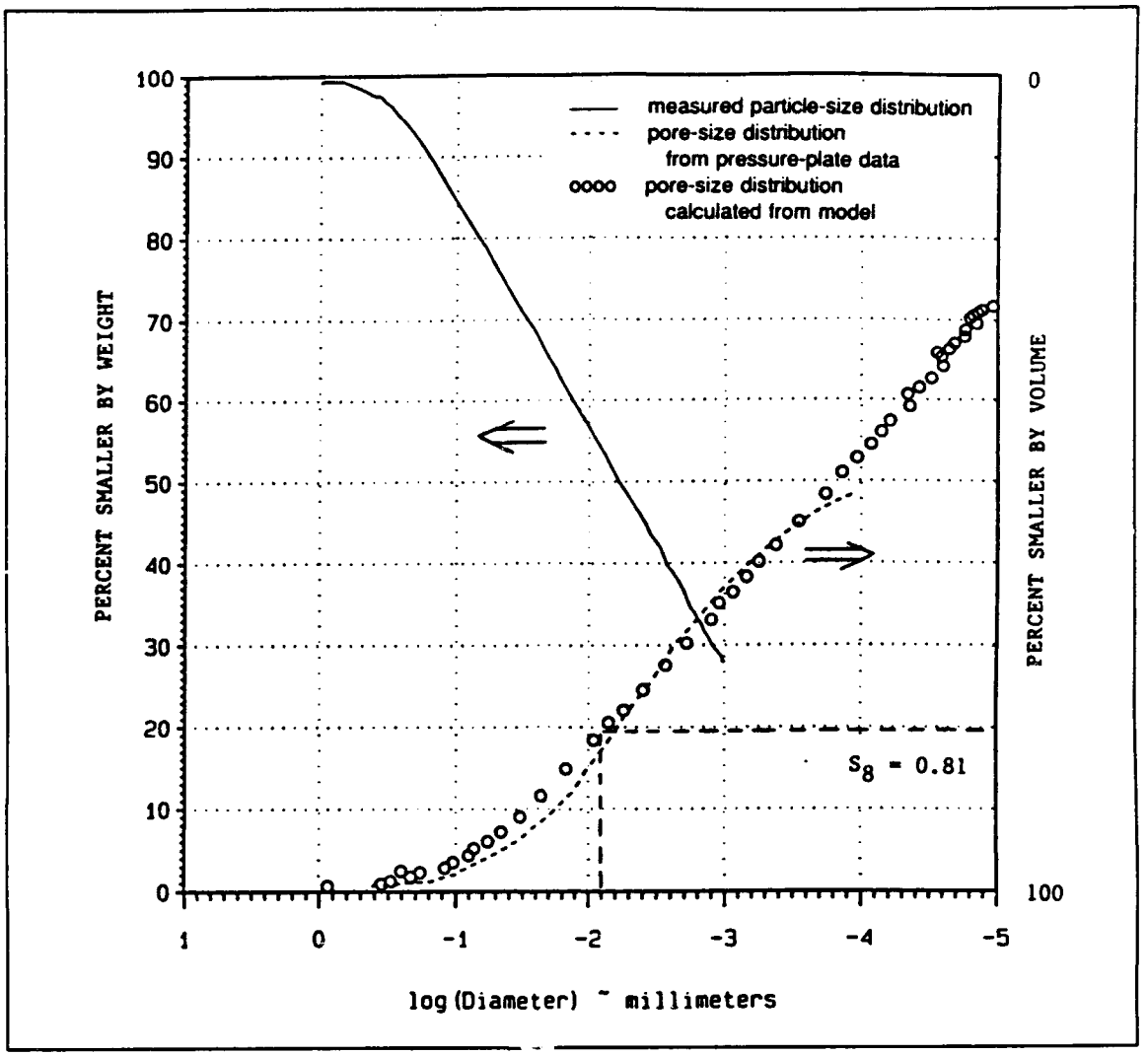

Figure 20. Comparison of measured and predicted pore-size distributions; 70 percent silty clay, 30 percent sandy loam (measurements from Arya and Paris (1981))

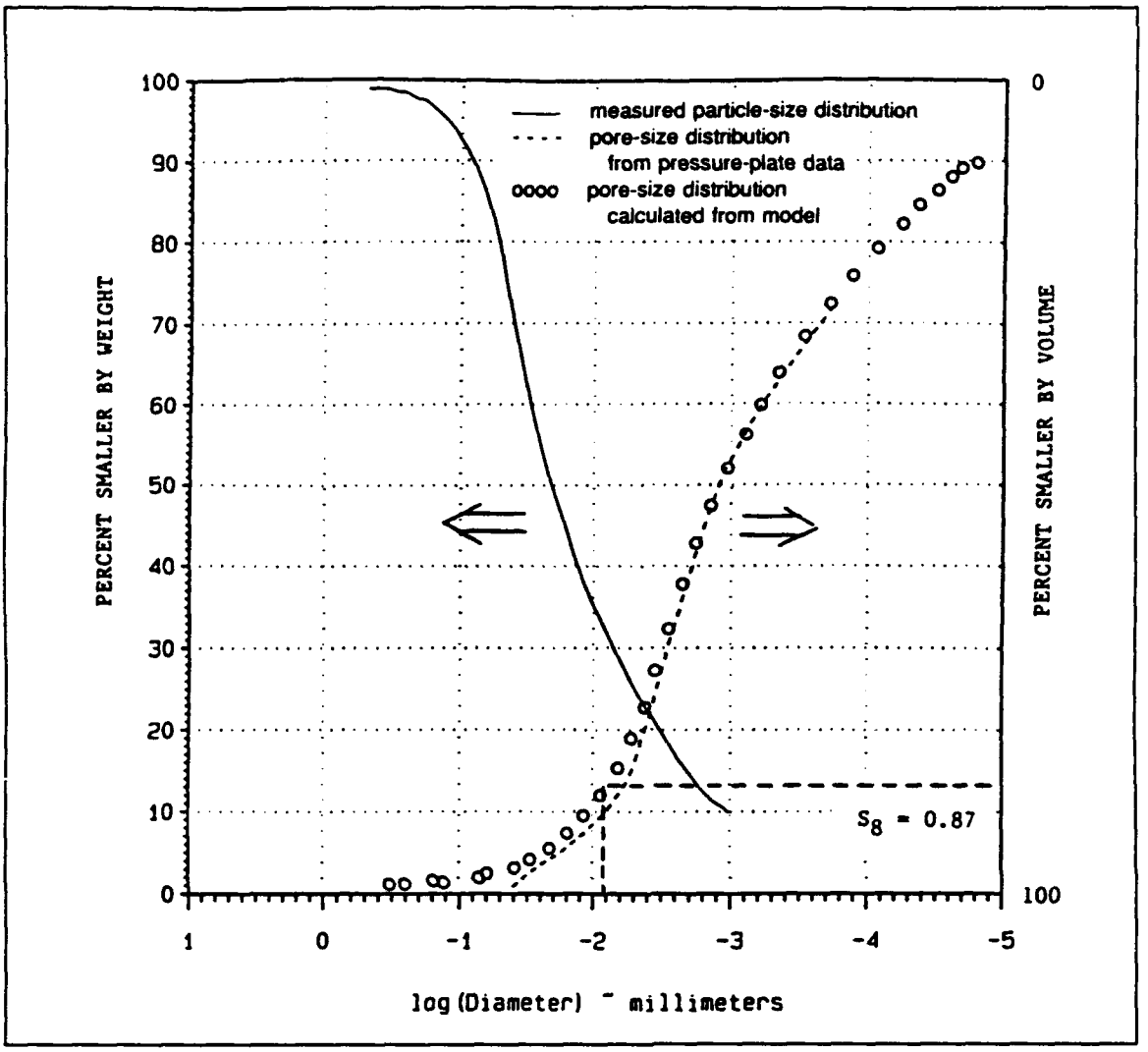

Figure 21. Comparison of measured and predicted pore-size distributions; loam 40- to 50-cm depth (measurements from Arya and Paris (1981))

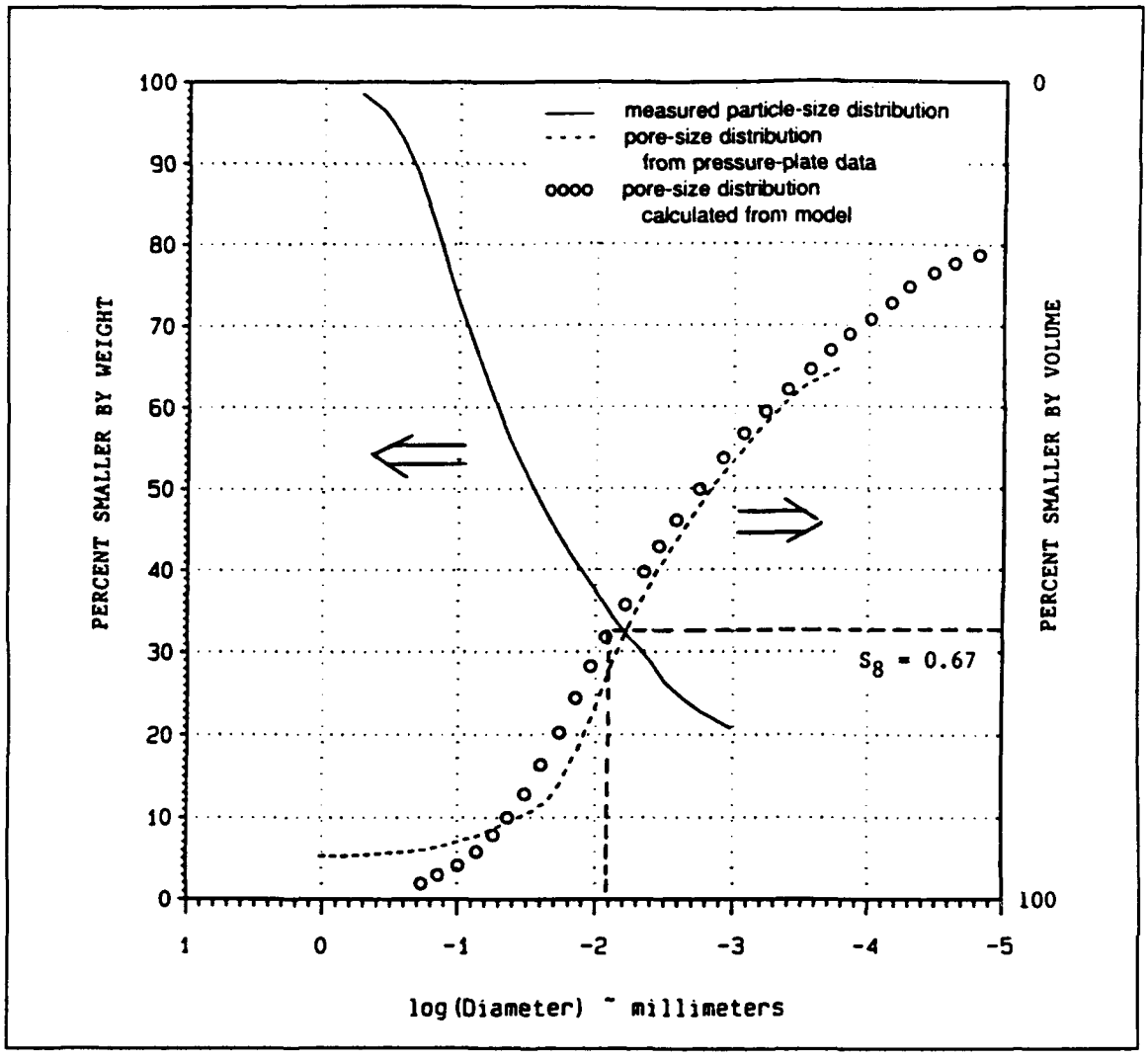

Figure 22. Comparison of measured and predicted pore-size distributions; 40 percent silty clay, 60 percent sandy loam (measurements from Arya and Paris (1981))

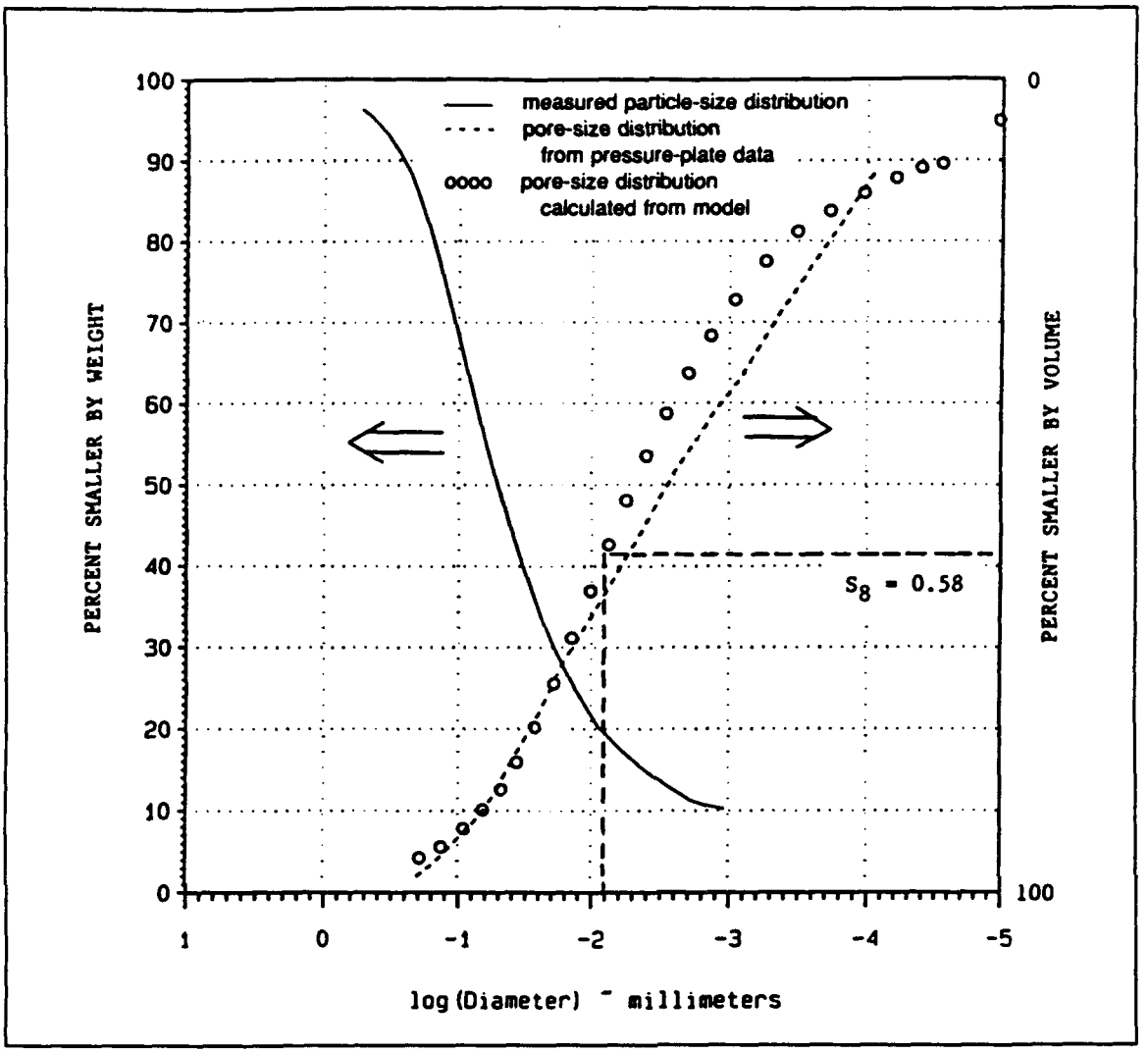

Figure 23. Comparison of measured and predicted pore-size distributions; loam 20- to 30-cm depth (measurement from Arya and Paris (1981))

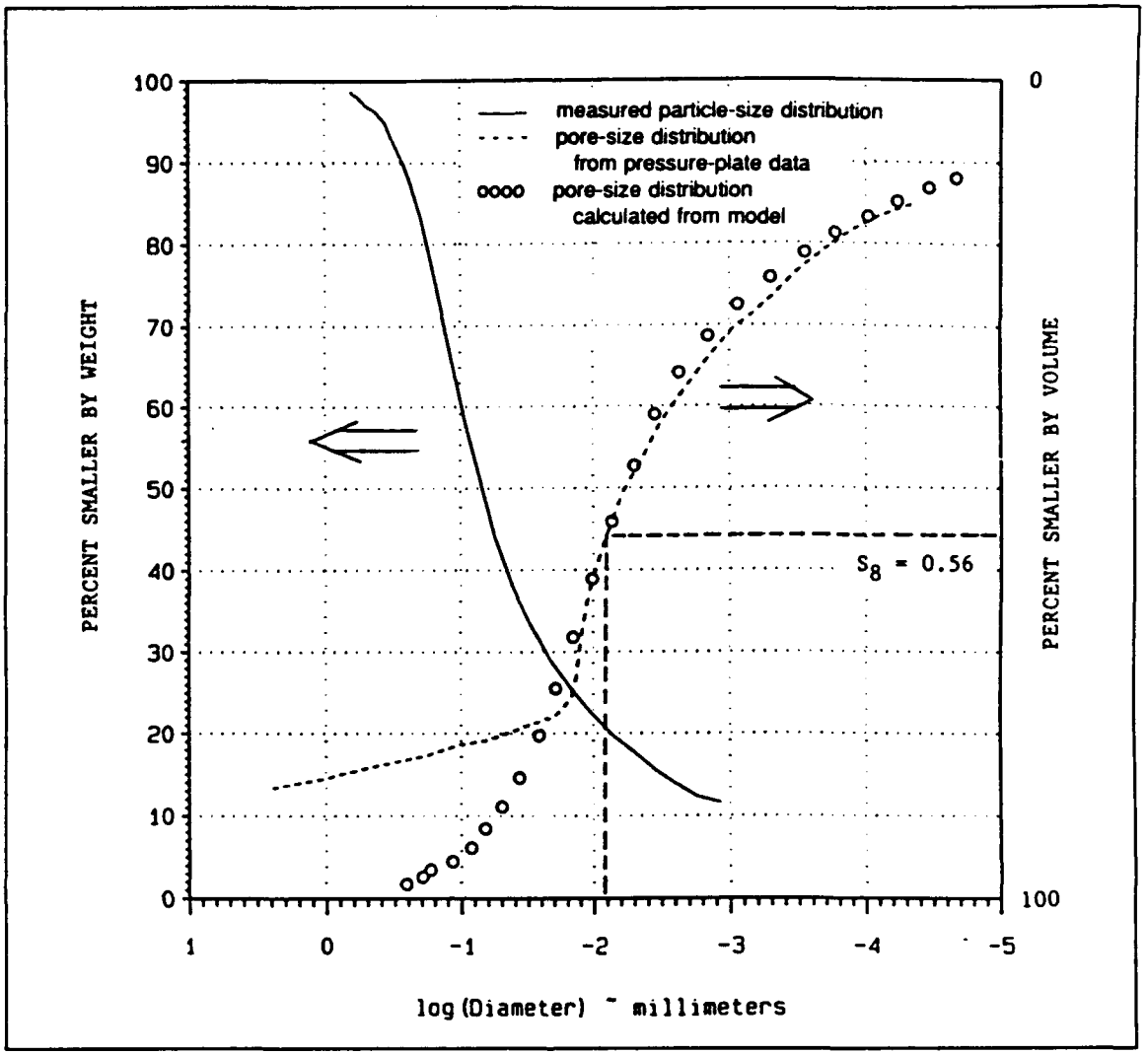

Figure 24. Comparison of measured and predicted pore-size distributions; 20 percent silty clay, 80 percent sandy loam (measurements from Arya and Paris (1981))

pressure-plate data and one from pore-size distribution data) produce quite similar results. As a brief aside, it is interesting to note that Campbell's earlier assumption of median pore size being equivalent to the median particle size is not true for these data. One might even say that based on this limited model exercise, the median pore size is approximately an order of magnitude smaller than the median particle size.

Now, how well does the fractal model for small pore structure apply to the Arya and Paris data? From their data, one can obtain the moisture content for each sample at field capacity, and from the previous figures, one can read S_8, the degree of saturation at a pore diameter of 8 μm. Equation 16 can then be used to compute the moisture content at the limits of fractal soil structure (particle density is taken to be 2.65 g/cc). These results are summarized in Table 1 and show a remarkable correlation.

Table 1
Fractal Cutoff Moisture Content Versus Measured Field Capacity Moisture (data from Arya and Paris (1981))

Sample	Dry Density	S_8	$(M_v)_{fractal}$	$(M_v)_{field\ capacity}$
B	1.400	0.81	0.38	0.39
C	1.416	0.87	0.41	0.42
D	1.480	0.67	0.30	0.33
E	1.456	0.58	0.26	0.28
F	1.517	0.56	0.24	0.25

Fractal Model Applied to This Study

Is the fractal structure model compatible with the data collected in this study? Most importantly, can the electrical response of the test soils be correlated with the fractal model? First of all, let us state the hypothesis:

a. Soil water fills the smallest pores first in a dry sample.

b. Soil structure can be modeled by a fractal geometry in the range of pore sizes in which water is held by capillary forces.

c. Within the small-pore fractal range, the fractal dimension can be calculated from knowledge of either the pore volume-pressure relationship (Equation 14) or the pore volume-pore size relationship (Equation 10).

d. The fractal model fails at pressures less than field capacity (1/3 bar), which, using the capillary equation and assumed values of surface tension and contact angle for water, is equivalent to a pore diameter of about 8 μm (in other words, the fractal model applies for pore diameters less than 8 μm).

e. The upper bound on moisture content associated with the small-pore fractal model is the field capacity, which can be estimated from the product of sample porosity (which is calculated from dry density and particle density) and the degree of saturation at the 8-μm mark on the pore volume-pore size curve (Equation 16).

f. The critical moisture content at which there is a transition from series to parallel-like electrical behavior is identical to the field capacity.

Items a - e were examined in the previous sections. Item f contains the physics of the relationship between soil moisture levels and the electrical response of the soil. What it says is that long-range connectivity becomes achievable when the pores governed by the capillary equation become filled with water. At moisture contents higher than this value, free water exists throughout the sample; i.e., the sample is no longer just "moist," it is now "wet."

The ideal set of data required to test this hypothesis would include enough *electrical response measurements* as a function of moisture content to determine the critical moisture content and field capacity measurements taken from pressure plate data at the same sample densities. Unfortunately, these data do not exist. The best that can be done is to use the electrical property measurements in this study and estimate the field capacity of the soil samples from the particle-size distribution curves using the Arya-Paris model to generate a pore-size distribution. This requires values of the fitting parameter α.

Although Arya and Paris (1981) were able to use values of the model parameter that fell within the range of 1.35 to 1.39 for the five soils discussed in the previous section, one can argue that these values may not be suitable for all soil samples. Their soils were well-graded and all contained some sand as well as some clay. The soils used in this study are, relative to the Arya-Paris soils, poorly graded. Recalling that the α parameter was a way of accounting for the fact that the length of a pore associated with an assumed spherical particle is something more than twice the particle radius, it seems likely that it could vary considerably for soils that are poorly graded and for which the basic particle shapes are distinctly different.

For example, pore spaces are likely to be parallel to the flat plate-like structure of kaolinite. The pore length contribution from each particle should be about the particle diameter. In other words, α for kaolinite should be on the order of 1.0. At the other extreme, Ottawa sand in a close-pack

geometry should possess pore channels that hug the surface of the almost-spherical particles, which means each particle contributes a path length much greater than its diameter. This would imply the largest values of α.

Since there is no a priori knowledge of the α parameter for these soils, one can take the reverse approach to testing the above hypothesis. Assume that the critical moisture content is the field capacity, which, in turn, is represented by the degree of saturation shown on the pore volume versus pore size curve at the 8-μm diameter mark. Following the generation of several pore-size distribution curves from the particle-size distributions, estimate α for each soil by the value that yields a pore-size distribution that matches the critical moisture and the 8-μm intersection. With this value of α, generate the most likely pore-size distribution curves for each of the soils and graphically determine the soil fractal dimension for each soil type using the relationship in Equation 10. The final test of the hypothesis will be to compare those values for fractal dimensions with data for similar soils that are published in the open literature.

First of all, Figures 25 to 28 show the results of applying the Arya and Paris' model to each soil used in this study with α allowed to vary from 1.0 to 2.0 in increments of 0.1. Secondly, values of critical moisture were assigned to the four soils based on the moisture-related data shown on Figures 11-14. These values, along with soil densities are used to calculate porosities and the required degrees of saturation shown in Table 2. Armed with this information, one can return to Figures 25 to 28 and estimate the value of α associated with each soil. These values are also shown in the table.

Finally, one can now take the slopes of the calculated pore-size distribution curve for each soil (using the estimated α value and the fractal model described above) and infer from those results a fractal dimension for the soil structure using Equation 10. Figures 29 to 31 show the results of this exercise and include the estimate of the soil fractal dimensions, varying from 2.0 for tan sand to 2.9 for kaolinite. Ottawa sand is not reported because it appears to have no critical moisture electrical response.

Supporting Data

Although very little data exist in the literature on fractal dimensions of minerals and/or soils, the extremes are supported by at least a couple of references. For example, Pfeifer (1984) calculated a fractal dimension for kaolinite of 2.92 using a dye adsorption and photometric measurement technique. On the other hand, he and other colleagues (Farin, Avnir, and Pfeifer 1984) report from another source a dimension of about 2.15 for quartz sands using a nitrogen adsorption technique.

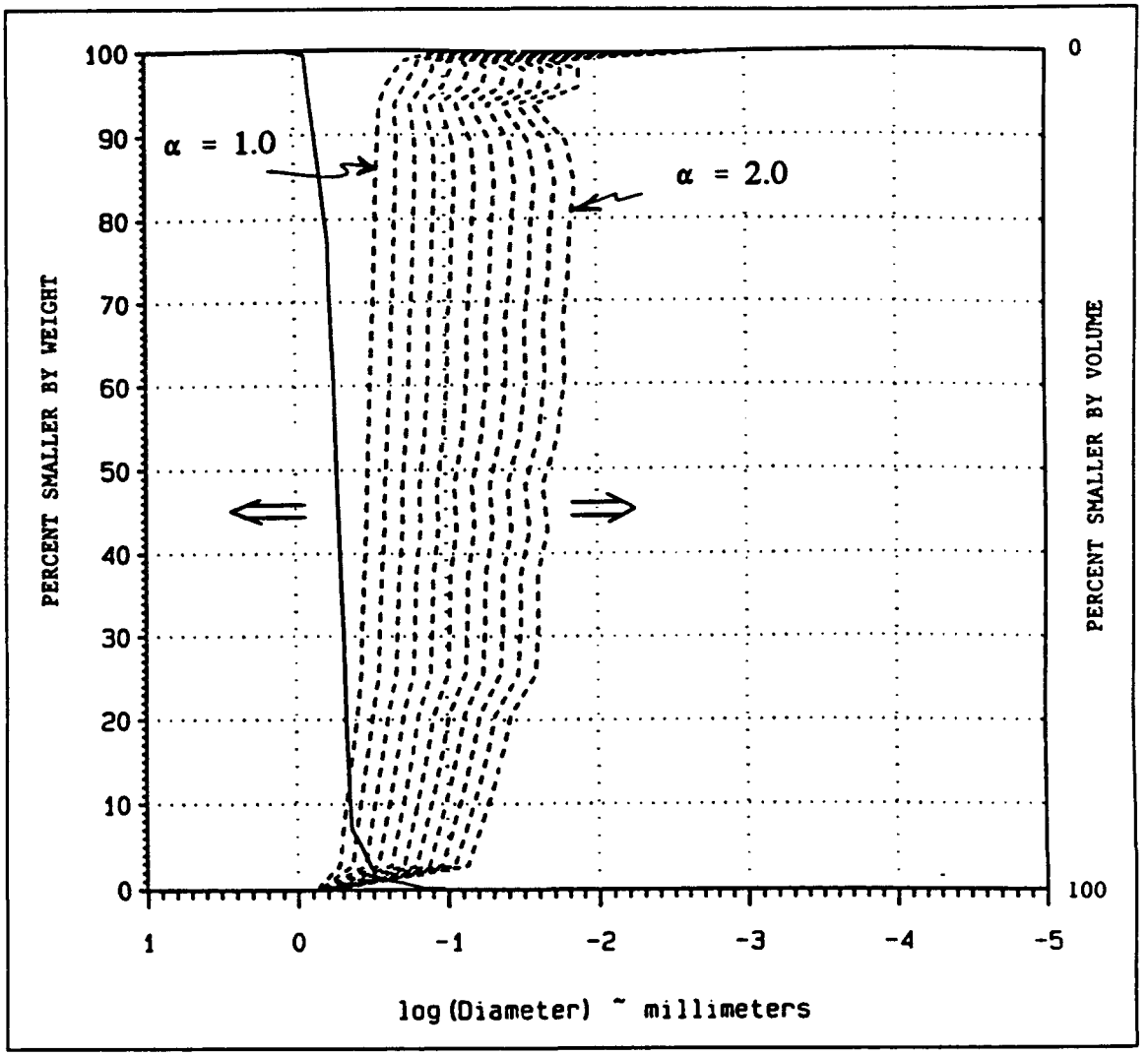

Figure 25. Predicted pore distribution curves for Ottawa sand

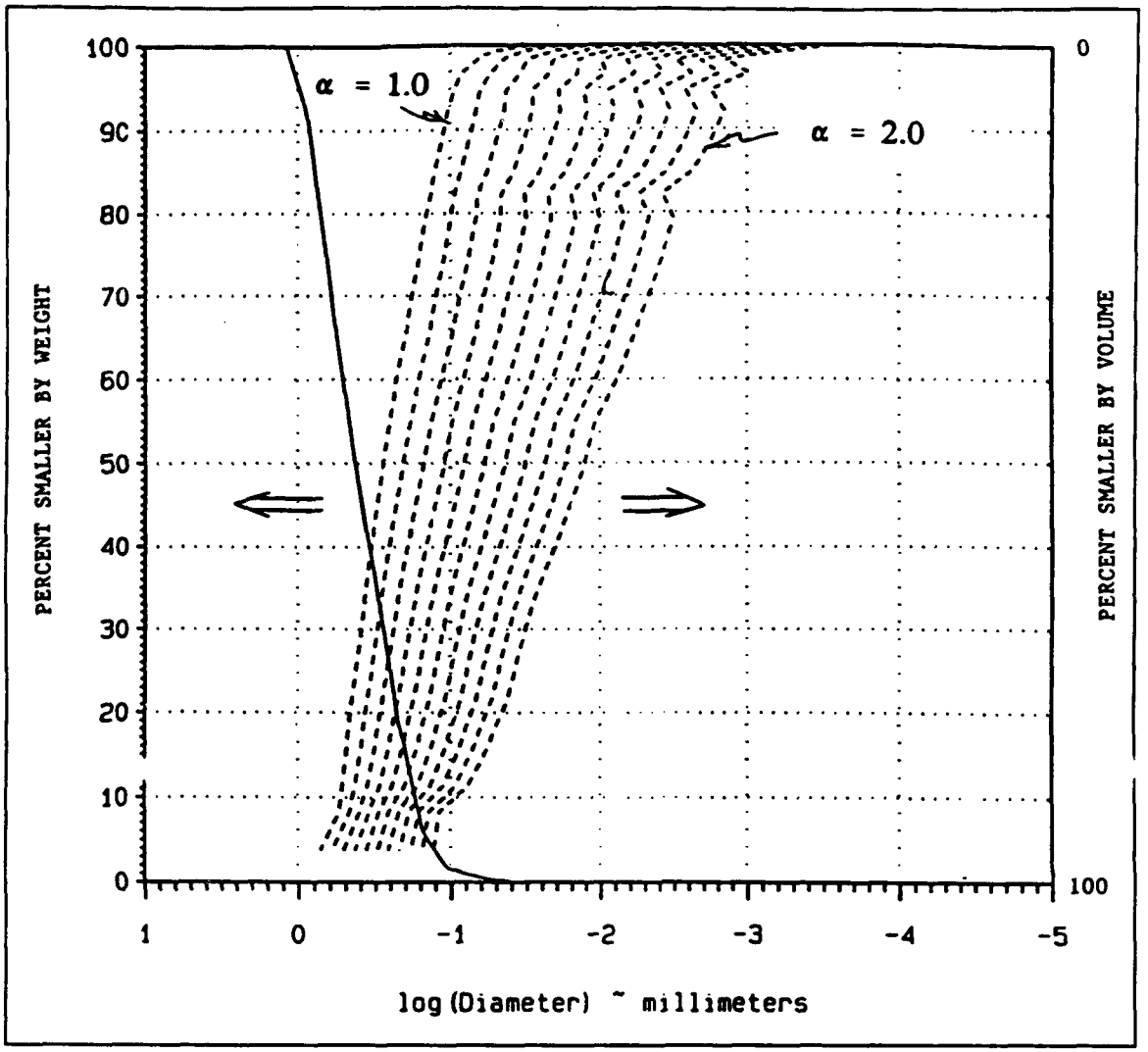

Figure 26. Predicted pore distribution curves for tan sand

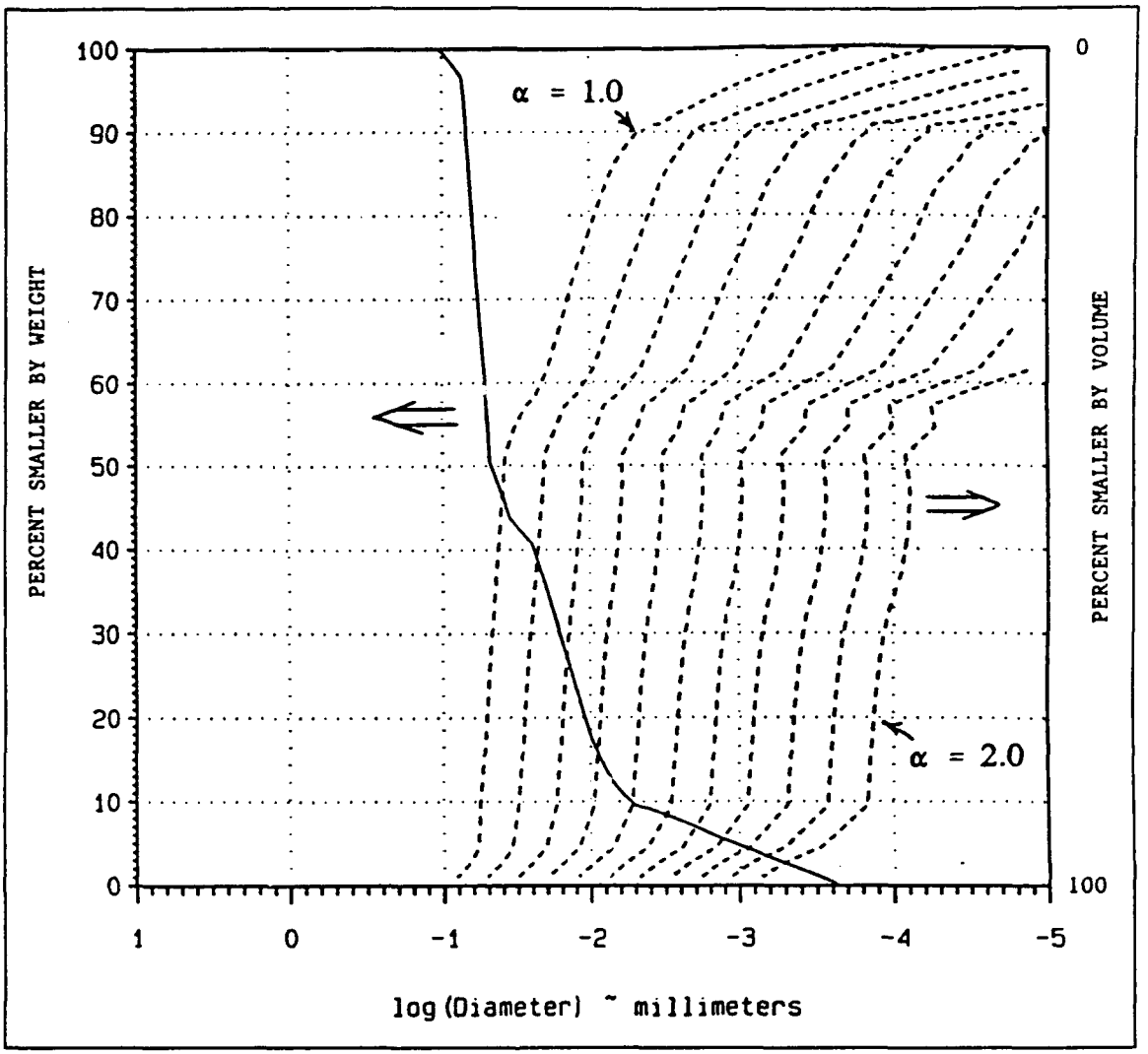

Figure 27. Predicted pore distribution curves for tan silt

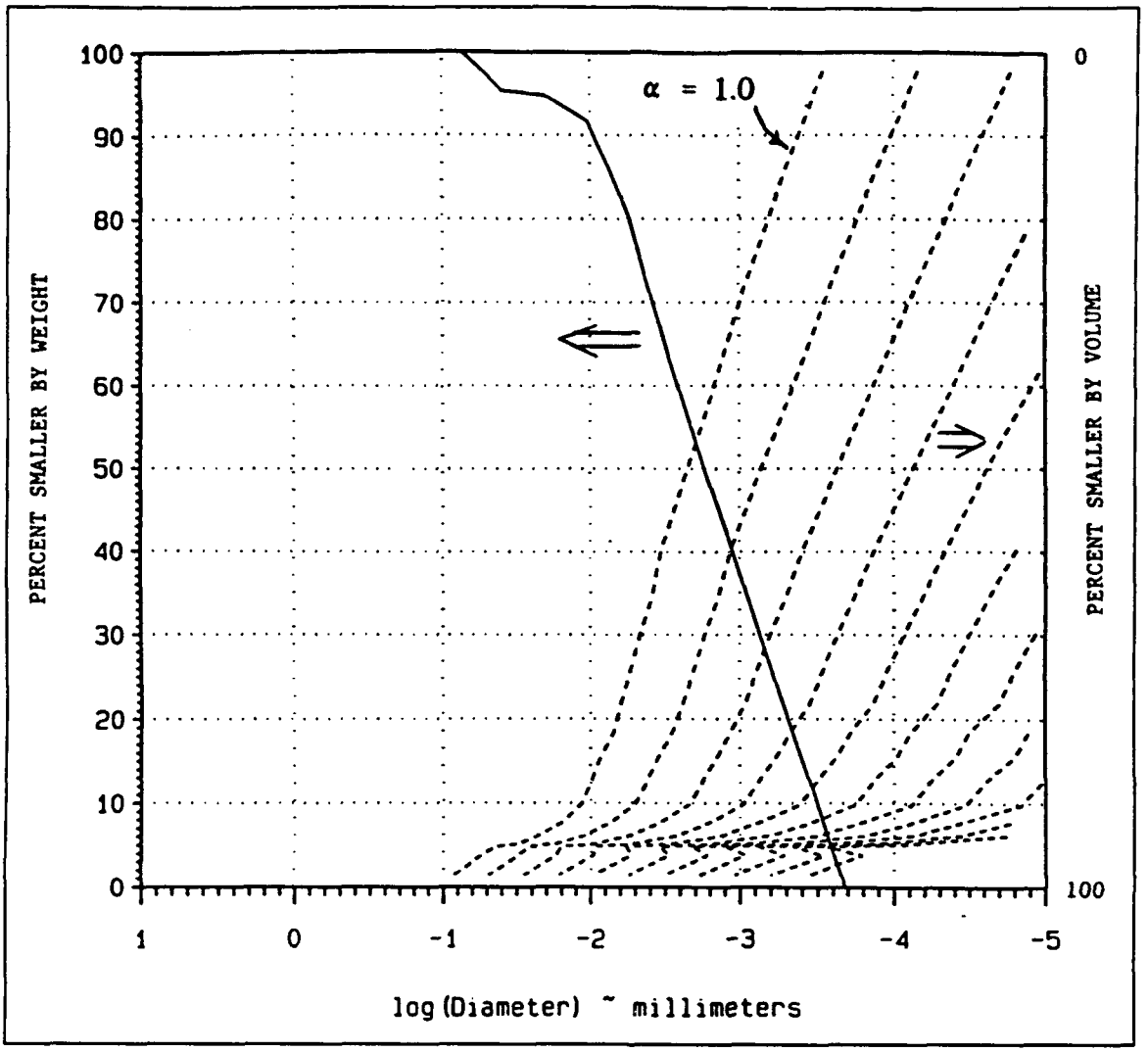

Figure 28. Predicted pore distribution curves for kaolinite

Table 2
Estimating α for the Soils in This Study

Soil	$(M_v)_{critical}$	ρ dry	ρ part	n	$S_e = (M_v)_{critical}/n$	α
Ottawa Sand	0.00	1.7	2.67	0.36	0.00	1.8*
Tan Sand	0.10	1.7	2.66	0.36	0.28	1.8
Tan Silt	0.35	1.4	2.71	0.48	0.73	1.3
Kaolinite	0.35	0.9	2.61	0.66	0.53	0.9

* Assumed to be like that of the tan sand.

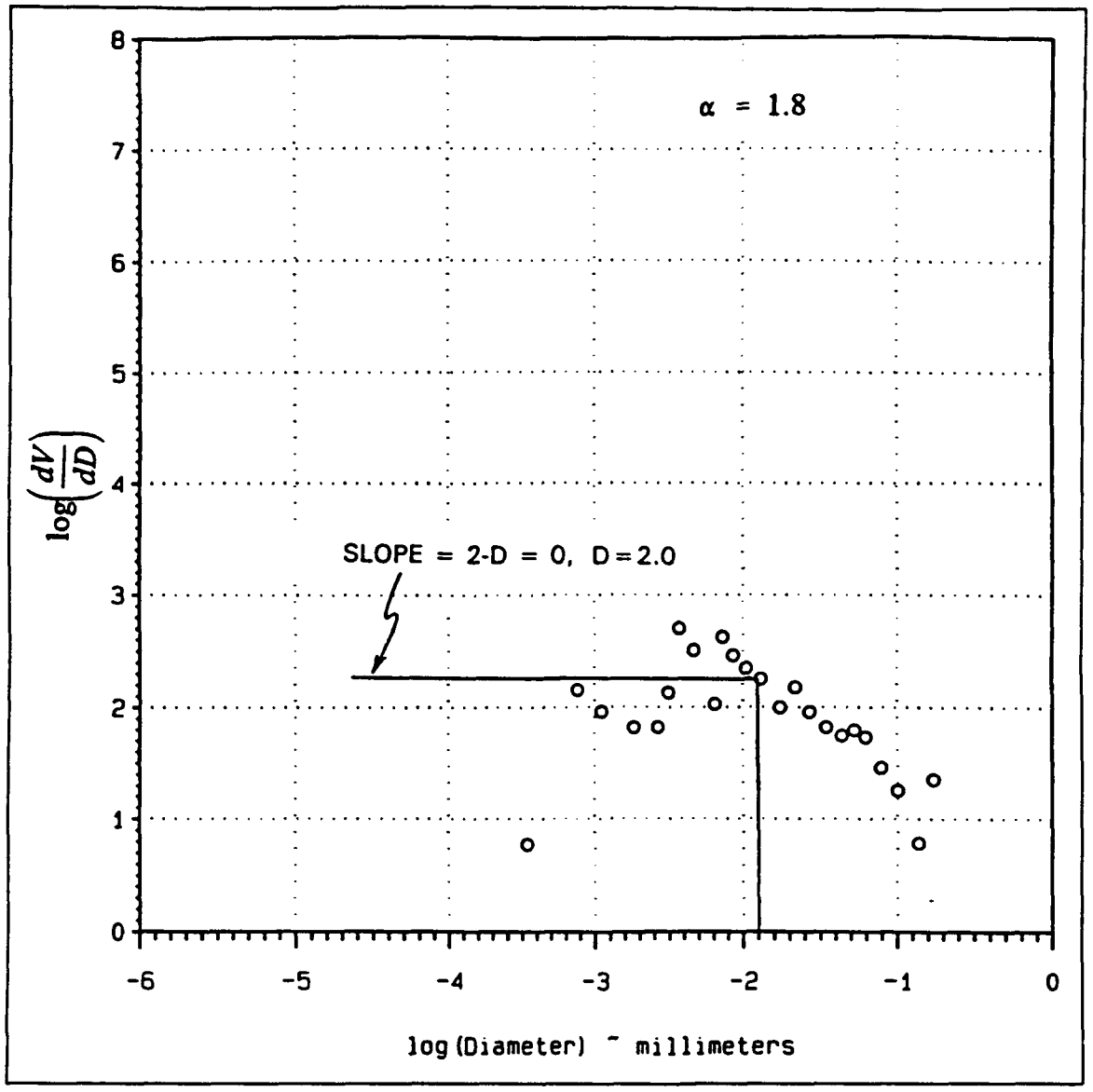

Figure 29. Inferred fractal dimension for tan sand

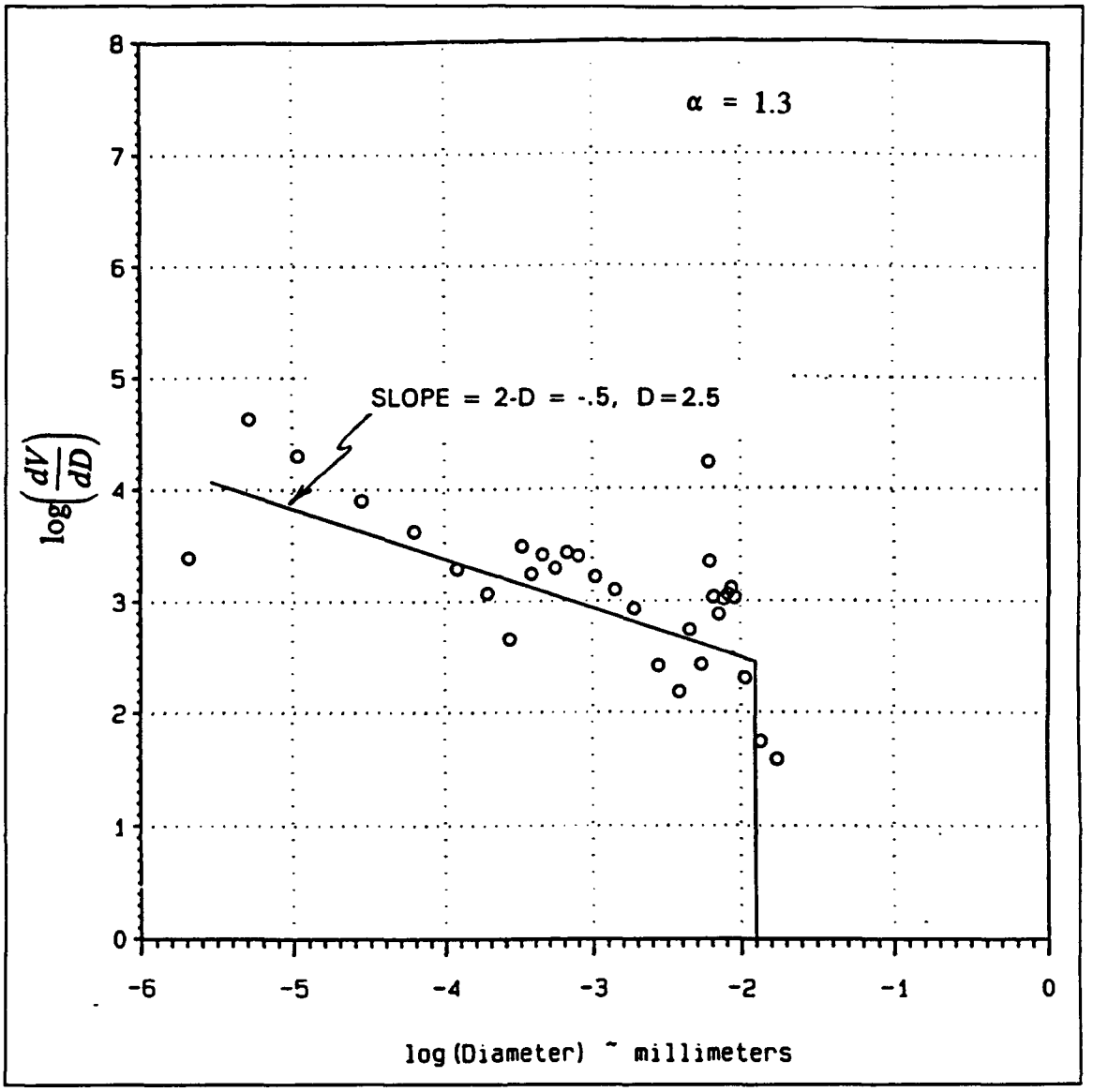

Figure 30. Inferred fractal dimension for tan silt

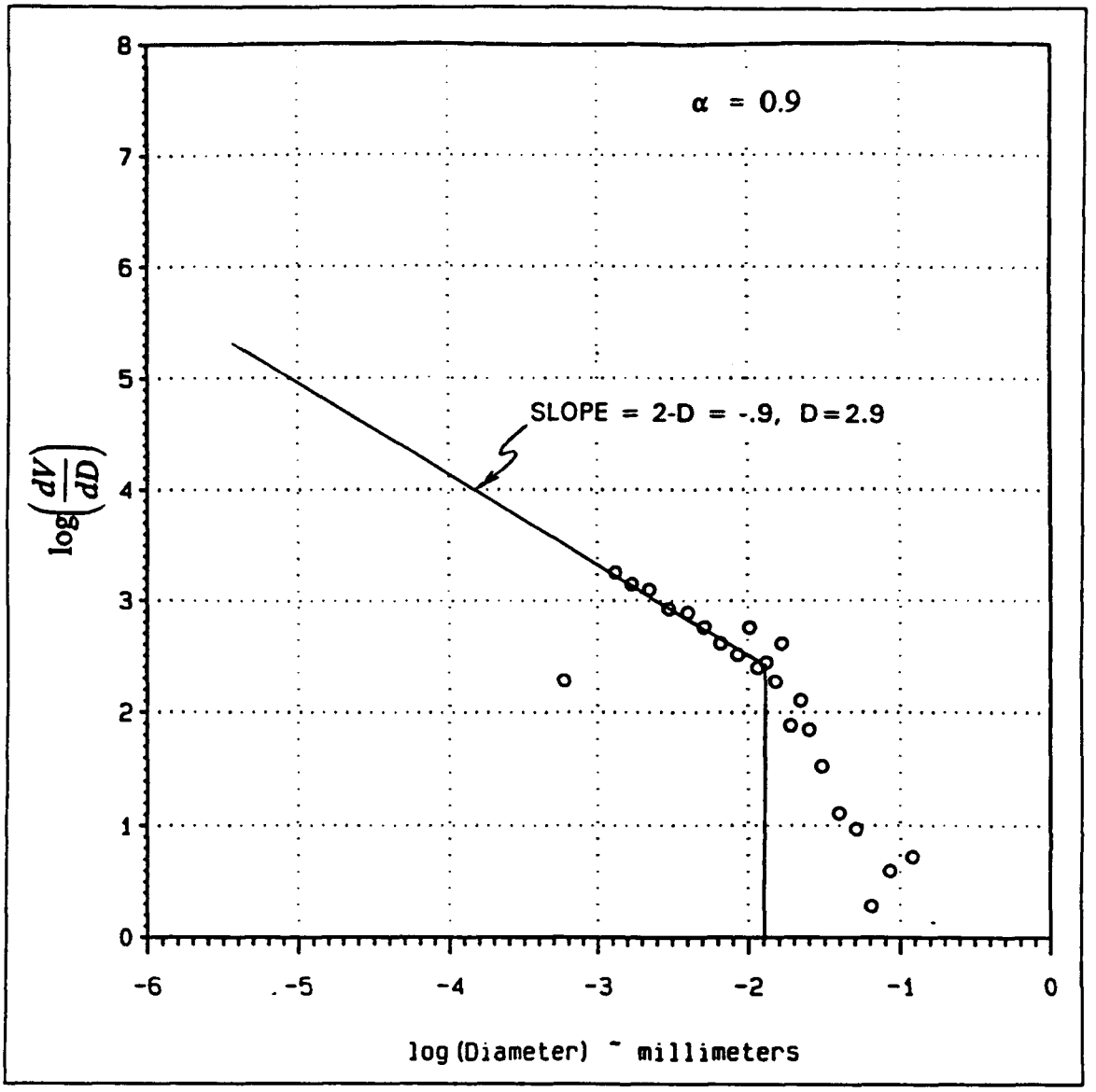

Figure 31. Inferred fractal dimension for kaolinite

5 Conclusions

The response of moist soils (or any other moist heterogeneous mixture) to active microwave sensors is controlled by surface geometry and the dielectric properties of the medium. A review of the literature reveals that what data do exist on dielectric properties suffer from a number of shortcomings. In most cases, the soils are simply not properly characterized in terms of their physical parameters such as the distribution of particle sizes, the dry density under which tests were conducted, or the temperature of the soil, all of which have some impact on the dielectric properties. The volumetric moisture content of the soil, which is usually the most important factor controlling dielectric response, is often not specified or is not computable. And, finally, the data are usually collected at a limited number of frequency values and over a very limited range of frequencies.

Attempts to model the dielectric response of these soils are also limited in several respects. Many models are strictly empirical and, therefore, apply only to that data set with its few variations. Equivalent circuit models have been successfully applied to data over a small frequency range, but the model parameters seldom have any physical meaning.

This study began with an attempt to supplement existing data on the complex dielectric properties of moist soils. A coaxial measurement apparatus for which measurements are controlled by a vector network analyzer was fabricated to allow property measurements in nominally moist soils to frequencies above 10 GHz, which allowed one to see the beginning of the dipole loss mechanism. Sample temperatures were controlled by an external bath, and sample moisture contents were varied by incremental drying of the samples. Actual test moisture values were determined after each series of measurements were completed by weighing the completely dry sample. Distilled, deionized water was used to saturate dry soil samples.

Soil samples were chosen to reflect a broad span of responses. They varied from a poorly graded clean sand to a very pure nonswelling clay mineral. The physical properties of the soil samples were characterized by the development of grain-size distribution curves and measurements of specific gravity and specific surface. With hindsight, either mercury porosimetry measurements or pressure plate measurements should have been conducted to obtain a relationship between pore volume and pore size.

As expected, the soil dielectric response was found to be a strong function of volumetric moisture content for nonfrozen soils. Low-frequency losses because of either ionic conductivity or Maxwell-Wagner effects, or both, were quite apparent, as were high-frequency losses because of the free-water dipole relaxation loss mechanism. Minimum losses occur in the 1- to 2-GHz range.

Sample temperature did not have a significant effect on the dielectric response of nonfrozen soils over a range of temperatures from 0 to 40 °C at any frequency. Data collected on frozen soils at -10 and -5 °C also did not show any significant difference. The pronounced transition from frozen to nonfrozen soils took place within the -5 to 0 °C range, but the spacing of data within this range was not enough to completely define that transition.

Data collected in the study supported the claim of previous researchers that there is a definite transition in normal soils from a series-like capacitive response to a parallel-like response with increasing volumetric moisture content. For the silt and clay samples, that transition occurred in the 30- to 35-percent moisture content range, while for the well-graded sand, it occurred in the 10- to 15-percent range. For equal moisture contents, then, the sands had a higher permittivity than silts and nonswelling clays.

Two approaches were taken to modeling the dielectric response of these soils. One was an equivalent circuit that allowed for both series-like and parallel-like responses of soil and water elements. An iterative solution technique was used to arrive at the weighting parameters for each element that varied in a sensible way with moisture content. The permittivities assigned to the circuit elements were held fixed at acceptable values, and excellent fits to the data over the entire range of frequencies were achieved for all of the soil types.

The second model was one that assumed the small pore geometry of a porous medium like soils could be described by fractal methods. The result was an expression for pore volume as a function of pore size or capillary pressure that included a fractal dimension of the soil structure. When applied to a set of pressure plate data taken from the open literature, this model showed that the fractal geometry assumption held for the small-pore portion of the data and collapsed at the field capacity of the soils (1/3 bar pressure, or 8-μm pore diameter). The model goes on to hypothesize that the critical moisture content of the soils at which its electrical response makes a transition from series to parallel behavior is, in fact, the moisture content at field capacity. Lacking a measured pore volume distribution for these soils in terms of either pressures or pore size, a pore volume-pore size distribution was estimated from the measured particle size distribution curves and used to evaluate bounds on the small-pore fractal dimension of the idealized soils used in this study. The results indicate that while real soils are likely to have fractal dimensions of 2.5 to 2.7, the value for coarse sands tends toward 2.0 and the value for fine nonswelling clay minerals tends toward 3.0.

References

Arulanandan, K., and Smith, S. S. (1973). "Electrical dispersion in relation to soil structure," ASCE, *Journal of the Soil Mechanics and Foundations Division* SM12, 1113-1133.

Arya, L. M., and Paris, J. F. (1981). "A physicoempirical model to predict the soil moisture characteristic from particle-size distribution and bulk density data," *Soil Science Society of America Journal* 45, 1023-1030.

Ballard, R. F. (1983). "Cavity detection and delineation research; Report 5, Electromagnetic (radar) techniques applied to cavity detection," Technical Report GL-83-1, U.S. Army Engineer Waterways Experiment Station, Vicksburg, MS.

Bear, J., and Verruijt, A. (1987). *Modeling groundwater flow and pollution.* D. Reidel Publishing Company, Dordrecht, the Netherlands.

Berlin, G. L., Tarabzouni, M. A., Al-Naser, A. H., Sheikho, K. M., and Larson, R. W. (1986). "SIR-B subsurface imaging of a sand-buried landscape: Al Labbah Plateau, Saudi Arabia." *IEEE transactions on geoscience and remote sensing.* GE-24(4), 595-602.

Birchak, J. R., Gardner, C. G., Hipp, J. E., and Victor, J. M. (1974). "High dielectric constant microwave probes for sensing soil moisture." *Proceedings of the IEEE.* 62(1), 93-98.

Brunfeldt, D. R. (1987). "Theory and design of a field-portable dielectric measurement system." *Proceedings of IGARSS '87 Symposium.* Ann Arbor, MI, 559-563.

Campbell, J. E. (1988). "Dielectric properties of moist soils at RF and microwave frequencies," Ph.D. diss., Dartmouth College, Hanover, NH.

Campbell, M. J., and Ulrichs, J. (1969). "Electrical properties of rocks and their significance for lunar radar observations," *Journal of Geophysical Research* 74(25), 5867-5881.

Colwell, R. N., ed. (1983). *Manual of remote sensing.* 2nd ed., American Society of Photogrammetry, Falls Church, VA.

Curtis, J. O. (1992). "Moisture and temperature effects on the microwave dielectric behavior of soils," Ph.D diss., Dartmouth College, Hanover, NH.

_____. "Microwave dielectric behavior of soils; Report 1, Summary of related research and applications," Technical Report in preparation, U.S. Army Engineer Waterways Experiment Station, Vicksburg, MS.

_____. "Microwave dielectric behavior of soils; Report 2, A unique coaxial measurement apparatus," Technical Report in preparation, U.S. Army Engineer Waterways Experiment Station, Vicksburg, MS.

Delaney, A. J., and Arcone, S. A. (1982). "Laboratory measurements of soil electric properties between 0.1 and 5 GHz," Report 82-10, U.S. Army Cold Regions Research and Engineering Laboratory, Hanover, NH.

Farin, D., Avnir, D., and Pfeifer P. (1984). "Fractal dimensions of surfaces. The Use of adsorption data for the quantitative evaluation of geometric irregularity," *Particulate Science and Technology* 2, 27-35.

Friesen, W. I., and Mikula, R. J. (1987). "Fractal dimensions of coal particles," *Journal of Colloid and Interface Science* 120(1), 263-271.

Gabriel, C., Grant, E. H., and Young, I. R. (1986). Use of time domain spectroscopy for measuring dielectric properties with a coaxial probe," *Journal of Physics, E: Scientific Instrumentation*, 19, 843-846.

Hallikainen, M. T., Ulaby, F. T., Dobson, M. C., El-Rayes, M. A., and Wu, L. (1985). "Microwave dielectric behavior of wet soil - Part I: Empirical models and experimental observations." *IEEE transactions on geoscience and remote sensing.* GE-23(1).

Hasted, J. B. (1973). *Aqueous dielectrics.* Chapman and Hall, London.

Hayre, H. S. (1970). "Geophysical dielectric constant determination." *IEEE transactions on geoscience electronics.* GE-8(4), 289-295.

Hoekstra, P., and Doyle, W. T. (1971). "Dielectric relaxation of surface adsorbed water," *Journal of Colloid and Interface Science* 36(4), 513-521.

Jakkula, P., Ylinen, P., and Tiuri, M. (1980). "Measurement of ice and frost thickness with an FM-CW radar." *Proceedings of the 10th European microwave conference.* Warszawa, Poland, 584-587.

John, B. (1992). "Soil moisture detection with airborne passive and active microwave sensors," *International Journal of Remote Sensing* 13(3), 481-491.

Katz, A. J., and Thompson, A. H. (1985). "Fractal sandstone pores: Implications for conductivity and pore formation," *Physical Review Letters* 54(12), 1325-1328.

Krepfl, M., Moore, C., and Lee, W. (1989). "A quantitative description of soil microstructure using fractals, Volume I of II, research results," Report WL-TR-89-48, Vol. 1, Weapons Laboratory, Kirtland AFB, NM.

Lundien, J. R. (1966). "Terrain analysis by electromagnetic means; Report 2, Radar responses to laboratory prepared soil samples," Technical Report 3-693, U.S. Army Engineer Waterways Experiment Station, Vicksburg, MS.

_____. (1972). "Determining presence, thickness, and electrical properties of stratified media using swept-frequency radar," Technical Report M-72-4, U.S. Army Engineer Waterways Experiment Station, Vicksburg, MS.

Madden, T. R. (1974). "Near surface electrical properties of rocks as a guide to mechanical properties," Report AFCRL-TR-75-0179, Air Force Cambridge Research Laboratories, Hanscom, AFB, MA.

Mandelbrot, B. B. (1983). *The Fractal geometry of nature.* W. H. Freeman and Company, New York.

McCauley, J. F., Breed, C. S., Schaber, G. G., McHugh, W. P., Issawi, B., Haynes, C. V., Grolier, M. J., and el Kilani, A. (1986). "Paleodrainages of the Eastern Sahara - The Radar Rivers Revisited (SIR-A/B Implications for a Mid-Tertiary Trans-African Drainage System." *IEEE transactions on geoscience and remote sensing.* GE-24(4), 624-648.

Moore, C. A., and Krepfl, M. (1991). "Using fractals to model soil fabric," *Geotechnique* 41(1), 123-134.

Nelson, S. O. (1973). "Microwave dielectric properties of grain and seed." *Transactions of the ASAE.* 16(5), 902-905.

_____. (1983). "Dielectric properties of some fresh fruits and vegetables at Frequencies of 2.45 to 22 GHz." *Transactions of the ASAE.* 26(2), 613-616.

Olhoeft, G. R. (1983). "Impulse radar studies of near surface geological structure." *Proceedings of the conference on lunar and planetary science X.* Houston, TX, 943-945.

O'Neill, K., and Arcone, S. A. (1991). "Investigations of freshwater and ice surveying using short-pulse radar," CRREL Report 91-15, U.S. Army Engineer Cold Regions Research and Engineering Laboratory, Hanover, NH.

Parchomchuk, P., Wallender, W. W., and King, R. J. (1990). "Calibration of a waveguide sensor for measuring soil moisture. *IEEE transactions on geoscience and remote sensing.* 28(5), 873-878.

Pfeifer, P. (1984). "Fractal dimension as working tool for surface-roughness problems," *Applications of Surface Science* 18, 146-164.

Sachs, S. B., and Spiegler, K. S. (1964). "Radiofrequency measurements of porous conductive plugs. Ion-exchange resin solution systems," *Journal of Physical Chemistry* 68(5), 1214-1222.

Smith, S. S. (1971). "Soil characterization by radio frequency electrical dispersion," Ph.D. diss., University of California at Davis.

Sridharan, A., Altschaeffl, A. G., and Diamond, S. (1971). "Pore size distribution studies," ASCE, *Journal of the Soil Mechanics and Foundations Division* SM5, 771-787.

Stewart, M. T. (1982). "Evaluation of electromagnetic methods for rapid mapping of salt-water interfaces in coastal aquifers," *Ground Water* 20(5), 538-545.

Swanson, R., Zoughi, R., Moore, R. K., Dellwig, L. F., and Soofi, A. K. (1988). "Backscatter and dielectric measurements from rocks of southeastern Utah at C-, X-, and K_u- Bands," *International Journal of Remote Sensing*, 9(4), 625-639.

Telford, W. M., Geldart, L. P., Sheriff, R. E., and Keys, D. A. (1984). "Electrical properties of rocks." *Applied geophysics*. Chapter 5, Cambridge University Press.

Thomas, A. M. (1966). "In situ measurement of moisture in soil and similar substances by 'fringe' capacitance," *Journal of Scientific Instruments* 43, 21-27.

Topp, G. C., Davis, J. L., and Annan, A. P. (1980). "Electromagnetic determination of soil water content: Measurements in coaxial transmission lines," *Water Resources Research* 16(3), 574-582.

Ulaby, F. T., Cihlar, J., and Moore, R. K. (1974). "Active microwave measurement of soil water content," *Remote Sensing of Environment* 3, 185-203.

Wang, J. R., and Schmugge, T. J. (1980). "An empirical model for the complex dielectric permittivity of soils as a function of water content," *IEEE transactions on geoscience and remote sensing.* GE-18(4), 288-295.

Wegmuller, Urs. (1990). "The effect of freezing and thawing on the microwave signatures of bare soil," *Remote Sensing of the Environment* 33, 123-135.

Wright, D. L., Olhoeft, G. R., and Watts, R. D. (1984). "Ground-penetrating radar studies on Cape Cod." *Proceedings of NWWA/EPA conference on surface and borehole geophysical methods in ground water investigations.* San Antonio, TX, 666-681.

Appendix A
Soil Properties

Particle-size distribution curves for each of the four soils used in these experiments were developed by technicians in the Geotechnical Laboratory at the U.S. Army Engineer Waterways Experiment Station, Vicksburg, MS, and are shown on the following four figures. Also included on each figure is the specific surface for that soil that was measured by laboratory personnel at Quantachrome Corporation, in Syosset, NY, using a nitrogen gas adsorption technique (Krypton gas for the Ottowa sand).

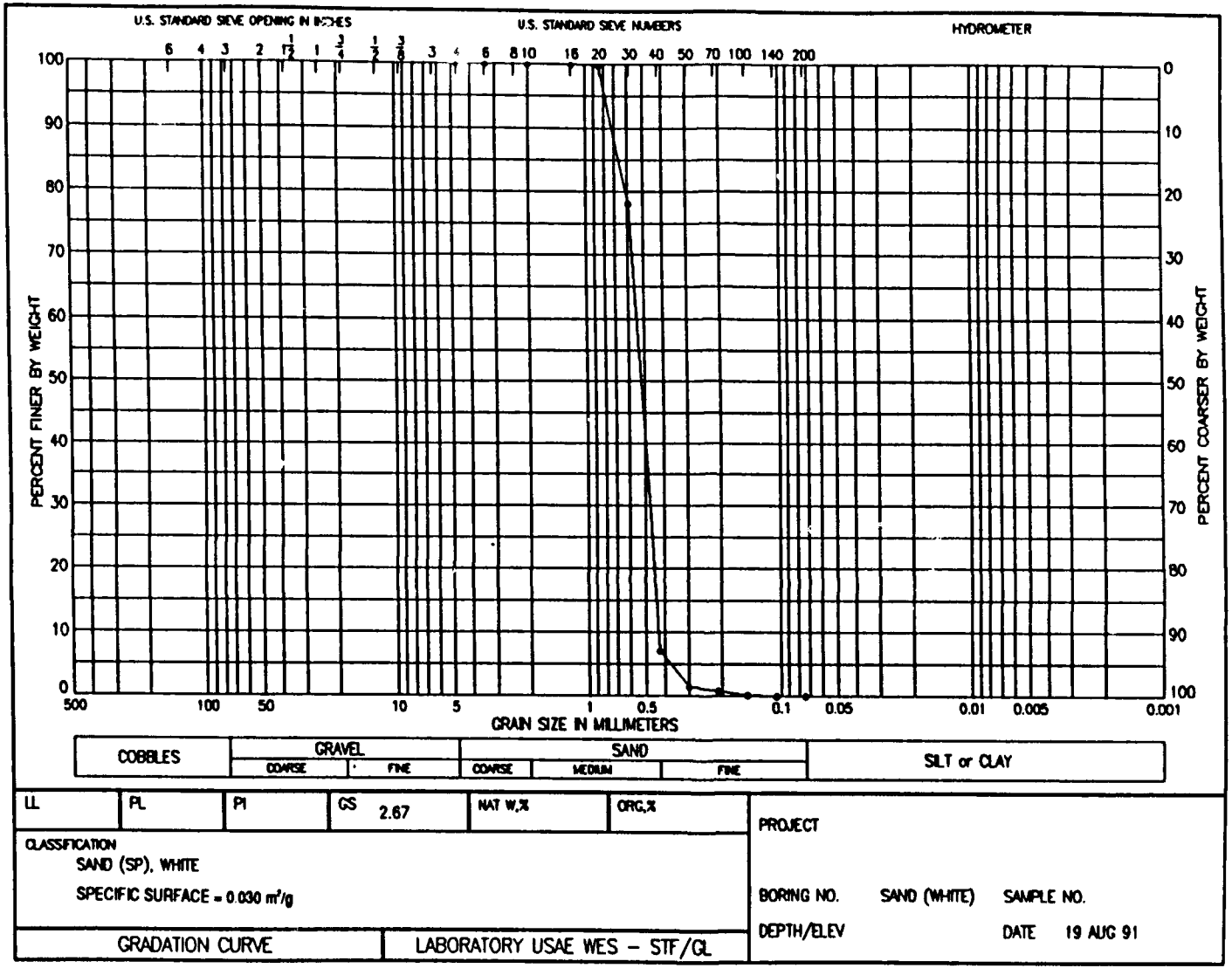

Figure A1. Gradation curve for Ottawa sand

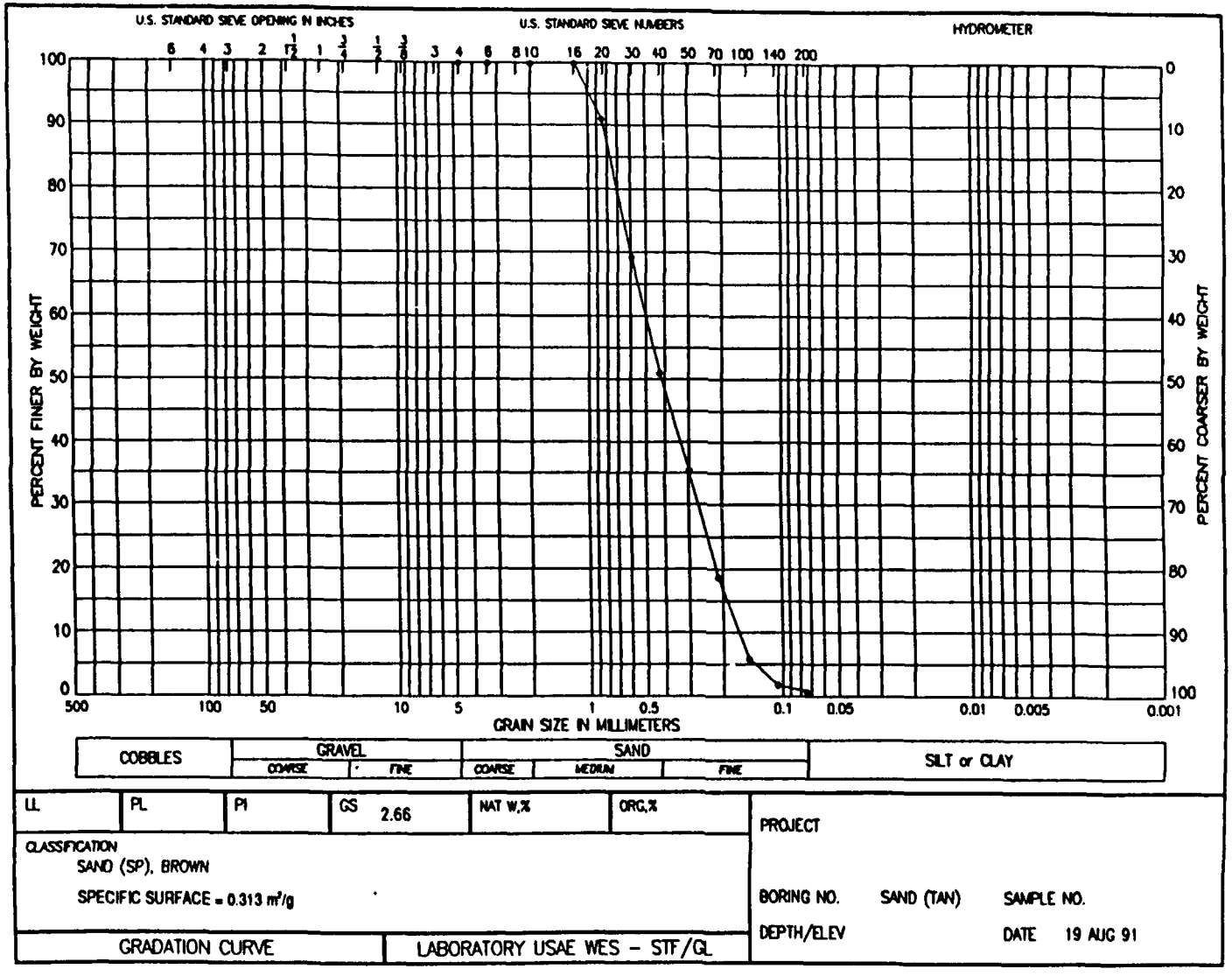

Figure A2. Gradation curve for tan sand

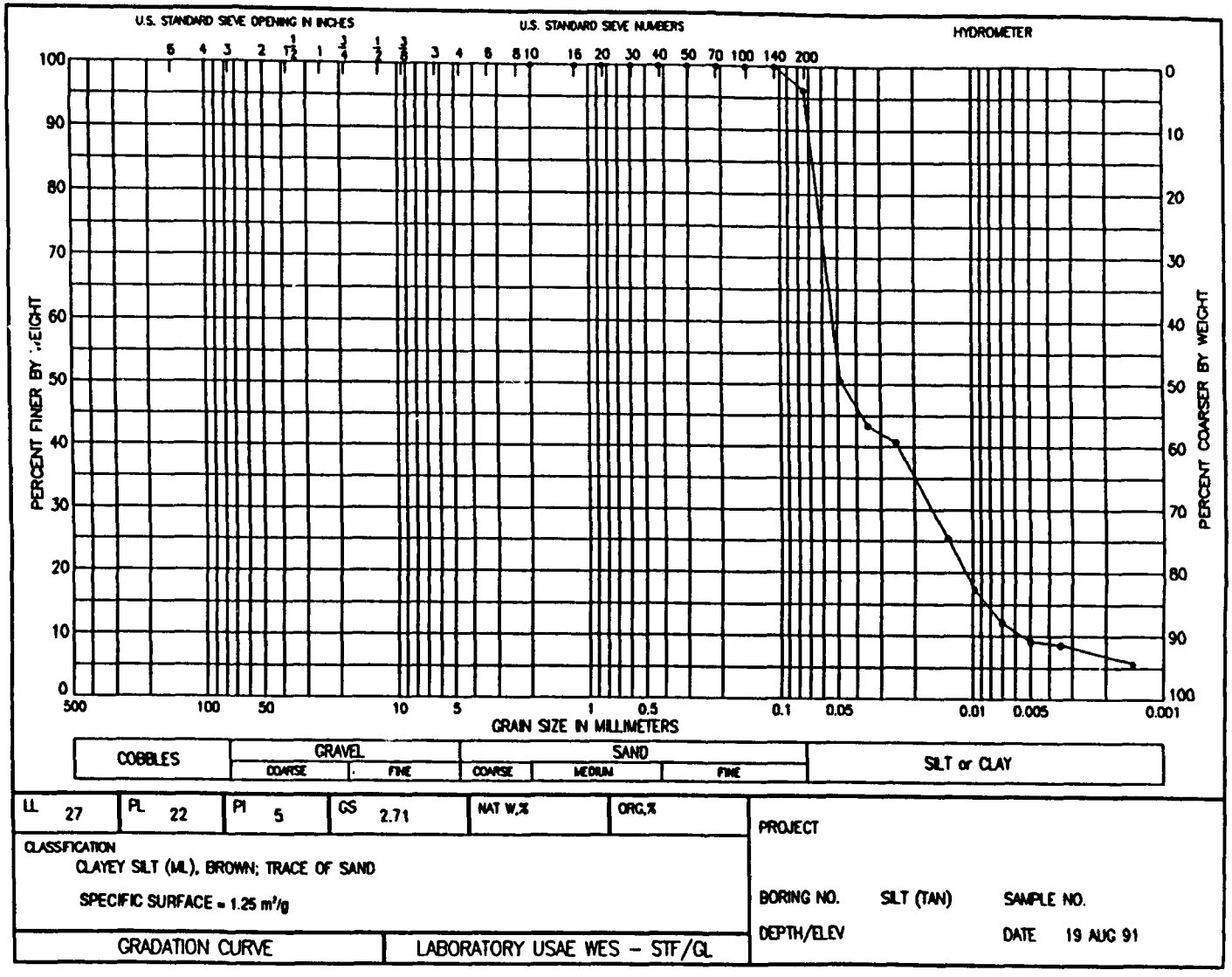

Figure A3. Gradation curve for tan silt

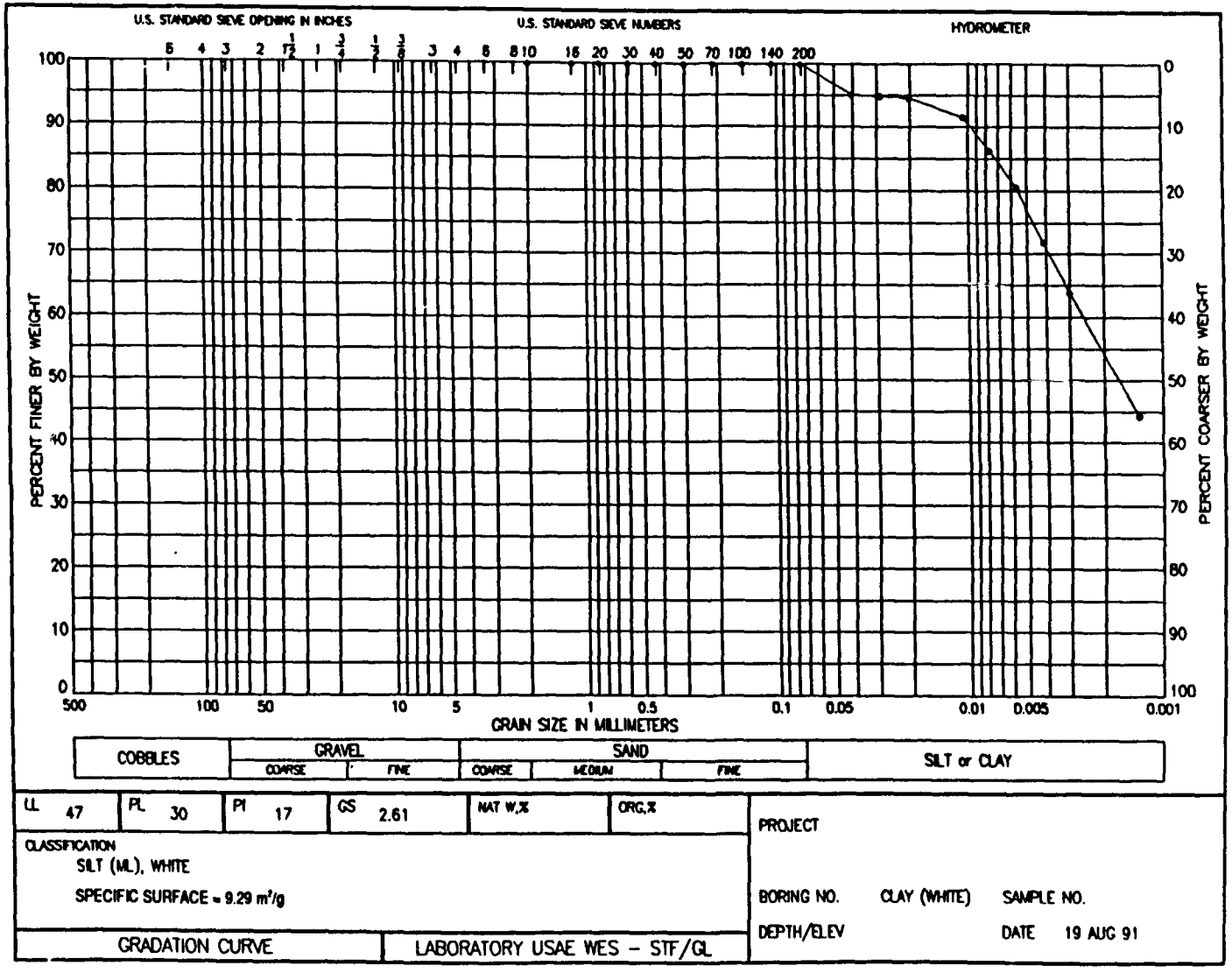

Figure A4. Gradation curve for kaolinite

Appendix B
Fractal Models of Soil Structure

Fractals

In recent years, some very interesting work has been done on the conductive behavior of porous media using the concept of self-similar geometries, or fractals, to model the behavior of certain physical quantities of that media. Mandelbrot, the guru of fractals, defines self-similar shapes as those in which a certain part of the shape can be broken up into N smaller parts, each looking like the original, but reduced in size by a fractional factor labeled r (Mandelbrot 1983).[1] The fractal dimension D of this self-similar shape can be written as

$$D = \frac{\log(N)}{\log\left[\frac{1}{r}\right]} \tag{B1}$$

or

$$N r^{D} = 1 \tag{B2}$$

Mandelbrot insisted that the exponent D be thought of as a dimension, because it arose from a method of measuring the perimeter of an object having an irregular boundary.

Fractals are often used to generate complex, or textured, curves or surfaces from very simple initiator geometries. For example, consider Figure 1 in which the initiator (or the initial segment of the geometry that

[1] References cited in this appendix are located at the end of the main text.

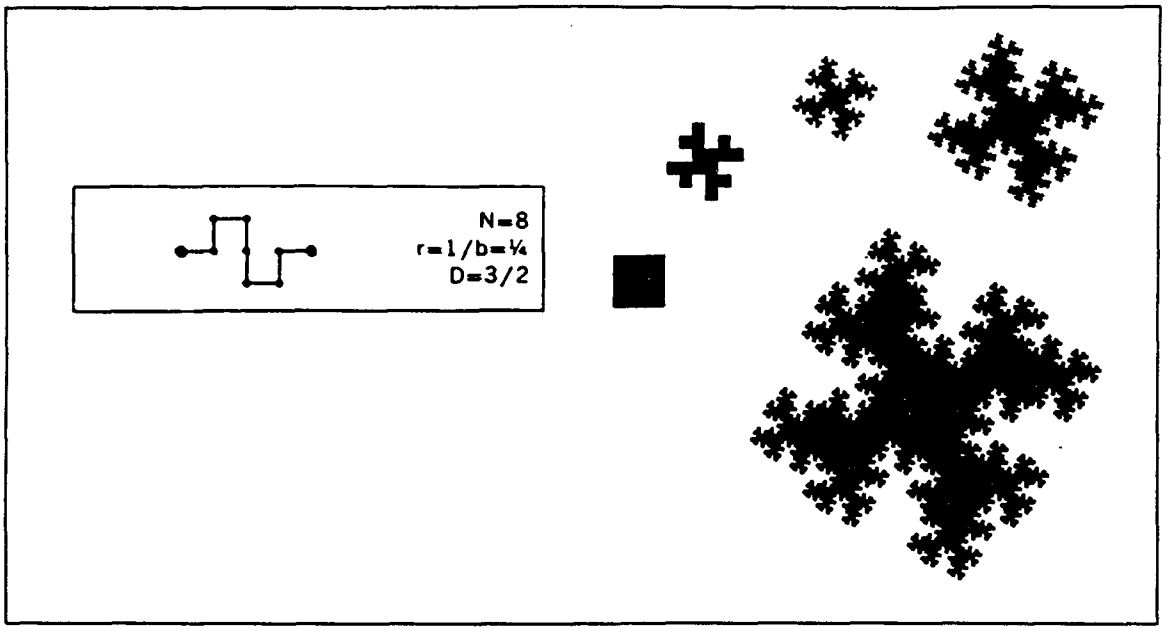

Figure B1. A fractal snowflake of dimension 1.5 (from Mandelbrot (1983))

will be fractalized) is a solid square (precisely stated, each side of the square is an initiator), and the generator (or the desired geometry) is the broken-line segment as shown. Moving clockwise from the initiator, the first two applications of the generator are shown at full scale, while the next two are enlarged to show the edge detail. Figure B2 shows another construction initiated with a solid square in which the generator results in the formation of both "lakes" and "islands."

Soil Structure

A third example of a fractal construction that is useful for studying porous media, and may be particularly useful for studying soil structure, is that shown in Figure B3 in which the initiator is a cube with square holes centered on each face and joining in the center. The generator is the same object but reduced by a factor of 1/3. Therefore, in the first stage, the initiator is divided into 20 smaller cubes, resulting in a fractal dimension of 2.7268. Mandelbrot referred to this construction as a Menger sponge. Friesen and Mikula (1987) used the Menger sponge to model the fractal dimension of the surface area of coal in such a way that the slope of the isotherm (fractional volume change versus pressure for porosimetry measurements) plotted on a log-log scale is linearly related to the fractal dimension. At least one recent study attempted to measure the fractal dimensions of sandstone solid-void interfaces (Katz and Thompson 1985). Measured values of interface fractal dimensions on five different samples using electron microscope techniques varied from 2.57 to 2.87.

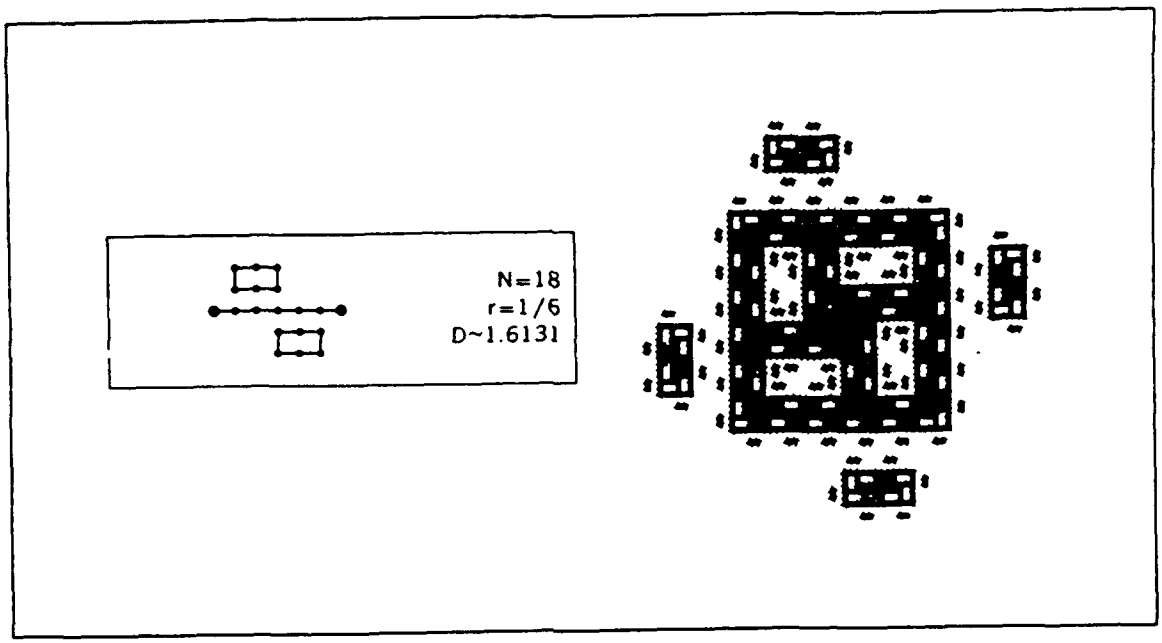

Figure B2. Fractal islands and lakes of dimension 1.6131 (from Mandelbrot (1983))

Work has been done very recently on modeling the microstructure of soil using fractals (Krepfl, Moore, and Lee 1989; Moore and Krepfl 1991). A two-dimensional representation of a three-dimensional model using hexagonal-shaped flakes as the generator is shown in Figure B4. Such models may be useful as a representation of pure clays. This particular fractal structure is strongly reminiscent of microphotographs of the pure kaolinite mineral structure.

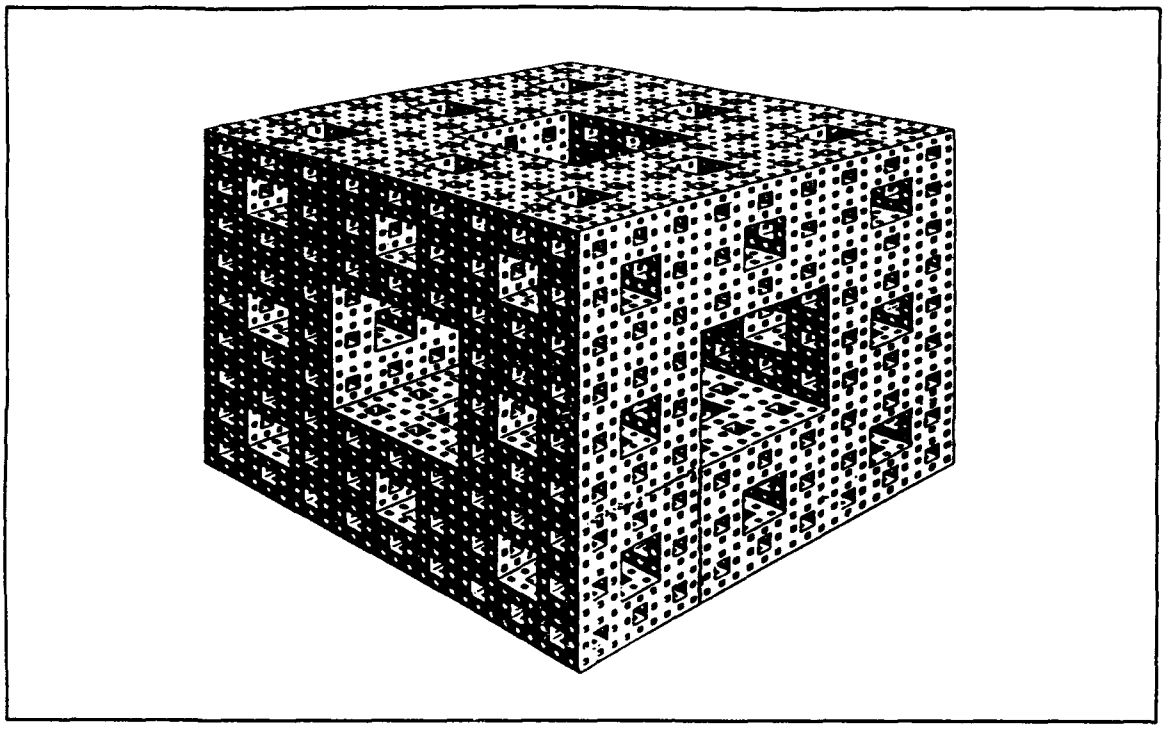

Figure B3. Menger sponge, fractal dimension 2.7268 (from Mandelbrot (1983))

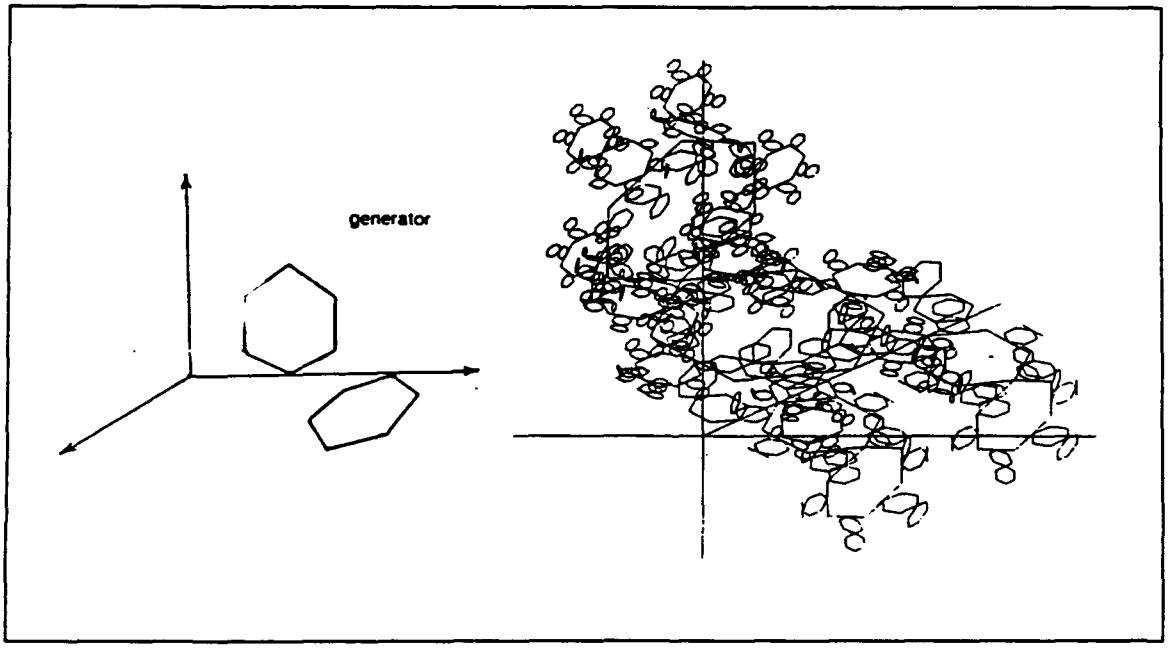

Figure B4. Fractal representation of soil fabric (from Moore and Krepfl (1991))

REPORT DOCUMENTATION PAGE

Form Approved
OMB No. 0704-0188

Public reporting burden for this collection of information is estimated to average 1 hour per response, including the time for reviewing instructions, searching existing data sources, gathering and maintaining the data needed, and completing and reviewing the collection of information. Send comments regarding this burden estimate or any other aspect of this collection of information, including suggestions for reducing this burden, to Washington Headquarters Services, Directorate for information Operations and Reports, 1215 Jefferson Davis Highway, Suite 1204, Arlington, VA 22202-4302, and to the Office of Management and Budget, Paperwork Reduction Project (0704-0188), Washington, DC 20503

1. AGENCY USE ONLY (Leave blank)	2. REPORT DATE	3. REPORT TYPE AND DATES COVERED
	December 1993	Report 3 of a series

4. TITLE AND SUBTITLE
Microwave Dielectric Behavior of Soils; Report 3, Measurements and Modeling

5. FUNDING NUMBERS

6. AUTHOR(S)
John O. Curtis

7. PERFORMING ORGANIZATION NAME(S) AND ADDRESS(ES)
U.S. Army Engineer Waterways Experiment Station
Environmental Laboratory
3909 Halls Ferry Road, Vicksburg, MS 39180-6199

8. PERFORMING ORGANIZATION REPORT NUMBER
Technical Report
EL-93-25

9. SPONSORING/MONITORING AGENCY NAME(S) AND ADDRESS(ES)
U.S. Army Corps of Engineers, Washington, DC 20314-1000

10. SPONSORING/MONITORING AGENCY REPORT NUMBER

11. SUPPLEMENTARY NOTES
Available from National Technical Information Services, 5285 Port Royal Road, Springfield, VA 22161.

12a. DISTRIBUTION/AVAILABILITY STATEMENT
Approved for public release; distribution is unlimited.

12b. DISTRIBUTION CODE

13. ABSTRACT *(Maximum 200 words)*

Making use of a coaxial reflection/transmission experimental procedure described in Report 2 of this series, a large number of complex dielectric property measurements were made of soil samples that ranged in texture from a poorly graded sand to a pure nonswelling clay mineral. Two methods of modeling the results are discussed. One is an equivalent circuit representation that accounts for both low-frequency conductivity and higher frequency dielectric relaxation losses in the soil/water mixture. The other model consists of a fractal description of soil structure combined with the concept of long-range electrical connectivity at less than 100 percent saturation.

14. SUBJECT TERMS
Complex dielectric constant
Conductivity
Equivalent circuits
Microwave
Permittivity
Soil

15. NUMBER OF PAGES
87

16. PRICE CODE

17. SECURITY CLASSIFICATION OF REPORT	18. SECURITY CLASSIFICATION OF THIS PAGE	19. SECURITY CLASSIFICATION OF ABSTRACT	20. LIMITATION OF ABSTRACT
UNCLASSIFIED	UNCLASSIFIED		